R. & M. No. 3421

MINISTRY OF AVIATION

AERONAUTICAL RESEARCH COUNCIL
REPORTS AND MEMORANDA

Boundary-Layer Separation in Supersonic Propelling Nozzles

By M. V. HERBERT and R. J. HERD

LONDON: HER MAJESTY'S STATIONERY OFFICE
1966

PRICE £1 8*s.* 0*d.* NET

Boundary-Layer Separation in Supersonic Propelling Nozzles

By M. V. Herbert and R. J. Herd

Communicated by the Deputy Controller Aircraft (Research and Development), Ministry of Aviation

*Reports and Memoranda No. 3421**

August, 1964

Summary.

A comparison has been made between the pressure rise at separation in convergent-divergent nozzles and that in other models with supersonic flow and a turbulent boundary layer. In the case of nozzles with uniform divergence, close similarity is found to the characteristics of separation induced on surfaces with initially zero pressure gradient. Where exceptions to this general agreement occur, three special categories of nozzle data can be distinguished. The first, involving a change of behaviour in the vicinity of separation, is attributable to the existence of a laminar boundary layer or of one in a state of transition. A critical value of Reynolds number at separation, based on equivalent flat-plate length, is found to be around 0·7 million. The second form of abnormality corresponds to an unusually large amount of pressure rise in the region between separation and nozzle outlet; this can occur in nozzles of low divergence angle with either turbulent or laminar separation, the effect being most pronounced with the latter. Third comes the case of a shock system in close proximity to nozzle outlet, where the full interaction pressure rise with a turbulent boundary layer is unable to develop.

LIST OF CONTENTS

* Replaces N.G.T.E. Report No. R.260—A.R.C. 26 102.

LIST OF CONTENTS—*continued*

LIST OF APPENDICES

LIST OF ILLUSTRATIONS

---

1. *Introduction.*

The performance of a supersonic internal-expansion propelling nozzle operating at a pressure ratio below that required to produce correct expansion depends, as is well known, upon the occurrence of flow separation within the nozzle. This takes place when the oblique shock, formed to recompress the overexpanded jet to the back pressure of the exhaust system, moves inside the walls of the nozzle. In inviscid flow, the shock would remain at outlet down to a much lower pressure ratio, and would only enter the nozzle after increasing in strength to the form of a plane shock. However, a boundary

layer is unable to withstand the pressure rise associated with so strong a shock at outlet, and consequently in practice the shock starts to move inside while still oblique in form.

Shock-induced boundary-layer separation in other supersonic flow systems has been studied quite extensively, and sufficient knowledge is available to estimate the quantities there associated with it. Several authors have applied the results of this work to separation from the walls of convergent-divergent propelling nozzles. They have found that experimental measurements of the pressure rise in nozzles exhausting into quiescent air agree fairly well with appropriate values for other systems with turbulent boundary layers. This suggests that no great differences are introduced by the factors of pressure gradient and wall divergence which exist in a nozzle.

However, some recent tests, carried out partly in the presence of an external stream, have indicated patterns of separation different from those obtained previously. There is in consequence need for a fresh appraisal of the factors upon which separation in a supersonic nozzle depends, in order to determine by what agency the observed difference in results is produced.

2. *The General Picture.*

A large body of experimental data exists on boundary-layer separation due both to obstacles and incident shocks, in supersonic flow with initially zero pressure gradient. The cases of forward-facing steps, curved surfaces, and compression corners, wedges or ramps, have been quite comprehensively studied two-dimensionally for both laminar and turbulent flow, as have incident shocks on flat plates. Limited evidence is available for separation at axisymmetric versions of steps, compression corners and curved surfaces, and for the interaction of a plane shock with a cylindrical body. It seems that the behaviour of two-dimensional and axisymmetric obstacles is qualitatively similar. Various theoretical approaches have been tried in order to describe the mechanism and occurrence of separation, generally including some factor for which an empirical value has to be taken.

Two points of immediate interest to us stand out when surveying this field of work (Refs. 1 to 21). First: in every experimental model studied, re-attachment of the boundary layer follows quite soon after separation. Second: the early part of the pressure rise (associated with separation) has features closely similar between all models, while the later part (associated with re-attachment) has not.

The second point may be put another way; in the words of Mager[14], the boundary layer does not 'know' what combination of circumstances creates the pressure rise leading to separation; it only knows what pressure rise is required at given conditions of Mach number and Reynolds number to cause it to separate. In this context Chapman *et al*[1] use the term 'free interaction', with relation to regions of flow 'which are free from direct influences of downstream geometry', and *ipso facto* 'independent of the mode of inducing separation'. Experimental results from several sources show that, at least as far as their respective separation points, an incident shock and all the forms of obstacle mentioned above are indeed 'free interactions' in this sense. But, once separated, the effects of geometry—either physical in the case of obstacles, or that imposed by mainstream requirements such as shock reflection—which the boundary layer must negotiate during the process of re-attachment, put the latter phase outside the category of a free interaction, and similarity of the various models ceases to be found.

In passing, it may be noted that Mager[14] had earlier coined the phrase 'free shock-separation' with reference to 'that type of separation where the flow downstream of the separation region is free

to adjust to any direction that may result from the shock-boundary-layer interaction process'. This condition seems to be restricted to cases in which re-attachment either does not occur or only does so some considerable distance after separation. Overexpanded nozzles and 'sufficiently large' steps are cited as possible examples, while other systems such as incident shocks (with early re-attachment) are termed 'restricted shock-separations'. Mager notes that 'at least in some cases, the interaction process of the restricted shock-separated boundary layer starts as a free shock-separation', which is another way of saying that up to the separation point all models behave similarly. Although there is no basic conflict of ideas, some confusion could arise between this terminology and that of Chapman *et al* quoted above, with regard to use of the word 'free' and what it is taken to imply. The two definitions are strictly incompatible, to the extent that Mager specifically refers to conditions 'downstream of the separation region' as deciding whether the interaction as a whole is 'free' or 'restricted' (according to which the great majority of the cases investigated must be regarded as not free), whereas Chapman *et al* ascribe the word to that part of a flow system which is independent of the downstream conditions (when part of the process in all models can generally be called free). Where used in the present paper, it will have the latter meaning.

Now the following stations in the flow may be recognised:

1 ~ the undisturbed stream just ahead of the initial compression.

s ~ the point of actual boundary-layer separation (upstream end of the 'bubble' or recirculation, usually determined by optical or oil-film methods).

2 ~ a point of higher pressure which can be regarded, rather arbitrarily, as a division between the processes of separation and re-attachment. This is defined according to some characteristic of the pressure distribution curve, variously termed the 'plateau' in laminar separation, and 'first peak' (for forward-facing steps) or 'inflection point' (for wedges or incident shocks) in turbulent flow. In the laminar case, this plateau of pressure extends over an appreciable distance ahead of the surface discontinuity or point of shock impingement. With a turbulent boundary layer, the selected feature of the pressure curve is a local one, and occurs at the maximum bubble width behind an incident shock-induced separation*, corresponding to the point of shock impingement, at or very slightly ahead of the surface discontinuity on a wedge or ramp, where the separation bubble again has its greatest width, and in the case of a forward-facing step about 60 per cent of the distance along the separated or recirculation region, i.e. measuring from the separation point towards the step.

r ~ the point of re-attachment or end of the separated region, occurring at the edge of a forward-facing step, and in the cases of wedges and incident shocks some distance downstream of the surface discontinuity or point of shock impingement.

3 ~ where parallel flow is finally restored and pressure rise ceases.

In the literature it seems to be generally established that all the models investigated exhibit pressure-rise characteristics which correspond closely to one another under similar conditions of Mach and Reynolds numbers as far as station 2 for laminar flow, and at least up to station s for turbulent. Thus far they conform with the concept of a free interaction in the sense used by Chapman *et al*[1].

---

* It should be noted that station 2 as here defined for incident shock interactions is *not* the same as the point of 'kink pressure' used by Gadd, Holder and Regan[8]. The latter occurs considerably nearer the separation point, and is not always easy to identify in data from other sources.

A difficulty appears, however, in respect of the further pressure rise from s to 2 in turbulent flow, where the detailed pressure distributions from various models are no longer identical. Chapman *et al*[1] conclude that in general this region must be regarded as outside the category of a free interaction. Nevertheless, in some instances similarity of pressure distribution has been observed between different geometries of model over a considerable part of the rise from s to 2. Two striking examples are available, both at $M_1 \simeq 3$:

(i) From Ref. 4 (Fig. 19 of Bogdonoff and Kepler, or Fig. 26 of Bogdonoff): this compares the pressure distribution for a strong incident shock (14° deflection) with that for a step (height $h = 1{\cdot}8\ \delta_1$).

(ii) From Ref. 1 (Fig. 39b): a comparison is given of the pressure distributions for a step (estimated $h = 2{\cdot}1\ \delta_1$) and a 25° compression corner.

Both these pictures show similar features:

(a) There is a lack of dependence on geometry of model not only up to the separation point but as far beyond as the 'inflection point' in the curves for incident shock and compression corner.

(b) These inflection points occur at pressure levels slightly below 'first peak' for the step in both sets of experiments. (A similar observation is made by Lange[7].)

(c) On the whole, values of pressure rise and interaction length (where l is measured from station 1) are in fairly good quantitative agreement between the different tests, as shown in the following table.

	Values of P/P_1			Values of l/δ_1		
	Separation (s)	Inflection (2)	First peak (2)	Separation (s)	Inflection (2)	First peak (2)
Incident shock: Ref. 4	2·10	2·55	—	$2\frac{1}{2}$	$5\frac{1}{2}$	—
Step: Ref. 4		—	2·67		—	7
Step: Ref. 1	2·06	—	2·43	$2\frac{1}{4}$	—	7
Compression corner: Ref. 1		2·34	—		$5\frac{3}{4}$	—

It is unfortunately true that in general no unique relation for P_2/P_1 exists for the case of a turbulent boundary layer. So far as the present paper is concerned, however, where the object is mainly to make a comparison with data on separation in nozzles, we are only seeking a condition which fairly describes the end of the separation process and the beginning of re-attachment in other models, and for this a reasonable but approximate estimate of P_2/P_1 will suffice. This is especially the case since the pressure rise to station s, which is unique and capable of fairly certain determination, represents

at least 80 per cent of the whole rise between 1 and 2. Of the various geometries of model studied in the literature, the most comprehensive data for P_2/P_1 as here defined come from forward-facing steps. This is perhaps not surprising as their 'first peak' is the feature most readily identifiable among the turbulent pressure distributions for any of the models. The value of P_2/P_1 at 'first peak' for certain types of step is considered near enough to that at 'inflection' for incident shocks and wedges to justify us, for the present purpose, in treating such step data as typifying the end of the separation process in all models.

There remains the complication of step height, which at times has been found to exert a quite pronounced effect. It seems to be generally agreed[1, 4, 11] that when step height is small the pressure rise to first peak—but not that to the separation point—diminishes as step height is reduced. A similar effect has been noted[4] in the case of weak incident shocks, and it is thought probable that small-angle wedges behave in like manner.

Bogdonoff and Kepler[4] show curves of P_2/P_1 for varying step height which level off when h/δ_1 reaches a value around 1·5 to 2. They did not, however, test much above 2. Love[9] did, and states that no effect of height was observed when $h/\delta_1 \geqslant 2$, although his upper limit is not given. On the other hand, Chapman *et al*[1] in their Fig. 46 present data which show a considerable further increase in P_2/P_1 as h/δ_1 rises from 2 to 6. This effect is apparently related to Mach number: departure from the general trend shown by the data of Ref. 4 (for $h/\delta_1 \simeq 2$) and Ref. 9 only becomes pronounced as M_1 increases above 2·5. It is advisable, therefore, when considering the use of step data as typifying P_2/P_1 for different geometric models in turbulent flow, to restrict the presumption of similarity to values of h/δ_1 around 2.

The first peak data available in this category cover the range of Mach number 1·4 to 6, as shown in Fig. 2b. They are derived from three sources:

(i) Love[9]: as already mentioned, these results relate to steps with h/δ_1 between 2 and some unknown higher value such that no effect of step height was produced.

(ii) Sterrett and Emery[11]: h/δ_1 is estimated to be within the range 1·6 to 3·0.

(iii) Bogdonoff[4]: only the results for $h/\delta_1 > 1{\cdot}5$ are included.

2.1. *Separation Criteria.*

Many relations, some wholly empirical and some based on theoretical considerations, are given in the literature for the ratios

$$\frac{P_s}{P_1}, \quad \frac{P_2}{P_s} \quad \text{and} \quad \frac{P_2}{P_1},$$

and kindred functions associated with the mainstream flow, such as Mach number ratio and shock deflection angle, are also employed to relate conditions at stations 1, s and 2. All analytical treatments assume two-dimensional flow.

2.1.1. *Turbulent flow.*—

Mager[13] seems to have been the first to derive the relation

$$\frac{M_s}{M_1} = K^{1/2} \tag{1}$$

where K is some constant.

In order to convert this into a simple expression for pressure ratio, he then uses a linearised approximation to the oblique shock, and obtains

$$\frac{P_s}{P_1} \simeq 1 + \frac{(1-K)\frac{\gamma}{2}M_1^2}{1+\frac{\gamma-1}{2}M_1^2} \tag{2}$$

or

$$C_{P,s} \simeq \frac{1-K}{1+\frac{\gamma-1}{2}M_1^2} \tag{2a}$$

where

$$C_P = \frac{P-P_1}{\frac{\gamma}{2}P_1M_1^2}.$$

The value suggested for K in Ref. 13 is 0·494, giving $M_s/M_1 = 0{\cdot}703$. In a later paper[14], Mager changes to $K = 0{\cdot}55$ on the grounds that a better fit is obtained to experimental measurements of the separation point[5]. This would give $M_s/M_1 = 0{\cdot}742$.

Numerical comparison of equations (1) and (2), using correct oblique shock relations in the former, discloses a gross discrepancy. At $M_1 = 2$, equation (1) yields a value of P_s/P_1 24 per cent above that given by equation (2), taking $K = 0{\cdot}55$, while at $M_1 = 4$ the figure has risen to 60 per cent. This was pointed out by Reshotko and Tucker[15] who, no doubt correctly, attribute the discrepancy to Mager's use of a shock-wave approximation. It seems, therefore, that equations (2) and (2a) should not be used.

What is hard to understand is that Mager in his later paper does nothing to answer this criticism or to correct the situation. He reiterates both equations (1) and (2), and then proceeds to develop an expression for P_2/P_s in terms of M_s and λ_2, for the case of his 'free shock-separation ' model in which re-attachment does not occur (*see* Section 2). This gives him

$$\frac{P_2}{P_s} = 1 + \frac{0{\cdot}328\,\gamma K M_1^2\lambda_2}{1+\frac{\gamma-1}{2}KM_1^2}. \tag{3}$$

By regarding the flow outside the boundary layer as adjusting itself to the conditions of the 'jet-like' separated boundary layer at station 2, he is able to invoke conditions across a two-dimensional mainstream shock to connect M_1 with λ_2. For this shock he introduces a further approximate relation

$$\lambda_2 \simeq \frac{(M_1^2-1)^{1/2}}{\gamma M_1^2}\left(\frac{P_2}{P_1}-1\right) \tag{4}$$

and suggests its use in conjunction with equations (2) and (3), giving the combined expression,

$$\frac{P_2}{P_1} = \left\{1 + \frac{(1-K)\frac{\gamma}{2}M_1^2}{1+\frac{\gamma-1}{2}M_1^2}\right\}\left\{1 + \frac{0{\cdot}328\,K(M_1^2-1)^{1/2}\left(\frac{P_2}{P_1}-1\right)}{1+\frac{\gamma-1}{2}KM_1^2}\right\}. \tag{5}$$

Reshotko and Tucker[15] give a general theoretical analysis for the 'change of boundary-layer-thickness parameters and form factor caused by a discontinuity in the absence of friction effects'.

Since friction effects are considered negligible compared with those of pressure gradient during separation, these authors conclude 'the form of the result suggests that the Mach number ratio across the shock is a characteristic parameter for defining shock-induced separation'. It should be noted, as Mager[14] points out, that they do not specifically distinguish between stations s and 2 in their analysis, and it is probably reasonable to regard it as applying strictly only to what we have agreed to call 'free interactions'. In turbulent flow, this covers s but not necessarily 2. Reshotko and Tucker do in fact quote different values for the ratio M_2/M_1 as between 'first peak' data for forward-facing steps (0·762) and 'inflection point' data for wedges (0·81).

Love[9] suggests that a value of M_s/M_1 around 0·85 is required to fit experimental data, which would give $K = 0{\cdot}722$. This figure is much higher than either of those taken by Mager[13,14]. However, since $P_2/P_1 > P_s/P_1$, it is necessary to have $M_2/M_1 < M_s/M_1$, and Love[9] shows a very fair correlation of experimental 'first peak' data for steps up to $M_1 = 3$ using the value $M_2/M_1 = 0{\cdot}762$ copied from Reshotko and Tucker[15]. More separation point data have recently become available, collected in Fig. 2a, covering Mach numbers between 1·5 and 6. A fair average fit over the whole range of M_1 is given by $M_s/M_1 = 0{\cdot}82$* ($K = 0{\cdot}67$).

So far as the validity of either Mach number ratio to correlate separation performance is concerned, it seems that we should accept M_s/M_1 as being a parameter which analysis suggests to be significant in the mechanism of separation, and as having at least in theory an unique value, while the use of M_2/M_1 may be justified by experimental data for any particular geometric arrangement, the values in this case being not necessarily independent of geometry.

An alternative and wholly empirical relation is offered by Love[9] to describe more closely his 'first peak' data on forward-facing steps over the range $1{\cdot}4 < M_1 < 3{\cdot}5$, namely

$$C_{P,2} = \frac{3{\cdot}2}{8 + (M_1 - 1)^2}. \tag{6}$$

This range is extended up to $M_1 = 6{\cdot}3$ by Sterrett and Emery[11], who show that equation (6) is in approximate agreement with their data up to $M_1 = 5$ and an increasingly poor fit thereafter. They give a further empirical equation to fit their own data, but it cannot be sensibly applied when $M_1 < 3{\cdot}5$. Use of any constant value for M_2/M_1 over the whole range is again found to be not completely satisfactory†.

Another semi-theoretical expression for P_s/P_1 is developed by Gadd[17]. This is explicitly given for the case of an incident shock in two-dimensional flow, but in an earlier version of the same work‡ similarity is suggested to the case of a compression corner. According to previous discussion, it should in fact be applicable to any 'free interaction'. Gadd considers a one-seventh power velocity profile as having a 'shoulder' at some characteristic fraction J of the free-stream velocity, and, again taking friction forces as negligible by comparison with those due to the pressure gradient, he

---

* The mean line in Fig. 2a fits $M_s/M_1 = 0{\cdot}825$ very closely over the range $1{\cdot}85 < M_1 < 3{\cdot}6$; at values of $M_1 < 1{\cdot}85$ the effective Mach number ratio drops sharply (0·79 at $M_1 = 1{\cdot}5$), and at high values of M_1 it falls again more gently (0·81 at $M_1 = 6$). Hence the accuracy in practice of this form of criterion, particularly at low Mach number, is only approximate.

† The value of M_2/M_1 required to fit the data for forward-facing steps, collected in Fig. 2b, rises from 0·762 at $M_1 < 3$ to 0·78 at $M_1 = 4$ and then falls rapidly to about 0·74 at $M_1 = 6$.

‡ A.R.C. 15 543. January, 1953.

evaluates the pressure increase required to bring the fluid on this streamline to rest isentropically. This pressure rise he argues is approximately equal to that at the separation point, whence

$$\frac{P_s}{P_1} = \left\{ \frac{1 + \frac{\gamma - 1}{2} M_1^2}{1 + \frac{\gamma - 1}{2}(1 - J^2) M_1^2} \right\}^{\gamma/(\gamma-1)} . \tag{7}$$

Gadd initially recommends[17] taking J as $0 \cdot 6$, but this is later revised[18] to $0 \cdot 54$; with the latter value of J equation (7) is shown[18] to give quite good fit to experiment.

A modification to equation (7) is proposed by Arens and Spiegler[22, 23] for the case in which the characteristic streamline is initially supersonic (which, for $\gamma = 1 \cdot 4$, works out to be when $M_1 \geqslant 2 \cdot 08$), when they then assume a normal shock followed by isentropic subsonic stagnation. This leads to the relation

$$\frac{P_s}{P_1} = \frac{\left(\frac{\gamma + 1}{2} J^2 M_1^2 \right)^{\gamma/(\gamma-1)}}{\left\{ 1 + \frac{\gamma - 1}{2}(1 - J^2) M_1^2 \right\} \left\{ \frac{M_1^2}{2} \left[(\gamma + 1) J^2 - \frac{(\gamma - 1)^2}{\gamma + 1} \right] - \frac{\gamma - 1}{\gamma + 1} \right\}^{1/(\gamma-1)}} . \tag{8}$$

Good agreement is claimed[22] between experimental data (for steps, compression surfaces and incident-shock models) and equation (8) using the value $J = 0 \cdot 56$.

Various other wholly empirical relations are available. Cooke[21] suggests that the data of Chapman *et al*[1] are reasonably well described by the equation

$$\frac{P_s}{P_1} = 0 \cdot 079 \, M_1^2 + 1 \cdot 52 - \frac{0 \cdot 22}{M_1} . \tag{9}$$

This does not satisfactorily fit the data of Sterrett and Emery[11] at higher Mach numbers, and should not be used when $M_1 > 4$. For relating stations s and 2, Cooke[21] notes that various compression-corner and incident-shock data fit the formula

$$\frac{P_2}{P_1} = 1 \cdot 15 \frac{P_s}{P_1} . \tag{10}$$

Guman[20], referring simply to 'peak' pressure, without specifying the intended meaning in relation to different geometric arrangements, proposes

$$C_{P,2} = 1 \cdot 54 \, C_{P,s} \tag{11}$$

which, in conjunction with equation (2) and $K = 0 \cdot 55$, is said to give 'fair to good agreement' with the data of Chapman *et al*[1].

2.1.2. *Agreement with experiment.*—At this stage it is worth sifting equations (1) to (11) in the light of experimental evidence, taken from Figs. 2a and b. In order to achieve greater sensitivity, reciprocal pressure ratios will be used in future: that is to say P_1/P_s, etc. rather than the form P_s/P_1, etc. which appears in the preceding equations. The value $\gamma = 1 \cdot 4$ is taken throughout.

On Fig. 1 relating to P_1/P_s are shown the following curves:

(a) Experimental mean line from Fig. 2a

(b) Equation (1) with $K = 0{\cdot}55$ (after Mager[14])

(c) Equation (1) with $K = 0{\cdot}67$

(d) Equation (2) with $K = 0{\cdot}55$ {said by Mager to be a sufficient approximation to (b)}

(e) Equation (7) with $J = 0{\cdot}6$

(f) Equation (7) with $J = 0{\cdot}56$

(g) Equation (8) with $J = 0{\cdot}6$

(h) Equation (8) with $J = 0{\cdot}56$.

It can be seen that curves (b), (e) and (g) all overestimate the value of P_s/P_1. Curves (f) and (h) show that when $J = 0{\cdot}56$, there is little difference between equations (7) and (8), and the simpler form of equation (7) may be preferred. Quite good agreement with the experimental data is given by curves (c), (f) and (h), except that none of the equations fits satisfactorily when $M_1 < 1{\cdot}7$.

An experimental curve of P_s/P_2 for forward-facing steps has been obtained by combining the data of Figs. 2a and b. Fig. 2c then compares the following curves for P_s/P_2:

(i) Experimental mean line derived as above

(j) Equation (3) for $K = 0{\cdot}55$ (after Mager[14])

(k) Equation (3) for $K = 0{\cdot}67$

(l) Equation (10)

(m) Equation (11) in conjunction with the experimental curve of P_1/P_s as used in Fig. 1.

Equation (3) was evaluated using correct shock deflection relations for λ_2 rather than Mager's approximation in equation (4). Fig. 2c shows that none of the relations giving curves (j) to (m) is very satisfactory. Equation (3) is insensitive to the value of K, and evidently much underestimates the ratio P_2/P_s. A slight improvement would be obtained by use of the expression

$$\frac{P_2}{P_s} = 1{\cdot}05 + 0{\cdot}05\, M_1. \tag{12}$$

Finally, Fig. 3 gives curves for P_1/P_2 as follows:

(n) Experimental mean line for forward-facing steps from Fig. 2b

(o) Equation (5) for $K = 0{\cdot}55$ (after Mager[14])

(p) Equation (6)

(q) $M_2/M_1 = 0{\cdot}762$

(r) Equation (7) with $J = 0{\cdot}56$ in conjunction with equation (12)

(s) Equation (8) with $J = 0{\cdot}56$ in conjunction with equation (12).

Also evaluated, but not shown in the figure, was

(t) equation (1) with $K = 0{\cdot}67$ in conjunction with equation (12).

Curve (o) bears little resemblance to the experimental line; there is no particular reason why it should, since it is made up of two expressions at least one of which {curve (d) of Fig. 1} has been

found to be inaccurate. Curve (p) from the empirical equation (6) gives the best fit so long as $M_1 \leqslant 4{\cdot}5$, as it was designed to do. For the complete range of M_1 up to 6, there is little to choose between curves (q), (r), (s) and (t), any of which agree with the experimental line about as well as its peculiar form will allow.

Summing up, of the semi-theoretical relations given:

equations (2), (3) and (5) should not be used;

equation (1) with $K = 0{\cdot}67$, and

equations (7) and (8) with $J = 0{\cdot}56$ are satisfactory in predicting P_s/P_1;

while of the empirical expressions:

equation (6) and the relation $M_2/M_1 = 0{\cdot}762$ are both of some value in determining P_2/P_1 for forward-facing steps;

equations (10) and (11) are not very satisfactory, and

equation (12) is slightly better in giving P_2/P_s.

2.1.3. *Laminar flow.*—The case of a laminar boundary layer is more susceptible to exact analytical treatment than is the turbulent.

Gadd[17] derives the following expression for an incident shock

$$C_{P,s} = 1{\cdot}56\,Z\left\{\frac{\left(1+\frac{\gamma-1}{2}M_1^2\right)\left[1-\frac{0{\cdot}636\tan^{-1}\left\{\left(\frac{\gamma-1}{2}\right)^{1/2}M_1\right\}}{\left(\frac{\gamma-1}{2}\right)^{1/2}M_1}\right]}{1+0{\cdot}693\,(\gamma-1)M_1^2}\right\}^{1/2} \tag{13}$$

where

$$Z = [(M_1^2-1)Re_X]^{-1/4}$$

and more generally[19] for separation in any two-dimensional supersonic flow

$$C_{P,s} = 1{\cdot}13\,Z.$$

Another and less rigorous analysis by Hakkinen *et al*[10] gives the almost identical relation

$$C_{P,s} = 1{\cdot}15\,Z$$

while the same authors present an argument suggesting that

$$\sqrt{2} < \frac{C_{P,2}}{C_{P,s}} < 1{\cdot}9$$

on the basis of which they propose

$$C_{P,2} = 1{\cdot}9\,Z.$$

Their own data for incident shocks at $M_1 \simeq 2$ agree quite well with their relations for both $C_{P,s}$ and $C_{P,2}$. Other and more comprehensive data up to $M_1 = 3{\cdot}5$ from the work of Chapman *et al*[1] have been shown to fit

$$C_{P,s} = 0{\cdot}93\,Z \text{ (due to Gadd[19])}$$

$$C_{P,2} = 1{\cdot}82\,Z \text{ (due to Sterrett and Emery[11])}.$$

Guman[20] suggests

$$C_{P,2} = 2{\cdot}2\,Z$$

as fitting the same data.

Taking the average of all experimentally supported values except Guman's, we get

$$C_{P,s} = \frac{1{\cdot}04}{[(M_1{}^2-1)Re_X]^{1/4}} \tag{14}$$

and

$$C_{P,2} = \frac{1{\cdot}86}{[(M_1{}^2-1)Re_X]^{1/4}}. \tag{15}$$

It is worth noting that equations (13) and (14) give coefficients of Z which agree quite closely (within $\pm$ 6 per cent in the range $2 < M_1 < 5$, taking values of γ between 1·2 and 1·4), so that the rather tedious computation involved in the use of equation (13) can be avoided.

2.2. *Effect of Reynolds Number.*

In the foregoing review of separation criteria, equations (1) to (11) for a turbulent boundary layer are all independent of Reynolds number, and equations (13) to (15) for a laminar boundary layer all have a dependence on $Re_X{}^{-1/4}$.

General analyses of the effect of Reynolds number have been attempted by several workers. The earliest is that given by Donaldson and Lange[6] for the case of shock-induced separation, who advance the suggestion that the 'critical' pressure coefficient (defined as being based on the pressure rise across a shock wave which just causes separation of the boundary layer) is proportional to the skin-friction coefficient. Hence

$$C_{P,\text{crit}} \propto Re_X{}^{-1/2} \text{ in laminar flow}$$

or

$$C_{P,\text{crit}} \propto Re_X{}^{-1/5} \text{ in turbulent flow.}$$

These expressions are apparently intended to take full account of Mach number as well as Reynolds number. The same authors cite work by Stewartson* as predicting that for laminar flow

$$C_P \propto Re_X{}^{-2/5}.$$

Apart from those relations given above, there seems to be general unanimity in favour of the square root of the skin-friction coefficient, with some additional dependence on Mach number. This leads to expressions, for constant Mach number, of the form

$$C_P \propto Re_X{}^{-1/4} \text{ in laminar flow}$$

or

$$C_P \propto Re_X{}^{-1/10} \text{ in turbulent flow.}$$

It will be observed that the laminar result is in agreement with equations (13) to (15). Chapman *et al*[1] give their derivation of the form

$$C_P \propto \sqrt{C_f}$$

as applying generally to any free interaction, which therefore covers both $C_{P,s}$ and $C_{P,2}$ in laminar flow and $C_{P,s}$ in turbulent. They add a rather tentative suggestion of $(M_1{}^2-1)^{-1/4}$ for the further Mach number dependence, which is also in line with equations (13) to (15). A later analysis by Erdos and Pallone[16] produces the same indices of $-1/4$ and $-1/10$ for Reynolds number.

* K. Stewartson. On the interaction between shock waves and boundary layers. *Proc. Cambridge Phil. Soc.*, Vol. 47, Part 3, p.545, July, 1951.

A great deal of the available experimental evidence covers too narrow a range of Reynolds number and exhibits too much scatter for any certain correlation to be made. In this category for laminar flow come the data from Refs. 6, 7, 10 and 11. Donaldson and Lange[6] claim that the data they show support their predicted dependence on $Re_X^{-1/2}$, but the correlation is unconvincing. All that can really be said of the laminar data published by Hakkinen *et al*[10] and Sterrett and Emery[11] is that a better fit is given by the index $-1/4$ than by 0. The most comprehensive correlations are those presented by Chapman *et al*[1], and these leave little doubt that $Re_X^{-1/4}$ is at least very close to the truth for both $C_{P,s}$ and $C_{P,2}$ in laminar interactions.

Turning to turbulent separation, data on the effect of Reynolds number can be found in Refs. 1 to 3, 6 to 9, and 11. Once again Donaldson and Lange[6] claim to find agreement between their prediction of $Re_X^{-1/5}$ and a collection of experimental data at varying Mach number, of which their own forms the whole of the high Reynolds number end. However, the trend shown is more obviously with Mach number than with Reynolds number, and the validity of their own data is in any case called in question by Lange[7]. Other collections[7, 9, 11] of data relating to $C_{P,2}$ create a fairly clear impression that a large dependence on Mach number exists but none at all on Reynolds number.

Chapman *et al*[1] publish data in the form $C_{P,s}$ versus Re_X, and show a quite good and distinct correlation of this quantity with $Re_X^{-1/10}$ for forward-facing steps and compression corners. When, however, they come to plot $C_{P,2}$ the picture changes somewhat, a fact which they associate with its exclusion from the category of a free interaction. The effects they observe in the latter case are a variation of the Reynolds number index with Mach number and type of model, both above and below the value $-1/10$, with zero in several cases. Similarly Kuehn[2, 3] shows that the overall pressure ratio for incipient separation at compression corners, curved surfaces and incident shocks, does not depend in a consistent manner on Reynolds number, but is again subject to changes with Mach number and geometry. In general the trend is towards zero dependence when the Mach number is low and the Reynolds number high, with a quite large effect being experienced when the Mach number is high and the Reynolds number low.

All this is rather a nuisance if one is seeking a general criterion for use in other circumstances. One may note, however, that there is no disagreement with

$$C_{P,2} \propto Re_X^{0}$$

for a turbulent boundary layer at $M_1 \leqslant 2$, and that no lower index than $-1/10$ is found up to $M_1 = 2{\cdot}5$. This is quite trifling, and for approximate estimates within that range of M_1 no significant error should result from neglecting the effect altogether.

3. *Regimes of Nozzle Operation.*

As the applied pressure ratio of a convergent-divergent nozzle with internal expansion is reduced from above its design pressure ratio towards unity, it is well known that four flow regimes occur successively:

(i) The flow is everywhere attached to the walls, when the nozzle is said to be running full. Either an expansion fan or an oblique shock is located at the nozzle outlet, depending upon whether the internal flow is under- or overexpanded. Transition from this regime to the next occurs at the 'kink point', at which the oblique shock commences to move inside the nozzle.

(ii) The flow separates from the walls inside the divergent portion of the nozzle, as a result of interaction between the internal oblique shock and the boundary layer.

(iii) Separation takes place close to the nozzle throat, the accompanying compression tending in form towards a normal shock, followed by subsonic diffusing flow. The change from regime (ii) is of course gradual, but various approximate estimates have been made of the condition at which a difference in flow model must be introduced. Arens and Spiegler[22, 23] have recently suggested for this case $M_1 < 1 \cdot 13$, while an earlier paper[24] proposed taking a normal shock at $M_1 = 1 \cdot 15$ as the 'limiting condition eventually reached as the shock system moves upstream in any nozzle' (*see* also Section 5).

(iv) The nozzle ceases to be choked, and runs with subsonic flow throughout.

In the present work we are concerned primarily with regime (ii), in which a parallel may be found to other models with separation in supersonic flow.

4. *Overexpanded Nozzles.*

Two salient differences set nozzles apart from the other models described in Section 2.

1. The fluid is expanding, and the pressure gradient ahead of the interaction is not zero.
2. Re-attachment generally does not occur, and the separation bubble is extended into a 'mixing region' continuing to the nozzle outlet (station b, Fig. 4), with ambient air entering to take part in the recirculatory flow system set up.

   Some further pressure rise is known to take place along the wall in this mixing region, and the amount may be expected to depend on the angle and Mach number of the separated main jet downstream of the interaction, on the wall angle, and on the level of Reynolds number controlling the mixing processes in the shear layer. This further rise in the mixing region has been called 'pressure recovery', having in mind some loose analogy with the behaviour of diffusing subsonic flow, and the terminology is retained here for convenience. In amount it is usually found to be small.

If, in the absence of data, the possible effect of a favourable pressure gradient in increasing the allowable shock strength be neglected, then there seems little doubt that the pressure rise in a nozzle should follow that in other models so far as they remain free interactions—i.e. up to station s in turbulent flow and station 2 in laminar. Beyond s, in the case of a turbulent boundary layer, the exact similarity in behaviour breaks down; but among various geometries of model some approximate correspondence was noted previously (Section 2) in the additional pressure rise to station 2, which may be regarded as the boundary dividing separation from re-attachment. It therefore seems quite likely that the pressure rise within the interaction region of a nozzle, which is experienced as the separation bubble develops, may also show some agreement as far as station 2. This it will be the purpose to demonstrate.

With subsequent and dissimilar pressure rises around re-attachment the present paper is happily unconcerned; instead there is the largely unknown quantity of the mixing pressure recovery. In the first instance, lacking any systematic measurements or method of theoretical prediction, no quantitative allowance for this final phase of pressure rise in a nozzle can be introduced. But where the amount of recovery must be small, as for instance in nozzles of rather wide divergence angle or with separation fairly close to the outlet, one can reasonably look for agreement between the overall pressure rise from 1 to b (Figs. 4 and 5) and those criteria which effectively describe behaviour up to station 2.

In certain special cases to be discussed later, the pressure recovery can assume much greater importance, and these exceptions to the general treatment will be noted as they arise.

4.1. *Previous Correlations.*

A recent contribution by Arens and Spiegler[22] became available as the present paper was in course of preparation. This constitutes an attempt, although not the first, to apply the results of work on other separation models to the case of an overexpanded nozzle, ignoring in the same way as ourselves the effects of pressure gradient. It is mentioned first because Arens' picture is similar to that shown in Fig. 4; he divides a nozzle into 'the initial region of compression terminating at the point of separation and the subsequent mixing region wherein the separated flow mixes with entrained air from atmosphere'. Other interaction models are also referred to as comprising zones of separation and mixing, where in that case 'mixing is terminated by further compression as the flow re-attaches'.

From the above description it appears that Arens and Spiegler regard the whole pressure rise in a nozzle beyond the separation point, i.e. the rise from s to 2 as well as that from 2 to b, as part of the 'mixing', which they then proceed to ignore*. A comparison is presented between the overall pressure rise to nozzle outlet from the data of numerous workers and the relations for P_s/P_1 in turbulent flow given by equations (7) and (8), taking Gadd's original value of $J = 0{\cdot}6$ in both. Rather surprisingly, in view of the assumptions noted above, fairly good agreement with the mass of nozzle data is shown. A contributory reason for this evidently arises from the tendency, illustrated in Fig. 1, of equations (7) and (8) with this value of J to overestimate the ratio P_s/P_1. There is certainly no inherent reason why any valid relation for P_s/P_1 should agree with the overall pressure rise occurring in an overexpanded nozzle. In this connection it may be noted that Arens and Spiegler[22] show on the same graph a curve labelled 'separation pressure ratio' from Ref. 11, which lies well away from the nozzle data in the direction which the difference between stations s and 2 would lead one to expect. The authors of Ref. 22 seem to recognise the fortuitous and empirical nature of the agreement which they present, as they go on to suggest that a more accurate value of J for use in equation (8) is around $0{\cdot}56$.

Much earlier Le Fur[25] applied the relation $M_2/M_1 = 0{\cdot}762$ from Refs. 9 and 15 with fair success to some rather limited experimental separation data from convergent-divergent nozzles, assuming $P_2 = P_b$.

Other attempts at correlation of nozzle data have been essentially empirical, and two sets of workers[24, 26] have found a convenient criterion to be constant flow deflection angle (λ) corresponding to the separation shock, again assuming $P_2 = P_b$. A fairly wide survey of data[24] on separation in nozzles with obviously turbulent boundary layers suggests a value of $\lambda = 13\frac{1}{2}°$.

Love[9] gives curves of λ corresponding to $M_2/M_1 = 0{\cdot}762$, which show a substantially constant value ($13\frac{1}{2} \pm 1°$) for $M_1 > 1{\cdot}9$ when $\gamma = 1{\cdot}4$†, but there is a pronounced effect of large changes in γ, λ increasing with reduction of γ.

---

* In another version of the same paper[23], Arens specifically neglects 'the small pressure rise occurring in the mixing region between the separation point and the nozzle exit plane'.

† Rather more generally, reference to shock tables ($\gamma = 1{\cdot}4$) shows that for any value of Mach number ratio in this neighbourhood, the corresponding deflection angle λ is nearly constant once the initial Mach number is fairly high, so that some theoretical support can be found for the efficacy of such a criterion.

This predicted effect of γ on separation is of considerable importance, and it is difficult to obtain any very conclusive picture from the evidence so far available. In general, the data of Refs. 1 to 12 are all for $\gamma = 1{\cdot}4$, and although the various relations quoted in preceding sections are functions of γ, its effect cannot be checked from conventional separation models. A single experiment is cited by Love[9] in which helium ($\gamma = 1{\cdot}667$) was used in a two-dimensional nozzle with separation at $M_1 = 3{\cdot}48$, yielding a value of $C_{P,2}$ in good agreement with that predicted by the relation $M_2/M_1 = 0{\cdot}762$—agreement at least as close as given by Love's own data for $\gamma = 1{\cdot}4$ to the same relation. To that extent prediction is apparently borne out.

All other separation data in which γ departs appreciably from $1{\cdot}4$ relate to rocket nozzles with lower values of γ. Summerfield *et al*[26] reproduce the results of Foster and Cowles[35], for axisymmetric nozzles with $M_1 > 3$ and $\gamma = 1{\cdot}23$, which they suggest show some value of λ around 16°, but the correlation is poor. When compared with collections of other nozzle separation data for which $\gamma = 1{\cdot}4$, it is found[24, 27] that the results of Foster and Cowles do not differ at all significantly from the general pattern.

Other data cited by Summerfield *et al*[26] are those of McKenney[34] on two-dimensional nozzles, with M_1 in the range 3 to $3{\cdot}4$ and $\gamma = 1{\cdot}4$. These results form a much better curve, giving values of λ between $14\frac{1}{2}$ and 13°, which agree quite well with those corresponding to the relation $M_2/M_1 = 0{\cdot}762$ at this γ.

Mager[27] uses his expression for P_2/P_1 {obtained by combining equations (2) and (3), with $K = 0{\cdot}55$} to correlate a variety of nozzle data including his own, but the form of presentation is insufficiently sensitive to give any true indication of its merits in the region where most data exist ($M_1 < 3{\cdot}5$). At higher Mach number, some few data* for low γ do indeed fall around Mager's computed curves for $\gamma = 1{\cdot}2$ and $1{\cdot}25$ and well away from that for $\gamma = 1{\cdot}4$, but it is not yet clear whether this deviation is caused by variation of γ or by the use of a faulty equation (*see* Section 2.1.2 and Fig. 3).

4.2. *Reynolds Number Change along a Nozzle.*

In experiments relating to separation in flow with initially zero pressure gradient, the local state of the boundary layer is usually represented by the Reynolds number based on distance from the leading edge of the surface. When considering a nozzle with finite pressure gradient and wall divergence, it is necessary to determine an 'equivalent flat-plate length'†. Stratford and Beavers[28] propose a method for calculating this length for axisymmetric flow with a turbulent boundary layer, which yields the following relation for $\gamma = 1{\cdot}4$

$$X = \left[\frac{1 + 0{\cdot}2M^2}{M}\right]^4 \frac{1}{y^{1{\cdot}25}} \int_0^x \left[\frac{M}{1 + 0{\cdot}2M^2}\right]^4 y^{1{\cdot}25}\, dx. \tag{16}$$

For two-dimensional flow with a turbulent boundary layer, the expression reduces to

$$X = \left[\frac{1 + 0{\cdot}2M^2}{M}\right]^4 \int_0^x \left[\frac{M}{1 + 0{\cdot}2M^2}\right]^4 dx. \tag{17}$$

---

* Produced by Elko and Stary, cited in Ref. 32, original not available.

† For definition see Appendix II.

Comparable relations for a laminar boundary layer are developed in Appendix III, giving for axisymmetric flow

$$X = \left[\frac{1 + 0{\cdot}2M^2}{M}\right]^4 \frac{1}{My^2} \int_0^x \left[\frac{M}{1 + 0{\cdot}2M^2}\right]^4 My^2 \, dx \tag{18}$$

and for two-dimensional flow

$$X = \left[\frac{1 + 0{\cdot}2M^2}{M}\right]^4 \frac{1}{M} \int_0^x \left[\frac{M}{1 + 0{\cdot}2M^2}\right]^4 M \, dx. \tag{19}$$

In each case the treatment assumes that $\gamma = 1{\cdot}4$.

It can be shown (e.g. Appendix IV of Ref. 51) that the effect upon conditions farther down a nozzle of ignoring the boundary-layer thickness at the throat is generally small. Consequently, it is assumed throughout this work that the throat boundary-layer thickness is zero.

Fig. 6 gives two examples of the variation of Reynolds number down the divergent part of a nozzle, based upon the equivalent flat-plate length as above (Re_X). For convenience the throat Reynolds number (Re^*) has been used as reference quantity, and the difference between laminar and turbulent boundary layers is shown.

5. *Nozzle Separation Data: Quiescent Air.*

The form of presentation adopted relates the overall separation pressure ratio P_1/P_b (denoted by k; *see* Figs. 4 and 5) to nozzle applied pressure ratio (A.P.R. = P_l/P_b). Knowledge of the complete pressure rise from station 1 to b is what a power-plant designer requires, and is all that the relatively crude instrumentation in general use permits to be measured. In comparing nozzle separation data in these terms with the results from other models, it must be remembered from Section 4 that no special allowance can at present be made for the pressure rise from station 2 to b occurring in a nozzle. With this limitation in mind, it may still be instructive to examine how values of the ratio P_1/P_2 obtained according to the expressions given in Section 2.1 agree with the quantity k as above. There is of course a direct connection between M_1 and P_l/P_1 (= A.P.R./k), while the assumption of $P_2 = P_b$ enables any relation in terms of M_1, M_2 or λ to be translated into one between k and A.P.R.

Figs. 7 to 10 show a collection of data obtained from nozzles with constant divergence half-angles in the range 10 to 30°, taken from Refs. 27 and 32 to 42. In most cases values of k are quoted directly, or pressure distributions are available from which to obtain it. Ref. 34, however, gives separation area ratios which have been converted to pressure ratios by means of isentropic relations for $\gamma = 1{\cdot}4$; any error so introduced should be well within the general spread of results.

One point which should be noted concerns the values of γ quoted for the data in Figs. 7 to 10, a number of which are around $1{\cdot}2$. These values relate to rocket-motor exhaust and are, so far as can be ascertained, for the initial condition at entry to the nozzle. Since the effect of γ is to receive some attention in the following pages, it could well be asked whether γ may not have risen much nearer to $1{\cdot}4$ during the expansion process preceding separation. This, however, seems not to be the case: a fairly typical example taken for the propellant mixture of Ref. 38 suggests that over an expansion pressure ratio of 1000 the relevant γ increases by less than 7 per cent†. One should therefore be justified in regarding the quoted values of γ as representative of the whole flow sequence of expansion and subsequent shock compression occurring in the nozzle.

† The authors are indebted to the Rocket Propulsion Establishment, Westcott, for this information.

A certain amount of the rather wide scatter appearing in Figs. 7 to 10 is no doubt caused by failure to account properly for the pressure rise occurring in the mixing region downstream of the interaction (*see* Section 5.2). Pressure distributions published by many authors show some variation in the extent of this rise, which might depend upon divergence angle and length of mixing region, i.e. upon area ratio or design pressure ratio. With this exception, no dependence on nozzle D.P.R. would be expected, as may be realised by considering Fig. 5. With a turbulent boundary layer the initial pressure rise is steep, and were it not for the subsequent 'recovery' an idealised pressure pattern would be a vertical line at separation, followed by a horizontal line continuing to outlet. With such a model a change in D.P.R. only affects the extent of the horizontal line, so that the pressure P_1 and hence k can be seen to depend only on A.P.R.

Among the experimental scatter no significant influence can be found of any of the following properties:

(i) Nozzle D.P.R.

(ii) Wall divergence in the range 10 to 30° half-angle.

(iii) Axisymmetric or two-dimensional form (Fig. 7).

(iv) γ in the range 1·2 to 1·4 (Figs. 7 and 10, noting that solid symbols are used to denote values of γ near 1·2).

Comments made above cover the first of these observations. The third is also not remarkable, since boundary-layer separation can be regarded as locally two-dimensional, whatever the geometry of the surface as a whole. A similar correspondence was noted in Section 2 between the behaviour of two-dimensional and axially-symmetric versions of other separation models. It is the fourth point that may excite some surprise, calling for further attention.

The surprise is largely occasioned because we have been conditioned by the form of the various separation criteria given in Section 2.1.1* to expect a dependence on γ. Upon reflection, the absence of any distinguishable effect amongst the data does not in itself seem incredible. So far as the boundary layer can be considered incompressible, there will be no influence of γ on separation; this can only arise through the transformation necessary to take account of compressibility, and it is unlikely that we need look for the effect to be large in magnitude. That none apparently exists is a fact which reflects mostly upon the validity of the criteria.

Three of the more satisfactory relations (Section 2.1.2) have been used, namely:

(i) Equation (1) with $K = 0{\cdot}67$
(ii) Equation (7) with $J = 0{\cdot}56$
} in conjunction with equation (12)

(iii) $M_2/M_1 = 0{\cdot}762$.

As can be seen from Figs. 7 and 8, any of these relations with $\gamma = 1{\cdot}4$ adequately fit the mass of data, suggesting that the pressure rise at separation in overexpanded nozzles of uniform divergence generally follows that in other models up to station 2. In order to show the agreement more clearly, the data for $\gamma \simeq 1{\cdot}2$, which exhibit much the worst scatter (Fig. 10), have been omitted from Fig. 8. Also shown on Figs. 7 and 8 is the curve of $\lambda = 13\frac{1}{2}°$ as suggested in Ref. 24; this is not a satisfactory fit at values of A.P.R. below 4 or above 60.

---

* *See also* Section 4.1.

Another line on Fig. 7 relates to the limiting condition of a normal shock reached when separation occurs close to the nozzle throat (*see* Section 3). Intersection of this line with the group of three other curves occurs around $M_1 = 1 \cdot 16$.

Fig. 9 shows just those data for which $\gamma \simeq 1 \cdot 2$ taken from Fig. 10, together with the same three relations as above for the value $\gamma = 1 \cdot 2$. There is now a much wider spread between the three criteria themselves than was the case with $\gamma = 1 \cdot 4$, and little pretence at agreement with the data. One has therefore to conclude that none of the foregoing relations for a turbulent boundary layer may permissibly be used with γ other than $1 \cdot 4$.

In some analytical treatments—for example that of Ref. 15 giving constant Mach number ratio—the quantity γ does not explicitly appear, and there is no reason to associate the validity of this form of criterion with particular values of γ. However, the empirical constant chosen to give agreement with experimental data could very well vary with γ. There is certainly no justification for taking the constant $0 \cdot 762$ in the above example as applying beyond the condition of $\gamma = 1 \cdot 4$ for which it was derived; likewise the constants K and J in equations (1), (7) and (8) could and evidently should depend on γ.

Note was made in Section 4.1 of a single experimental value obtained with helium for which $\gamma = 1 \cdot 667$, that was shown by Love[9] to support closely the relation $M_2/M_1 = 0 \cdot 762$. This point is included on Fig. 7, and appears very near to other data for $\gamma = 1 \cdot 23$ and $1 \cdot 4$ on the fringe of the scatter. It seems then that the agreement in Ref. 9 is fortuitous.

On the evidence of Figs. 7 and 10, we may conclude fairly definitely that this form of pressure-rise characteristic is independent of γ in the case of a turbulent boundary layer.

It is worth observing that the relations given for laminar separation also contain an effect of γ. Somewhat curiously, the trend is opposite in sense to that noted above for a turbulent boundary layer. Expressions of the form of equations (1) and (7) for turbulent separation give, as we have seen, values of k diminishing with reduction of γ; but, for a given value of Re_X, the type of equation (14) for laminar separation produces an increase in k with reduction of γ. In this case constants can be derived analytically[10, 19] which fairly well agree with the data for $\gamma = 1 \cdot 4$ (Section 2.1.3), and there is no obvious reason why they should be invalid for any other condition. Unfortunately there are no known data for laminar separation at values of γ other than $1 \cdot 4$, so the matter cannot be resolved; but on present evidence there is a likelihood that the pressure rise occurring with laminar separation, unlike that with turbulent, may vary with γ.

5.1. *The 'Kink Point'.*

The condition at which an oblique shock moves from the lip inside the nozzle is traditionally known as the 'kink point'.

It should of course be appreciated that, even when the shock is nominally still at the lip, some compression will feed up the boundary layer, raising the wall pressure immediately ahead of the outlet. As the shock strengthens, this zone of compression or 'foot' of the shock will spread farther inside the nozzle, until eventually the boundary layer just starts to separate at outlet; at this condition only the pressure rise from 1 to s will be experienced on the wall. Further change of nozzle pressure ratio will bring the shock wholly inside the nozzle, with the full pressure rise from 1 to 2.

Since this process occurs gradually, there is in reality no single 'point' which defines the difference between a nozzle running full and one with internal separation. However, as a general guide to the onset of separation, it is convenient to take the condition where the full pressure rise 1 to 2 is first

achieved. This we shall treat as being the 'kink point'. It occurs at a value of A.P.R. equal to $k \times$ nozzle D.P.R.; and at this condition the assumption $P_2 = P_b$ is obviously correct, since there is no 'mixing region' in which pressure recovery can take place. The relation between kink-point pressure ratio and nozzle D.P.R. for turbulent flow may thus be obtained from any of the three satisfactory criteria given in Fig. 8. This is presented in Fig. 11.

5.2. *Comments.*

Data collected in Figs. 7 to 10 are for nozzles with constant divergence half-angles between 10 and 30°, and suggest a negligible influence of wall angle over this range. Although one of the sources[35] claims to find some effect, it seems small enough to be lost amongst the general scatter. Arens and Spiegler[44] tested nozzles with 7, 15 and 22° divergence, and found no trend. Their work covered both two-dimensional and axisymmetric nozzles, and confirms that the separation behaviour is similar in both cases.

Divergence angles outside the above range have not received wide attention, no doubt because they would have little practical utility. Some few data are available[36, 45, 46], and the observed effects are discussed in Section 7. Also omitted from Figs. 7 to 10 are the quite numerous data[27, 37, 40, 42, 43] existing on contoured nozzles, which will be reviewed briefly in Section 8.

It was noted in Section 2.2 that turbulent boundary-layer separation might be expected to show a dependence on Reynolds number according to $Re_X^{-1/10}$, but that the overall pressure rise from station 1 to 2 in other models has in fact frequently been observed to be independent of Re_X. None of the workers contributing to the literature on nozzle separation has been able to isolate any effect; and, if it exists, this is likely to be masked by the amount of scatter generally obtained. For all practical purposes, it can be taken that Re_X is a further variable by which the system is unaffected when turbulent.

5.2.1. *Separation close to nozzle outlet.*—There is, however, one influence of which several authors[39, 40, 42, 44] have found evidence. They have observed that when separation takes place near the outlet of a nozzle, the pressure rise can be markedly less (k higher) than when the shock is well inside, and that such data depart with some consistency from general correlations of the type presented here as Figs. 7 *et seq.* Sunley and Ferriman[39] were apparently the first to appreciate the significance of this behaviour, and on the evidence of their own results and those of Ahlberg *et al*[40] (area ratio 6 or above), conclude that separation within the last 20 to 30 per cent of nozzle area must be regarded as forming an exception to normal behaviour. As a general rule, however, this statement cannot be accepted; abundant evidence exists that nozzles of smaller area ratio still behave quite normally when separation is taking place very much closer to the outlet.

Limiting ourselves to the case where no significant amount of pressure recovery occurs in the mixing region downstream of station 2, it is worth considering further what effect on k can be expected as the shock reaches the end of a nozzle. So long as the separation sequence up to station 2 is able to develop within the nozzle walls (fully-developed separation), so the system as a whole should conform to the usual pattern as given by Fig. 3—that is, up to what we have agreed to call the 'kink point'. But, as we have seen in Section 5.1, once station 1 moves nearer the outlet than the distance normally existing between 1 and 2, then the internal pressure rise must be reduced. After station s reaches the outlet, the boundary layer no longer separates at all, although some pressure rise will still be experienced immediately inside the walls. At any of these conditions outside the

range of fully-developed separation, a value of $k < 1$ should be detectable if wall pressure measurements are made sufficiently near the outlet. Thus a gradual rise in k away from the conventional level will occur with increase of A.P.R. beyond the kink point.

It remains to see what is the order of distance between stations 1 and 2 (the interaction length), and what proportion this may represent of nozzle area. Interaction length is likely to be related to boundary-layer thickness, and as an approximate and rather arbitrary estimate we will take 6 thicknesses†. Calculations for a turbulent boundary layer at $Re^* = 4$ million and $\gamma = 1{\cdot}4$ then show that departure from normal behaviour may be expected when the point of incipient separation (or incipient point: i.e. station 1) is nearer outlet than the following values of percentage nozzle area:

Nozzle area ratio	Percentage area from outlet
2	$4\frac{1}{2}$
5	$8\frac{1}{2}$
10	$11\frac{1}{2}$
25	17

The answer is dependent upon but not very sensitive to nozzle divergence angle, and these results are valid for half-angles around 10 to 15°. If the boundary-layer thickness δ be treated as effectively independent of γ, as it is of M_1, then at a given value of Re^* the interaction length is by assumption a function only of equivalent flat-plate length (X) and the ratio Re_X/Re^*. Alternative evaluation for $\gamma = 1{\cdot}2$, with the same Re^* as above, produces figures of percentage area which are somewhat smaller than those for $\gamma = 1{\cdot}4$.

One further piece of quantitative information may be added before returning to the data, and that concerns the value which k should reach at the limiting condition for separation of the boundary layer, when station s is at outlet. The pressure rise from 1 to s is known, and at this condition $k = P_1/P_s$. An appropriate curve is included on Fig. 10.

Of the sources cited above in connection with the effect of a shock near outlet, Arens and Spiegler[44] offer no data. Farley and Campbell[42] tested a conical nozzle of 15° half-angle and area ratio 25, containing four pressure tappings within the last 14 per cent of area, and values of k were recorded reaching about 17 per cent above normal at A.P.R. = 142. The last point is off the scale of Fig. 10, but the same nozzle can be seen to have behaved quite normally at A.P.R. = 119. Unfortunately the relevant pressure distributions are not published, but this result is quite in line with our estimates of where fully developed separation may be expected to cease. Some pressure distributions given by the same authors for contoured nozzles tend to support this explanation.

Ahlberg *et al*[40] also quote some abnormal results. These data, omitted from Figs. 7 and 8, are included in Fig. 10. Regrettably, no pressure distributions are available, nor any information as to the position of pressure tappings. All that one can say from Fig. 10 is that their three conical nozzles all show the same sort of trend, that in the case of the two higher area ratios the magnitude of the effect is well within expectation, and that only for the smallest nozzle could any doubts be raised as to the adequacy of the previous explanation. The data point at highest A.P.R. (= 29) would seem

† Assumed to be independent of Mach number M_1 and γ.

to suggest that the boundary layer was just not separating internally, implying measurement of an incipient point within perhaps the last 4 per cent of area. Only the missing pressure distribution could confirm or deny this.

Lastly we come to the data of Sunley and Ferriman[39]. While most of their results (included in our Figs. 7, 9 and 10) follow the conventional pattern, these authors show in their Fig. 10 a series of five points relating to their nozzle 'B' (area ratio 13·7 and half-angle 17°) which suggests another pronounced departure from normal behaviour. Although the trend which they illustrate is apparently the same as that shown by the data of Ahlberg *et al*[40] noted above, there is reason to think that the magnitude of the effect may in this case have been overestimated.

The process applied to their data by Sunley and Ferriman[39] was somewhat involved, and their quoted values of k were not taken directly from experimental readings*. Instead they plotted the ratio wall pressure/outlet pressure at each individual measuring station against A.P.R., and in each case estimated the value of A.P.R. at which separation was incipient at that station. From the station area ratio, they then obtained a 'derived' value of P_1/P_t by means of one-dimensional flow relations assuming $\gamma = 1{\cdot}2$, and such values were used in place of an experimental running-full line in arriving at the quantity k. Unfortunately, for separation approaching the nozzle outlet, the values of k given by this method are critically dependent on the accuracy of the running-full line chosen. An attempt by the present authors to estimate a running-full line, from experimental evidence contained in the same paper[39], suggests values of k in the 5 instances in question which are below those given by Sunley and Ferriman. For this reason these crucial points have been omitted from our Fig. 10.

To sum up, values of pressure rise from station 1 to 2 occurring in other models with turbulent boundary-layer separation agree quite well with a great many of the data for the overall pressure rise in overexpanded nozzles of uniform divergence in which separation is fully developed. A recognisable and to some extent predictable effect comes into play once the point of incipient separation moves close to the nozzle outlet, the critical distance varying with nozzle area ratio and divergence angle. When separation occurs well inside a nozzle, the pressure rise through the interaction is followed by a further gradual increase of pressure downstream—the so-called pressure recovery. This is at present a largely unknown quantity, tending to confuse the picture, and preventing any more definite or precise association between local separation effects in nozzles and those in other models. But it can be taken as fairly certain that the rise 1 to s is the same throughout in accordance with its status as a free interaction, while the evidence available suggests that approximate similarity of the additional rise from s to 2 also extends to the case of nozzles.

6. *Separation with External Flow.*

Some recent work has been done with nozzles immersed in external flow. This would not be expected to produce any change in separation characteristics when correlated in terms of nozzle base pressure, but behaviour has in fact been observed dissimilar from the 'conventional' so far discussed. Very much higher values of k were obtained than those shown in Figs. 7 to 10, and these data are termed 'unconventional'. Such nozzles ceased to run full at values of applied pressure ratio considerably greater than those given in Fig. 11, and in fact not far below the design point.

* H. L. G. Sunley. Private communication, 1963. Comments by the authors in Ref. 39 hint at some difficulties in their accuracy of measurement.

Musial and Ward[48] tested two conical convergent-divergent nozzles of area ratios 6 and 9, in each case with and without supersonic external flow. The quiescent-air separation results are conventional, but those obtained in the presence of external flow are not. For the area ratio 9 nozzle in an external stream, k has values of 0·85 and 0·875 for applied pressure ratio respectively 7 and 11·1, as shown in Fig. 12.

Reid and Hastings[49] examined the behaviour of a profiled convergent-divergent nozzle of area ratio 1·67, surrounded by a cylindrical afterbody, both in quiescent air and with supersonic external flow. Once again, the patterns of separation in the presence of an external stream are unconventional, but this time so also are those in quiescent air. In both cases the values of k are, as shown in Fig. 12, appreciably higher than usual for the same A.P.R., and the 'kink point' occurs at A.P.R. about 6·9 for a design pressure ratio of 7·6. For this nozzle, separation at lower A.P.R. is accompanied by a considerable amount of downstream pressure recovery, and a reduced level of k.

An examination of the boundary layer was carried out by Reid and Hastings[49] at a throat Reynolds number of 1·26 million, where it was found to be turbulent. However, their nozzle separation data were obtained with values of throat Reynolds number in the range 0·14 to 0·46 million.

Tests of a conical convergent-divergent nozzle of area ratio 2·9 in a supersonic stream have been carried out recently at the National Gas Turbine Establishment[50]. Some pressure distributions down the nozzle are reproduced in Fig. 13 for external Mach numbers 1·3 and 1·5. Values of k corresponding to these curves appear in Fig. 12, lying within the range 0·48 to 0·92. The 'kink point' pressure ratio is around 16 compared with a design pressure ratio of 20.

The same nozzle was also tested[50] in subsonic external flow and in quiescent air. Typical pressure distributions are reproduced in Figs. 14 and 15, while the values of k are included in Fig. 12. In both cases the separation is perfectly conventional, with a range of k between 0·38 and 0·56, and 'kink point' pressure ratios around 8·5 and 9·0. These latter values are in good agreement with the curve of Fig. 11.

Some further evidence comes from other recent work at N.G.T.E. on a quiescent-air thrust rig[51], where all of a family of conical convergent-divergent nozzles were found to exhibit somewhat unusual thrust characteristics. Fig. 16 shows the pressure distributions taken from Ref. 51 for a nozzle with internal shape exactly the same as that just described from Ref. 50. Corresponding values of k are given in Fig. 12, and it can be seen that the 'kink point' occurs around A.P.R 17 (D.P.R. = 20).

This particular nozzle had previously been tested on another quiescent-air rig using air close to saturation[33], where it yielded conventional values of k, included amongst the data of Figs. 7, 8 and 10.

It is instructive to compare Figs. 13 to 16 for exactly similar nozzle geometry and different operating conditions. There is a marked difference in character between the separation patterns corresponding to the conventional and unconventional cases, and this does not correlate with the presence of external flow. In two of the instances cited above, the unconventional pattern is observed in quiescent air, while conventional behaviour can be obtained with a subsonic external stream.

Some further evidence is offered by Meleney and Kuhns[47], who tested three 15° conical nozzles in quiescent air. Original pressure distributions are not published, but the large number of data presented by these authors fall into two categories: the first is entirely conventional, and these data agree well with the general pattern depicted on Fig. 7; the second exhibits generally higher values of k, which are in the range occupied by the unconventional results in Fig. 12. All three nozzles,

which had the same throat diameter, demonstrated both sorts of behaviour, occurrence of the unconventional correlating very well with nozzle supply pressure and not at all with nozzle area ratio.

6.1. *Laminar or Turbulent?*

Figs. 12, 13 and 16 suggest very strongly that the explanation of this anomaly lies in the state of the nozzle boundary layer. The unconventional results show a rise of pressure in the immediate vicinity of separation which in most cases is small enough to be convincingly laminar, and many of the values of k lie within the band which would be predicted by equation (15) for laminar separation.

Let us go on to consider the level of Reynolds number. Figs. 18 and 19, from which data for values of A.P.R. below 3 have been omitted, show fairly clear division between conventional data and unconventional in terms of both Re_X and Re^*. The former Reynolds number is plotted assuming a turbulent boundary layer throughout (Fig. 18), but computations have also been carried out on the alternative assumption of a laminar boundary layer for all the unconventional data. It is found that the values of Re_X are between 15 and 30 per cent lower in the laminar case, as might be expected from Fig. 6. Taking all the data shown on Fig. 12, which includes values of A.P.R. < 3, they can be divided into groups as follows:

Conventional:	Re^*	1·47 to 3·96 million
	Re_X	0·69 to 3·05 million
Unconventional:	Re^*	0·14 to 0·85 million
	Re_X	0·021 to 0·49 million if laminar 0·023 to 0·69 million if turbulent.

Table 1 gives the throat Reynolds number for most of the data used in Figs. 7 to 10, and these are in the range 1·03 to 25·6 million.

An unmistakable correlation seems to emerge, implying that a critical value of Reynolds number exists around

$$Re_X = 0{\cdot}7 \text{ million}\dagger$$

at which the boundary layer is normally in a state of transition. A corresponding figure for critical throat Reynolds number could be suggested from Fig. 19 to be

$$Re^* \simeq 1{\cdot}0 \text{ million},$$

which should constitute a useful guide to separation behaviour, so long as it be remembered that the throat Reynolds numbers given in Fig. 19 are restricted to nozzles with wall semi-angles in the range 10 to 15°‡. Where nozzles are considered with higher or lower wall angles, this value of throat Reynolds number may not be a satisfactory criterion of performance (*see* Section 7).

Corroborative evidence for this explanation comes from other test results quoted in Ref. 51. The nozzle which had produced unconventional separation patterns (Fig. 16) in quiescent air, was

† This value is given on the assumption that the boundary layer is always treated as turbulent, which is the most convenient course to adopt.

‡ 1. Fig. 6 showed, for 10° and 15° conical nozzles, that the throat Reynolds number is of the same order as the general level of length Reynolds number down the later portion of nozzle divergence.

2. A typical aircraft designed to cruise around Mach number 2 to 3 can be expected to have values of nozzle Re^* between 3 and 8 million throughout its flight path. Thus, unfortunately from the point of view of thrust performance, any internal separation taking place should conform to the conventional turbulent pattern.

tested on the same rig with the same inlet conditions, but with the addition of artificial surface roughening ahead of the throat. This was done by means of a $\frac{1}{2}$ in. wide band of grade 150 carborundum powder spread thinly on a paint base to make it adhere to the nozzle surface, and positioned so that the downstream edge of the band was $\frac{1}{2}$ in. from the plane of the 2 in. diameter throat. The aim was to ensure a turbulent boundary layer entering the throat, the method being based upon the work of Cook[52]. With this roughening, separation behaviour was found to have become conventional, so supporting the contention that the different types of data are attributable to boundary-layer condition. Fig. 17 gives pressure distributions down the roughened nozzle reproduced from Ref. 51, and values of k will be found in Fig. 12.

Two points require to be noted in connection with the critical values of Reynolds number given above. In the first place, there is no certainty that they are independent of incipient Mach number M_1. Chapman *et al*[1] observed that the Reynolds number determining occurrence of their transitional flow regime, that is to say the limiting Reynolds number for laminar re-attachment, increased with M_1; but they also present curves indicating that no clear dependence exists in the case of transition of an attached boundary layer on a flat plate, at least up to $M_1 \simeq 3 \cdot 5$. In nozzles we are not concerned with re-attachment, nor with transition downstream of separation except in so far as it may affect pressure recovery in the mixing region. This observation, namely that transition is substantially independent of Mach number, seems to be commonly agreed except at high Mach number (around 5), where the critical Reynolds number is known to increase.

In any particular nozzle, Re_X is directly related to M_1 throughout its length. The ranges of M_1 covered by the data shown in Figs. 18 and 19 are from $1 \cdot 8$ to $2 \cdot 9$ for the conventional, and from $1 \cdot 7$ to $2 \cdot 5$ for the unconventional data. For the range of M_1 of current interest for nozzle separation, it seems safe to assume that no dependence of the critical Reynolds number on M_1 need be considered.

Secondly, all the data contributing to Figs. 18 and 19 are for $\gamma = 1 \cdot 4$. In view of the conclusion just given regarding effects of Mach number, it can be reckoned improbable that transition is affected by γ within the same range of M_1.

If it be accepted that the differences in behaviour appearing on Fig. 12 can be explained by boundary-layer condition, then all the data shown there can be classified according to Reynolds number. Those data with values of Reynolds number below the critical given above may correspond to a state of transition in which clear trends with other variables are not discernible. Above the critical value, however, all can be taken as turbulent, and as a number of these data occur at low A.P.R., it is of interest to see how they would fill in that somewhat sparsely covered region in Fig. 7. A new plot, Fig. 20, includes additional turbulent data from two sources—those from Fig. 12 and various unpublished N.G.T.E. data for three nozzles in subsonic external flow.

Rather wide scatter is apparent in the lowest range of A.P.R. This is perhaps to be expected, since separation is then occurring quite near the throat, with a mixing region of large extent offering the greatest possible opportunity for pressure recovery downstream of the interaction. Neglect of this effect is therefore most significant at very low A.P.R., especially for nozzles of small divergence angle. With this exception, the spread of data straddles the curve for other separation models.

7. *Effect of Divergence Angle.*

It was observed in Section 5.2 that uniform wall divergence had no apparent effect on nozzle separation within the range 7 to 30° semi-angle. This is in line with the assumption that pressure

gradients in the approach flow may be neglected; so long as that remains true, wall angle (provided it is uniform) cannot affect conditions within the interaction, but could still have an influence in the subsequent mixing region. We may now look at Fig. 21, showing the behaviour of conical nozzles with divergence angles outside the above range.

In general it will be seen that data for angles greater than 30° have very high values of k, while those for angles less than 7° lie either at or below the conventional level.

Let us consider first the wide angle (45°) nozzle of Kuhns[46]. Published pressure distributions for this nozzle reveal separation patterns which we have now come to associate with a laminar boundary layer. Values of separation Reynolds number, Re_X, are in all cases less than 0·5 million, and comparison with Figs. 12 and 18 shows that no further explanation need be sought for the high level of k. But it is worth noting that, according to the critical value of throat Reynolds number suggested in Section 6·1 for nozzles of half-angle 10 to 15°, the boundary layer should be turbulent. Not only does increased divergence angle cause a given wall pressure to be achieved in shorter length (smaller Re_X), but in this particular nozzle of Kuhns the effect is much augmented by use of a small radius of curvature at the throat. Very rapid expansion in the neighbourhood of the throat brings the wall pressure far below the one-dimensional isentropic curve, and the Re_X corresponding to a given pressure is further lowered. For such nozzles a critical value of $Re^* = 1{\cdot}0$ million is evidently inappropriate.

It is extremely probable that similar circumstances exist in the case of the 33° nozzle of Scheller and Bierlein[45], although these authors unfortunately omit the relevant pressure distributions. But once again $Re^* > 1{\cdot}0$ million.

Turning now from high wall angles to low, the work of Kuhns[46] is again of primary interest. He tested a 5° nozzle, and observed some unusual effects reproduced in Fig. 22. Up to A.P.R. 8·5, the values of k are well below the conventional (Fig. 21); however, below A.P.R. 4·6 the separation appears to be typically laminar, a condition confirmed by values of separation Reynolds number from 0·23 to 0·71 million (computed as for a turbulent boundary layer). This low level of k is in fact the result of unusually high pressure recovery occurring steadily all the way down the nozzle beyond the interaction region (Fig. 22). By A.P.R. 5·2, the separation Reynolds number of 1·26 million implies that the boundary layer has become turbulent, and the shape of the pressure curve tends to confirm this (Fig. 22); appreciably more recovery still occurs after the interaction than is usual in nozzles of wider angle. It should be noted that the throat Reynolds number criterion again breaks down, this time in the opposite sense, for at A.P.R. 5·2 it has the value 0·74 million which incorrectly suggests a laminar boundary layer. Above this A.P.R., the amount of pressure recovery decreases, and at A.P.R. 9·8 the value of k agrees with the general level of data for turbulent separation.

Even lower values of k occur in the 5° nozzle of Scheller and Bierlein[45] (Fig. 21), and one of their illustrations shows that in one such case a turbulent boundary layer is again followed by high downstream recovery. In the same illustration, the pressure distribution closely follows the one-dimensional isentropic curve up to separation, and on this basis values of Re_X have been obtained for the group of data. These cover the range 1·64 to 28·6 million, confirming the presence of a turbulent boundary layer. Corresponding values of Re^* are 0·91 to 8·27 million.

From the foregoing observations relating to nozzles of wall angle above 30° or less than 7°, it is apparent that all departures from the conventional level of k are attributable to one or other of two factors: first, a laminar boundary layer; or second, exceptional pressure recovery. The latter arises

chiefly in very low angle nozzles with laminar separation. No data are available for nozzles with angle greater than 30° and a turbulent boundary layer, but there is no evidence amongst the known data of any effect of uniform divergence angle on the interaction itself. This rather negative conclusion upholds the assumption that pressure gradient in the approach flow is not an important factor.

The circumstance noted above, namely that laminar separation at low A.P.R. in 5° nozzles is accompanied by unusually high pressure recovery in the mixing region, excites interest in the effect of wall angle. Figs. 13, 16 and 23* all give pressure distributions for laminar separation in 10° nozzles, while Figs. 14, 15 and 17 show corresponding turbulent patterns. Comparison of these two groups suggests that, other things being equal, rather more recovery generally takes place after laminar separation than after turbulent, although the amount is always markedly less than was observed in a 5° nozzle.

7.1. *The Mixing Region.*

In sum, the features just discussed prompt the idea that the amount of recovery is associated with what may be called the effective angle of the mixing region—that is, the angle between the separated jet boundary and the wall, as shown diagrammatically in Fig. 4. The problem is to obtain the jet boundary. This may readily be done for the case of an inviscid free jet, regarded as discharging into a region of constant pressure—a situation which corresponds only to the case of zero pressure recovery after the interaction. The jet boundary is then at constant Mach number. For a given wall pressure distribution, implying a varying Mach number along the edge of the jet, the inviscid boundary could of course be constructed; but in the general case it is this wall pressure distribution which is sought. A further complication is introduced by the shear effects which are responsible for spreading of the jet boundary, and the uncertainty as to the nature of this shear layer. If the boundary layer is turbulent before separation, then one can confidently treat the shear layer as turbulent; but an initially laminar flow boundary could undergo transition as a result of separation (for example, cases of laminar separation followed by turbulent re-attachment are quoted in Ref. 1), so that in any particular case the shear layer could be either laminar or turbulent.

However, despite these acknowledged and severe limitations, it is quite instructive to examine some free jet boundaries. Figs. 24 and 25 show inviscid boundaries constructed by the method of Ref. 53 for axisymmetric nozzles, covering the following cases:

- Wall angle (α): 5 to 15°
- Mach number (M_1): 1·5 to 2·5
- Values of P_1/P_2 typical of laminar and turbulent separation.

The turbulent separation plots of Fig. 25 should be fairly realistic, since the jet boundary is always well away from the wall, and the assumption of a constant-pressure mixing region is not violently in error. On the other hand, Fig. 24, for laminar separation, should obviously be modified in accordance with the pressure rise known to be taking place in the mixing region; the effect of this will be to shift the inviscid boundary progressively farther inwards away from the wall. If a particular pressure distribution be assumed, the inviscid boundary changes as shown in Fig. 26.

* In the case of Fig. 23, this excludes the three highest values of A.P.R.

It can be seen that the shift is not great in extent, despite the considerable pressure gradient assumed. The effect is not, therefore, such as to upset the contrast which is apparent between Figs. 24 and 25, nor to alter the general trends displayed. These indicate that the effective angle of the mixing region referred to above is influenced by both wall angle and initial boundary-layer state; it will be reduced either by shallow nozzle divergence or by the smaller flow deflection angle occurring at separation with a laminar boundary layer. A combination of low wall angle and laminar separation will produce the smallest effective angle, as it does the highest pressure recovery. This may be thought of as somewhat analogous to the case of a wind-tunnel diffuser, where a small angle gives a high pressure recovery, and a wide angle means a completely detached jet with large reverse-flow region and little pressure rise.

Superimposed on the inviscid free jet boundaries in Figs. 24 and 25 are shown regions of jet spreading, again as for constant pressure discharge, and assuming a turbulent shear layer in all cases. Variation of the jet spreading factor with Mach number has been taken from the work of Korst and Tripp[54], and the shaded regions correspond to an error-function velocity profile between the limits 1 and 99 per cent of the inviscid jet velocity.

As already observed, in Fig. 24 the inviscid jet boundaries are much closer to the wall than in Fig. 25, and the wall is seen to interfere with the 'free' spreading in every example of laminar separation shown. While there is no pretence at this picture being quantitatively realistic, it serves to illustrate how turbulent jet spreading augments the influences of wall angle and initial boundary-layer state on the feature of most significance—the angle of the reverse-flow region. The conclusion to emerge qualitatively is that those factors which would reduce the angle of the reverse-flow region also tend in practice to give high recovery.

One may note that, were the shear layer to remain laminar after separation, the subsequent amount of spreading shown in Fig. 24 would be greatly reduced. This would of course result in less interference by the wall and a wider angle of the reverse-flow region. In such a case, high pressure recovery would no longer be expected. This situation seems most likely to arise with a combination of low Reynolds number and high Mach number.

Within the mixing region exists a system of low-velocity flow recirculation intermingling with the spreading jet (as indicated in Fig. 4), and we may distinguish two regimes:

(i) 'Free mixing', where the flow boundary is allowed to spread freely without interference by the wall. A reverse-flow region of wide angle allows easy recirculation of air for entrainment at the jet boundary, and effectively constant pressure is maintained.

(ii) 'Confined mixing', where the wall interferes with the spreading flow boundary. Here a narrow-angle reverse-flow region means that a longitudinal pressure gradient is required, in order to sustain the passage of sufficient reverse flow adjacent to the wall to feed the entrainment process at the jet boundary.

Two points may then be noted for the case of confined mixing. First, the total amount of the pressure rise will depend markedly on the length of mixing region available. Secondly, as will be observed from Fig. 24, the angle of the reverse-flow region varies with distance, being least immediately after separation, and greatest near the nozzle outlet. This implies that the rate of pressure rise will diminish with distance from separation. Reference to, for instance, Figs. 16, 22 and 23 confirms both these points.

Some rather interesting data have become available from recent unpublished tests at N.G.T.E. These are shown in Fig. 27. Three conical nozzles of design pressure ratios 3·75, 8 and 20 (area

ratios 1·19, 1·71 and 2·9), built up from the same throat section and having equal divergence angles, were run under conditions producing a laminar boundary layer. The 2·9 area ratio build had been used previously[51] to give the pressure distributions reproduced in Fig. 16. There seems to be more than a chance similarity between the three sets of curves in Fig. 27, suggesting that, so long as separation takes place at a given station, the subsequent pressure distribution in the mixing region is largely independent of where the nozzle walls may be ended. These results tend to support the idea that local geometry—that is, the local angle of the reverse-flow region—governs the pressure gradient at any position along a nozzle.

7.2. *Separation near the Throat of a Nozzle.*

A noteworthy feature of Fig. 27 is the steep pressure rise occurring shortly after separation when this takes place near the nozzle throat. In steepness this rise is comparable with many examples of turbulent separation.

Under conditions when, in the light of the foregoing analysis, the boundary layer should be laminar, previous data have yielded values of k at A.P.R. < 3 which on Fig. 12 are indistinguishable from the conventional turbulent level. Examples of such data occur in Figs. 13, 16 and 23 at the lowest values of A.P.R., and the behaviour of this same nozzle geometry is more clearly illustrated by the unbroken curves in Fig. 27. So steep an early pressure rise might prompt the thought that the boundary layer had in some fashion become turbulent at separation; and, indeed, a mechanism for producing transition during the interaction can be advanced.

This is based on observations reported by Haines, Holder and Pearcey[55, 56] relating to separation from the upper surface of an aerofoil. It was found that under certain conditions laminar separation can be followed by re-attachment to the surface as a turbulent layer, thereby enabling subsequent turbulent separation to occur with a high pressure rise. Such a situation is quoted as arising when the supersonic region at the leading edge is still small, causing the compression system from the laminar separation to be reflected from the sonic boundary, and producing an expansion which turns the separated layer back towards the wall. This brings about re-attachment and often transition as well, thus making possible almost immediate further turbulent separation with a large pressure rise. It is not impossible that an analogous situation could exist in the conical nozzles now considered. Expansion due to curvature on the surface around the throat produces a flow field in which the flow on the nozzle axis remains subsonic while that near the wall is supersonic[51], implying the existence of a sonic boundary as cited above for an aerofoil. If a similar sequence of events were to occur in the nozzle, then a steep pressure rise could be explained in terms of the final turbulent separation.

Certain features, however, detract from the probability of this explanation. In the first place, the sonic line in such a nozzle, although not confined to the geometric throat plane, is contained within a region closely adjacent, so making it most unlikely that any sonic boundary could exist far enough downstream to influence all stations where a steep pressure rise takes place (Fig. 27). Secondly, once separation moved beyond the neighbourhood of the sonic line, the reversion to normal laminar separation would be expected to appear as an abrupt change in the pattern of pressure distribution. This can be seen from Fig. 27 not to be the case; the decline in steepness near separation is quite gradual and steady as A.P.R. increases.

Furthermore, in any particular case where it occurs, the very steep rise is of short duration, thereafter blending smoothly into a curve of progressively diminishing steepness, along which the

later and less steep pressure rise is quite evidently attributable to processes within the mixing region. This later pressure rise is still considerable, and such recovery, as has already been observed, is not normally found after turbulent separation in a nozzle of this angle.

That the flow boundary is somehow and somewhere rendered turbulent, when the Reynolds number indicates an initially laminar boundary layer, is clear—otherwise it could not possibly support so steep a pressure rise. It is a question only of whether transition takes place before or after separation.

If, provisionally, we take it that the existence of a turbulent boundary layer at separation is precluded, then the onus of explanation for the steep pressure rise is thrown on the subsequent mixing region. The vigorous stirring and energy transfer taking place in the separated region make it quite likely for the processes of turbulent mixing to develop early. It may be conjectured that the separated shear layer remains laminar for a short distance, whereafter it becomes turbulent and able to support a steep pressure rise.

When separation occurs much farther from the nozzle throat, it seems quite possible from the evidence of Fig. 27 that the shear layer remains laminar throughout. This would imply a reduced intensity of mixing with increase of Mach number, which could conceivably be due to the fact that the ratio of external density to jet density decreases with rise in jet Mach number.

8. *Separation in Contoured Nozzles.*

Data on axisymmetric contoured nozzles may be found in Refs. 27, 37, 40, 42, 43, 49 and 51; of these sources we shall only concern ourselves with those wherein the data relate to turbulent boundary layers. As we have already seen (Section 6) the data of Reid and Hastings[49] are laminar. In the tests of Fradenburgh *et al*[43] the level of nozzle Reynolds number cannot be determined, but on the evidence of their pressure distributions many of these data are also laminar.

The nozzles of Eisenklam and Wilkie[37] were all of unusual shape; the wall angle increased continuously with distance from the throat, to form a trumpet-like profile quite different from the convex-concave shape of normal contoured nozzles.

Therefore only results from Refs. 27, 40, 42 and 51 are included in Figs. 30 and 31. All relate to the usual convex-concave form of contour save Ref. 51—in this case the nozzles were wholly concave or 'tulip' shaped with a sharp 16° corner at the throat. Although the value of Re^* in these tests was only 0·75 million, a turbulent boundary layer was assured by roughening the approach to the throat in the manner described in Section 6.1. The pressure distributions (reproduced as Figs. 28 and 29) were, however, very little different with or without this roughening, leading to the surmise[51] that transition could be produced by the abrupt discontinuity of wall angle at the throat in this design.

In Fig. 31 some of the data from Refs. 40 and 42 show an effect similar to that in Fig. 10. This type of behaviour was discussed in Section 5.2.1, and it seems most probable that the instances in Fig. 31 are attributable to the same situation—namely, insufficient length between the point of incipient separation and nozzle outlet for full development of the shock-boundary-layer interaction. Under these conditions the internal pressure rise is progressively reduced with increase of A.P.R. beyond the kink point.

The 'tulip' nozzle pressure distributions of Figs. 28 and 29 reveal some unusual effects, associated at least in part with the shape of wall in the vicinity of the throat. This sudden change of slope results locally in rapid two-dimensional supersonic expansion to a low level of wall pressure, and,

particularly in the nozzle of D.P.R. 10, the subsequent wall pressure in the absence of separation changes comparatively little. Apparently in consequence of this rather flat pressure distribution, a separation shock travels with unusual rapidity from one end of the nozzle to the other. When separation occurs near the throat, values of k are obtained in general agreement with those from other contoured nozzles (Figs. 30 and 31), except that k is here increasing with A.P.R.; after movement of the shock towards outlet (i.e. higher A.P.R.), the nozzle with D.P.R. 10 has still higher values of k, while that with D.P.R. 20 shows a sudden drop in level, rising again afterwards.

As the shock approaches closer to outlet in these nozzles, it is evident that the usual effect beyond the kink point is appearing*. In the case of the D.P.R. 20 nozzle, the last internal pressure tapping is less than one estimated boundary-layer thickness from outlet, where it can detect a very small pressure rise. It is almost certain that the results from this nozzle at A.P.R. 8·33 and 10·87 do not represent separation at all. At A.P.R. 3·98, the D.P.R. 10 nozzle is also experiencing less than the pressure rise for fully developed separation. These three points have been omitted from Figs. 30 and 31.

It has been said, from the evidence of previous sections, that nozzle wall angle and hence by inference longitudinal pressure gradient have no significant influence on the interaction and its accompanying pressure rise from 1 to 2. Were this all, a contoured nozzle should behave no differently to any other, subject to the same critical value of Re_X. However, it has also been noted that the amount of pressure rise taking place in the mixing region following the interaction is strongly influenced by nozzle wall angle when this is low; and the shallow local wall angles often found in contoured nozzles over much of the later part of their divergent length are comparable with those angles of nozzle in which this effect is most pronounced. One might therefore expect that any departure from the 'conventional' level of performance with a turbulent boundary layer will be in the direction of higher pressure recovery, and reduced values of k.

Examining Figs. 30 and 31, it can be seen that the data do in general lie quite appreciably below the range corresponding to nozzles with uniform divergence angles of 10° or above. Those from Ref. 42 are replotted in Fig. 32 so as to show the effect of mean wall angle; this is defined as the average of the wall angle at separation and that at outlet, which may in some measure characterise the mixing-region geometry. Values between 4 and 22° are encountered in these results. It is possible to discern some trend towards reduction of k at low mean wall angle, implying higher pressure recovery. But this by no means forms a complete or adequate explanation for the general level of results as compared with data for conical nozzles, and examination of the original pressure distributions[42] suggests that mixing-region geometry is not in fact the main cause of this difference; the pressure recovery is generally no greater there than for conical nozzles. Lower values of k in the contoured case seem to be associated with more pressure rise in the initial steep region than that which we are accustomed to seeing between 1 and 2.

In all the results appearing in Figs. 30 to 32, separation was taking place on the concave part of the nozzle profile. If an effect of curvature on shock-boundary-layer interaction be postulated at all, it would be natural to expect it in the direction of a boundary layer separating less readily on a wall of concave curvature (as here observed), and more readily on a convex one; this comes from

---

* A further example of behaviour beyond the kink point seems to occur in Fig. 17 at A.P.R. 9·69, where the incipient point is reckoned to be within the 6 boundary-layer thicknesses mentioned in Section 5.2.1. This data point was not included in Fig. 12.

considerations of geometry alone, independent of any further effect due to pressure gradients accompanying the curvature. Pearcey[57], in a comprehensive survey of associated work, cites instances where convex curvature was indeed found to reduce the pressure rise to the separation point in wholly laminar interactions, while in turbulent ones Bogdonoff and Kepler[4] refer to the effect of convex curvature as decreasing the peak pressure rise. But it is difficult to find any clear evidence in the literature relating to concave curvature.

In addition to any effect on the pressure rise to the separation point (1 to s), there is the further aspect that wall curvature could affect the growth of the separated region or bubble downstream, and hence the subsequent pressure rise from s to 2. In the same paper[4], Bogdonoff and Kepler suggest that in turbulent interactions the bubble width at station 2 bears some constant relation to initial boundary-layer thickness (provided that an incident shock is not too weak nor a forward-facing step too small). This, they go on to say, could mean that curvature of the wall after the separation point alters the length of the separated region between s and 2. For convex curvature, their argument is that, as the wall curves away from the separated flow boundary, the length required to achieve a given bubble width is reduced, and with it the amount of pressure rise. Similarly, this would imply increased length and pressure rise from s to 2 in the case of concave curvature. From the work of these authors, one can estimate the relevant bubble width at station 2 to be between $\frac{1}{2}$ and 1 boundary-layer thickness (except for small steps and weak shocks when it would be less).

It is worth noting here the order of curvature we are dealing with, also in terms of boundary-layer thickness. For the nozzles of Ref. 42, calculations suggest that typical figures for radius of curvature lie around 100 to 150 thicknesses. If a length of $4\delta_1$ be assumed between s and 2, then the corresponding amount by which the wall curves towards the separated layer is less than $0{\cdot}1\delta_1$. Comparing this with the order of bubble width noted above, it seems rather unlikely that so small a shift could be responsible for the whole of the observed effect. Were the difference restricted to the separated region, it would require that the pressure rise s to 2 increase by something like a factor of 2. A more probable conclusion, therefore, is that the pressure rise up to the separation point (1 to s) is also affected by curvature.

This is a feature of separation which calls for further study, with particular application to nozzles.

9. *Conclusions.*

(i) Various relations are available in the literature which are intended to describe the pressure rise occurring at shock-induced separation of laminar and turbulent boundary layers in two-dimensional supersonic flow with initially zero pressure gradient. These relations—some having semi-theoretical derivation and some being wholly empirical—have been compared with experimental data on systems such as forward-facing steps, compression corners and incident shocks. Any of the following expressions offer reasonably good accuracy over the range of Mach number 1·5 to 6 with a turbulent boundary layer:

for pressure rise to the separation point of any model,

$$\text{either (a)} \quad \frac{M_s}{M_1} = 0{\cdot}82 \text{ with } \gamma = 1{\cdot}4$$

$$\text{or} \quad \text{(b)} \quad \frac{P_s}{P_1} = \left\{ \frac{1 + 0{\cdot}2\, M_1^2}{1 + 0{\cdot}137\, M_1^2} \right\}^{3{\cdot}5}$$

and for pressure rise to the 'first peak' of forward-facing steps (with step height not less than $1\frac{1}{2}$ boundary-layer thicknesses),

$$\text{either (c)} \quad \frac{M_2}{M_1} = 0{\cdot}76 \text{ with } \gamma = 1{\cdot}4$$

$$\text{or} \quad \text{(d)} \quad \frac{P_2}{P_s} = 1{\cdot}05 + 0{\cdot}05\, M_1 \text{ in conjunction with either (a) or (b) above.}$$

(ii) Values of P_2/P_1 derived from these expressions have been compared with a variety of data for separation in overexpanded nozzles of uniform divergence. So long as the nozzle boundary layer is turbulent before separation, quite good agreement is obtained with the overall pressure ratio P_b/P_1, with two classes of exception. The first of these is divergence half-angles below 7°; the second is a shock system in close proximity to the nozzle outlet. For angles of 10° or greater, and shocks properly within the nozzle, there is no significant effect of angle, nozzle area ratio, geometry (i.e. two-dimensional or axisymmetric), or working fluid over the range of γ from 1·2 to 1·4. It appears from this correlation that the pressure gradient existing in a nozzle does not appreciably influence separation behaviour.

(iii) When the nozzle half-angle is 5° or less, departures are found from the general correlation, caused by increased pressure rise in the mixing region downstream of the interaction. This continuing rise of pressure, here termed recovery, is always present to some extent, but is not generally important in the case of a turbulent boundary layer for angles of 10° and above. When the angle is sufficiently small for pressure recovery to be significant, there is an influence of nozzle area ratio, since this governs the length of mixing region available.

(iv) As the point of incipient separation approaches nozzle outlet, a condition is reached when insufficient length remains to accommodate a fully-developed shock-boundary-layer interaction. Beyond this, the internal pressure rise will be progressively reduced, and the general correlation again ceases to apply. This critical distance is likely to increase with boundary-layer thickness, and in a nozzle of large area ratio it could represent a considerable proportion (over 15 per cent) of nozzle area.

(v) Certain other unconventional separation characteristics in nozzles of uniform divergence can be attributed to the existence of a laminar boundary layer, or of one in a state of transition. The critical value of separation Reynolds number appears to be around 0·7 million, based on equivalent flat-plate length, below which the boundary layer will not remain turbulent unless artificial means of promoting transition are employed. For conical nozzles with half-angles in the range 10 to 15°, a convenient general-purpose guide to separation behaviour is given by a critical value of throat Reynolds number around 1·0 million.

(vi) For Reynolds numbers below these critical values, the pressure rise in a nozzle can be greatly reduced, especially when separation takes place towards the outlet. However, the value of overall pressure ratio can in some circumstances reach the level normally observed with a turbulent boundary layer. This situation arises in nozzles of shallow divergence (half-angle 10° and below) with separation near the throat—i.e. a long mixing region—and is brought about by an exceptional measure of pressure recovery.

(vii) It is surmised that this process of recovery in a nozzle subsequent to the interaction is governed by what may be termed the angle of the reverse-flow region, that is, by the amount of

space available for upstream passage of the flow which the boundary of the separated jet is trying to entrain. The pressure gradient along the nozzle wall, which has been referred to as the recovery, must be that appropriate to the passage of this reverse flow adjacent to the wall. Low wall angle, and the smaller flow deflection angle through the weaker shock associated with laminar separation, both serve to narrow the angle of the reverse-flow region, and both in practice tend to promote higher pressure recovery.

(viii) Data from contoured nozzles, where separation occurs on surfaces with concave curvature, suggest that higher pressure rise is achieved within the shock-boundary-layer interaction than is the case with uniform divergence. This is a circumstance deserving further study.

Acknowledgements.

The authors wish to express their grateful thanks to Dr. B. S. Stratford for the valuable part taken by him in discussions during preparation of this paper. They are also much indebted to Mr. H. H. Pearcey of Aerodynamics Division, N.P.L., for the benefit of his advice in certain aspects of this work.

REFERENCES

No.	Author(s)	Title, etc.
1	D. R. Chapman, D. M. Kuehn and H. K. Larson.	Investigation of separated flows in supersonic and subsonic streams with emphasis on the effect of transition. N.A.C.A. Report 1356. 1958.
2	D. M. Kuehn	Experimental investigation of the pressure rise required for the incipient separation of turbulent boundary layers in two-dimensional supersonic flow. N.A.S.A. Memo 1–21–59A. February, 1959.
3	D. M. Kuehn	Turbulent boundary-layer separation induced by flares on cylinders at zero angle of attack. N.A.S.A. Tech. Report R–117. 1961.
4	S. M. Bogdonoff and C. E. Kepler	Separation of a supersonic turbulent boundary layer. *J. Ae. Sci.*, Vol. 22, No. 6, p.414. June, 1955.
	and	
	S. M. Bogdonoff	Some experimental studies of the separation of supersonic turbulent boundary layers. Paper V, proceedings of 1955 Heat Transfer and Fluid Mechanics Institute, held at University of California, Los Angeles. June, 1955.
5	H. Schuh	On determining turbulent boundary-layer separation in incompressible and compressible flow. *J. Ae. Sci.*, Vol. 22, No. 5, p.343. May, 1955.
6	C. du P. Donaldson and R. H. Lange.	Study of the pressure rise across shock waves required to separate laminar and turbulent boundary layers. N.A.C.A. Tech. Note 2770. September, 1952.
7	R. H. Lange	Present status of information relative to the prediction of shock-induced boundary-layer separation. N.A.C.A. Tech. Note 3065. February, 1954.
8	G. E. Gadd, D. W. Holder and J. D. Regan.	An experimental investigation of the interaction between shock waves and boundary layers. *Proc. Roy. Soc.* A, Vol. 226, p.227. 1954.
9	E. S. Love	On the effect of Reynolds number upon the peak pressure rise coefficient associated with the separation of a turbulent boundary layer in supersonic flow. *J. Ae. Sci.*, Vol. 22, No. 5, p.345. May, 1955.
	and	
	E. S. Love	Pressure rise associated with shock-induced boundary-layer separation. N.A.C.A. Tech. Note 3601. December, 1955.
10	R. J. Hakkinen, I. Greber, L. Trilling and S. S. Abarbanel.	The interaction of an oblique shock wave with a laminar boundary layer. N.A.S.A. Memo 2–18–59W. March, 1959.
11	J. R. Sterrett and J. C. Emery ..	Extension of boundary-layer-separation criteria to a Mach number of 6·5 by utilizing flat plates with forward-facing steps. N.A.S.A. Tech. Note D–618. December, 1960.

REFERENCES—*continued*

No.	*Author(s)*	*Title, etc.*
12	J. R. Sterrett and J. C. Emery ..	Experimental separation studies for two-dimensional wedges and curved surfaces at Mach numbers of 4·8 to 6·2. N.A.S.A. Tech. Note D–1014. February, 1962.
13	A. Mager	Prediction of shock-induced turbulent boundary-layer separation. *J. Ae. Sci.*, Vol. 22, No. 3, p.201. March, 1955.
14	A. Mager	On the model of the free, shock-separated, turbulent boundary layer. *J. Ae. Sci.*, Vol. 23, No. 2, p.181. February, 1956.
15	E. Reshotko and M. Tucker ..	Effect of a discontinuity on turbulent boundary-layer-thickness parameters with application to shock-induced separation. N.A.C.A. Tech. Note 3454. May, 1955.
16	J. Erdos and A. Pallone	Shock-boundary layer interaction and flow separation. Paper 17, proceedings of 1962 Heat Transfer and Fluid Mechanics Institute, held at University of Washington. June, 1962.
17	G. E. Gadd	Interactions between wholly laminar or wholly turbulent boundary-layers and shock waves strong enough to cause separation. *J. Ae. Sci.*, Vol. 20, No. 11, p.729. November, 1953.
18	D. W. Holder and G. E. Gadd ..	The interaction between shock waves and boundary layers and its relation to base pressure in supersonic flow. Paper 8 in 'Boundary layer effects in aerodynamics', proceedings of Symposium held at N.P.L. March/April, 1955.
19	G. E. Gadd	A theoretical investigation of laminar separation in supersonic flow. *J. Ae. Sci.*, Vol. 24, No. 10, p.759. October, 1957.
20	W. J. Guman	On the plateau and peak pressure of regions of pure laminar and fully turbulent separation in two-dimensional supersonic flow. *J. Ae. Sci.*, Vol. 26, No. 1, p.56. January, 1959.
21	J. C. Cooke	Separated supersonic flow. R.A.E. Tech. Note Aero. 2879. A.R.C. 24 935. March, 1963.
22	M. Arens and E. Spiegler ..	Shock-induced boundary layer separation in over-expanded conical exhaust nozzles. *A.I.A.A. Journal*, Vol. 1, No. 3, p.578. March, 1963.
23	M. Arens	The shock position in overexpanded nozzles. *J. R. Ae. Soc.*, Vol. 67, No. 628, p.268. April, 1963.
24	M. V. Herbert, E. T. Curran and J. B. McGarry.	Unpublished M.o.S. Report. June, 1958.
25	B. Le Fur	Etude des tuyères convergentes-divergentes de sortie avec écoulement externe supersonique. *Tech. Sci. Aero.* No. 4. 1958.
26	M. Summerfield, C. R. Foster and W. C. Swann.	Flow separation in over-expanded supersonic exhaust nozzles. *Journal A.R.S.*, p.319. September/October, 1954.

REFERENCES—*continued*

No.	*Author(s)*	*Title, etc.*
27	A. Mager *et al*	Final report of exit nozzle research under contract AF.04(645)22. Marquardt Corporation Report 5620. November, 1956.
28	B. S. Stratford and G. S. Beavers	The calculation of the compressible turbulent boundary layer in an arbitrary pressure gradient—a correlation of certain previous methods. A.R.C. R. & M. 3207. September, 1959.
29	N. Curle	The steady compressible laminar boundary layer, with arbitrary pressure gradient and uniform wall temperature. *Proc. Roy. Soc.* A, Vol. 249. January, 1959.
30	S. Goldstein	*Modern developments in fluid dynamics.* Vol. I. Clarendon Press, Oxford. 1938.
31	A. D. Young	The calculation of the profile drag of aerofoils and bodies of revolution at supersonic speeds. College of Aeronautics, Cranfield, Report 73. April, 1953. A.R.C. 15 970.
32	L. Green	Flow separation in rocket nozzles. *Journal A.R.S.*, p.34. January/February, 1953.
33	C. Overy	Unpublished M.o.A. work. 1961.
34	T. D. McKenney	Flow separation in over-expanded supersonic exhaust nozzles. *Journal A.R.S.*, p.320. September/October, 1954.
35	C. R. Foster and F. B. Cowles ..	Experimental study of gas-flow separation in over-expanded exhaust nozzles for rocket motors. Jet Propulsion Lab. Progress Report 4–103, California Inst. Tech. May, 1949.
36	H. G. Krull and F. W. Steffen ..	Performance characteristics of one convergent and three convergent-divergent nozzles. N.A.C.A. Research Memo. E52H12. September, 1952.
37	P. Eisenklam and D. Wilkie ..	On jet separation in supersonic rocket nozzles. I—The characteristics of flow. Imperial College Report J.R.L. 29. D.G.G.W. Report EMR/55/4. May, 1955.
38	H. E. Bloomer, R. J. Antl and P. E. Renas.	Experimental study of effects of geometric variables on performance of conical rocket engine exhaust nozzles. N.A.S.A. Tech. Note D–846. June, 1961.
39	H. L. G. Sunley and V. N. Ferriman.	Jet separation in conical nozzles. Rocket Propulsion Symposium, Cranfield. 1962.
40	J. H. Ahlberg, S. Hamilton, D. Migdal and E. N. Nilson.	Truncated perfect nozzles in optimum rocket design. *Journal A.R.S.*, Vol. 31, No. 5, p.614. May, 1961.
41	C. E. Campbell and J. M. Farley..	Performance of several conical convergent-divergent rocket type exhaust nozzles. N.A.S.A. Tech. Note D–467. September, 1960.
42	J. M. Farley and C. E. Campbell	Performance of several method-of-characteristics exhaust nozzles. N.A.S.A. Tech. Note D–293. October, 1960.

No.	*Author(s)*	*Title, etc.*
43	E. A. Fradenburgh, G. C. Gorton and A. Beke.	Thrust characteristics of a series of convergent-divergent exhaust nozzles at subsonic and supersonic flight speeds. N.A.C.A. Research Memo. E53L23. March, 1954.
44	M. Arens and E. Spiegler ..	Separated flow in overexpanded nozzles at low pressure ratios. *Bull. Research Council Israel*, Vol. 11C, No. 1, p.45. February, 1962.
45	K. Scheller and J. A. Bierlein ..	Some experiments on flow separation in rocket nozzles. *Journal A.R.S.*, p.28. January/February, 1953.
46	R. M. Kuhns	Flow separation in over-expanded supersonic nozzles. Report No. RT–124, Convair, San Diego. July, 1952.
47	R. H. Meleney and R. M. Kuhns..	Flow separation in over-expanded supersonic nozzles. Report RT–115, Convair, San Diego. October, 1951.
48	N. T. Musial and J. J. Ward ..	Overexpanded performance of conical nozzles with area ratios of 6 and 9 with and without supersonic external flow. N.A.S.A. Tech. Memo. X–83. September, 1959.
49	J. Reid and R. C. Hastings ..	The effect of a central jet on the base pressure of a cylindrical after-body in a supersonic stream. A.R.C. R. & M. 3224. December, 1959.
50	G. T. Golesworthy and M. V. Herbert.	The performance of a conical convergent-divergent nozzle with area ratio 2·9 in external flow. N.G.T.E. Memo. M.371. November, 1963.
51	M. V. Herbert and D. L. Martlew	The design-point performance of model internal-expansion propelling nozzles with area ratios up to 4. N.G.T.E. Report R.258. A.R.C. 26 495. December, 1963.
52	T. A. Cook	Some supersonic wind tunnel tests on the fixing of boundary-layer transition using distributed roughness bands. R.A.E. (Bedford) Tech. Note Aero. 2772. July, 1961.
53	J. B. Roberts	Unpublished M.o.A. work. 1963.
54	H. H. Korst and W. Tripp ..	The pressure on a blunt trailing edge separating two supersonic two-dimensional airstreams of different Mach numbers and stagnation pressures but identical stagnation temperatures. Mid-West Conference on Solid and Fluid Mechanics, University of Michigan. April, 1957.
55	A. B. Haines, D. W. Holder and H. H. Pearcey.	Scale effects at high subsonic and transonic speeds, and methods for fixing boundary-layer transition in model experiments. A.R.C. R. & M. 3012. September, 1954.
56	H. H. Pearcey	Shock-induced separation and its prevention by design and boundary layer control. Chapter in *Boundary layer and flow control.* G. V. Lachmann, editor. p.1333, Pergamon Press. 1961.
57	H. H. Pearcey	*Ibid.* p.1187.

TABLE 1

Nozzle Throat Reynolds Numbers
(Conventional Separation Data)

Authors	Reference	Range of Re^* (millions)
Marquardt	27	around 3
McKenney	34	1·25 to 2·40†
Foster and Cowles	35	1·03 to 2·30
Krull and Steffen	36	2·61 to 25·6
Eisenklam and Wilkie	37	2·62 to 6·56
Bloomer *et al*	38	1·15
Sunley and Ferriman	39	1·24 to 4·61
Campbell and Farley	41	3·72 to 18·80
Farley and Campbell	42	10·40 to 19·00

† Taking the throat dimension as the diameter of a circle enclosing the same throat area.

APPENDIX I

Notation

C_f	Skin-friction coefficient
C_P	Pressure coefficient
k	Separation pressure ratio (*see* Appendix II)
M	Mach number
P	Pressure (static pressure when used with no suffix)
Re	Reynolds number
T	Temperature
U	Velocity at free-stream edge of boundary layer
x	Distance along nozzle wall
X	Equivalent flat-plate length (*see* Appendix II)
y	Distance perpendicular to nozzle axis
α	Nozzle wall divergence semi-angle
δ	Boundary-layer thickness
θ	Boundary-layer momentum thickness
λ	Shock deflection angle
ν	Kinematic viscosity

Suffices and Superscripts

a	Values at free-stream edge of boundary layer
b	Values at nozzle base
s	Values corresponding to the separation pressure
t	Total head values
w	Values at nozzle wall
1	Values corresponding to the incipient pressure
2	Values corresponding to the peak or plateau pressure
*	Values at nozzle throat
∞	Values in external flow

APPENDIX II

Definitions

Applied pressure ratio (A.P.R.)	The ratio of nozzle upstream total pressure to nozzle base pressure $= P_t/P_b$.
Design pressure ratio (D.P.R.)	That pressure ratio corresponding to the ratio of nozzle outlet area to throat area in one-dimensional theory.
Separation pressure ratio (k)	The ratio of incipient pressure to nozzle base pressure $= P_1/P_b$ (*see* Figs. 4 and 5).
Kink point	The condition at which the oblique shock moves from the nozzle lip to inside the nozzle (*see* Section 5.1).
Equivalent flat-plate length (X)	That length over which a boundary layer growing at a constant Mach number equal to the local Mach number would attain the same thickness as the actual local boundary layer.
Separation Reynolds number (Re_X)	The Reynolds number at the point of incipient separation, based upon the equivalent flat-plate length.
Throat Reynolds number (Re^*)	The reference Reynolds number for a nozzle, based upon sonic throat flow conditions and the diameter of a circle having the same area as the nozzle throat.
Incipient pressure (P_1) Separation pressure (P_s) Peak or plateau pressure (P_2)	Detailed definition given in text (Section 2).

APPENDIX III

Momentum Thickness of a Laminar Boundary Layer

For a steady, compressible, laminar boundary layer, with arbitrary pressure gradient, Curle[29] derives the following relations:

$$\theta^2 = 0{\cdot}45\,\frac{\nu_a}{G}\int_0^x \frac{G}{U}\,dx \tag{A1}$$

where

$$G = \exp\left\{2\int_0^x \left(\frac{T_w}{T_a} + 2 - \frac{M_a^2}{2}\right)\frac{U'}{U}\,dx\right\} \tag{A2}$$

and

$$U' = \frac{dU}{dx}.$$

These relations are for two-dimensional flow, and it is assumed that there is no heat transfer through the walls.

If it be further assumed that the total temperature (T_t) is constant across any cross-section of a nozzle,

then

$$T_w = T_t.$$

Thus, when $\gamma = 1{\cdot}4$, $\dfrac{T_w}{T_a} = 1 + 0{\cdot}2\,M_a^2$. (A3)

Now

$$U = M_a(\gamma g R T_a)^{1/2},$$

i.e.

$$U = M_a(\gamma g R T_t)^{1/2}(1+0{\cdot}2\,M_a^2)^{-1/2}. \tag{A4}$$

Thus

$$\frac{dU}{dM_a} = (\gamma g R T_t)^{1/2}(1+0{\cdot}2\,M_a^2)^{-3/2}.$$

Whence

$$\frac{U'}{U}\,dx = \frac{1}{M_a(1+0{\cdot}2\,M_a^2)}\,dM_a. \tag{A5}$$

Substituting equations (A3) and (A5) into (A2):

$$G = \exp\left\{6\int_{M_0}^{M_a} \frac{(1-0{\cdot}1\,M_a^2)}{M_a(1+0{\cdot}2\,M_a^2)}\,dM_a\right\}$$

where M_0 is the value of M_a when $x = 0$.

Integration of this equation yields:

$$G = \frac{1}{B}\,M_a^6(1+0{\cdot}2\,M_a^2)^{-9/2} \tag{A6}$$

where

$$B = M_0^6(1+0{\cdot}2\,M_0^2)^{-9/2}.$$

Substituting equations (A4) and (A6) into (A1):

$$\theta^2 = \frac{0{\cdot}45\ \nu_a}{G(\gamma g R T_t)^{1/2}} \int_0^x \frac{M_a^6(1+0{\cdot}2\ M_a^2)^{-9/2}}{BM_a(1+0{\cdot}2\ M_a^2)^{-1/2}}\, dx$$

or

$$\theta^2 = \frac{0{\cdot}45\ \nu_a}{BG(\gamma g R T_t)^{1/2}} \int_0^x M_a^5(1+0{\cdot}2\ M_a^2)^{-4}\, dx. \tag{A7}$$

Let us define

$$P'' = M_a^5(1+0{\cdot}2\ M_a^2)^{-4},$$

and

$$X = \frac{1}{\overline{P''}} \int_0^x P''dx.$$

When M is constant, it can be seen that $X = x$. Hence we can regard X in the general case as an 'equivalent flat-plate length'. Combining equations (A4), (A6), (A7), and substituting P'' and X into the resultant equation, gives:

$$\theta = 0{\cdot}671\ XRe_X^{-1/2} \tag{A8}$$

where Re_X is the local Reynolds number based upon X. This expression may be compared with the classical relation for incompressible flow on a flat plate[30]:

$$\theta = 0{\cdot}664\ xRe_x^{-1/2}.$$

These should agree when $M = 0$, so that we shall adjust the constant in equation (A8) to give:

$$\theta = 0{\cdot}664\ XRe_X^{-1/2}. \tag{A9}$$

Let suffix $_2$ now refer to conditions at a point on the diverging boundary of a two-dimensional nozzle, and suffix $_3$ refer to conditions at a point on the diverging boundary of an axisymmetric nozzle. Let the free-stream flow conditions at these two points be the same. Now by equation (A9):

$$\theta_2 = 0{\cdot}664\ X_2 Re_{X_2}^{-1/2},$$

i.e.

$$\theta_2 = 0{\cdot}664\ X_2^{1/2} \left(\frac{Re_{X_2}}{X_2}\right)^{-1/2}.$$

Since the flow conditions at the two points are the same

$$\left(\frac{Re_{X_2}}{X_2}\right) = \left(\frac{Re_{X_3}}{X_3}\right).$$

If the transformation $\delta x_2 = (y_3/d)^2 \delta x_3$ is made, where d is some as yet unspecified reference length, it can be shown[31] that:

$$\theta_3 = \left(\frac{d}{y_3}\right) \theta_2.$$

Thus

$$\theta_3 = 0{\cdot}664 \left(\frac{d}{y_3}\right) P''^{-1/2} \left(\frac{Re_{X_3}}{X_3}\right)^{-1/2} \left[\int_0^{x_3} P'' \left(\frac{y_3}{d}\right)^2 dx_3\right]^{1/2}$$

$$= 0{\cdot}664\, X_3^{1/2} \left(\frac{Re_{X_3}}{X_3}\right)^{-1/2}$$

$\therefore$

$$\theta_3 = 0{\cdot}664\, X_3 Re_{X_3}{}^{-1/2}$$

where

$$X_3 = \frac{1}{P'' y_3{}^2} \int_0^{x_3} P'' y_3{}^2 dx_3 .$$

Thus, in general terms:

$$\underline{\theta = 0{\cdot}664\, X Re_X{}^{-1/2}}$$

where

$$X = \frac{1}{P''} \int_0^x P'' dx \text{ for two-dimensional flow}$$

or

$$X = \frac{1}{P'' y^2} \int_0^x P'' y^2 dx \text{ for axisymmetric flow}$$

and

$$P'' = M^5 (1 + 0{\cdot}2\, M^2)^{-4} .$$

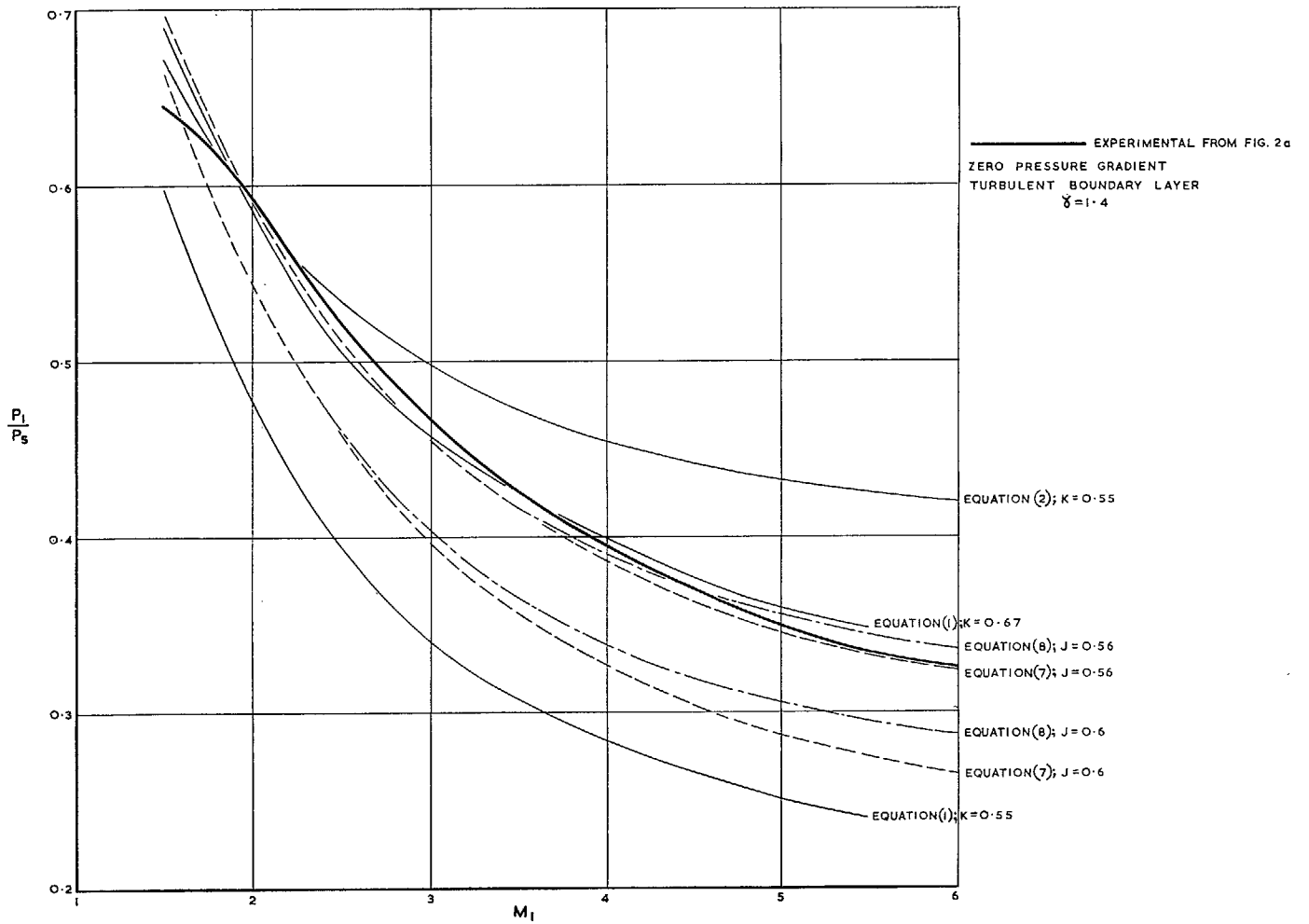

FIG. 1. Separation pressure ratio—I.

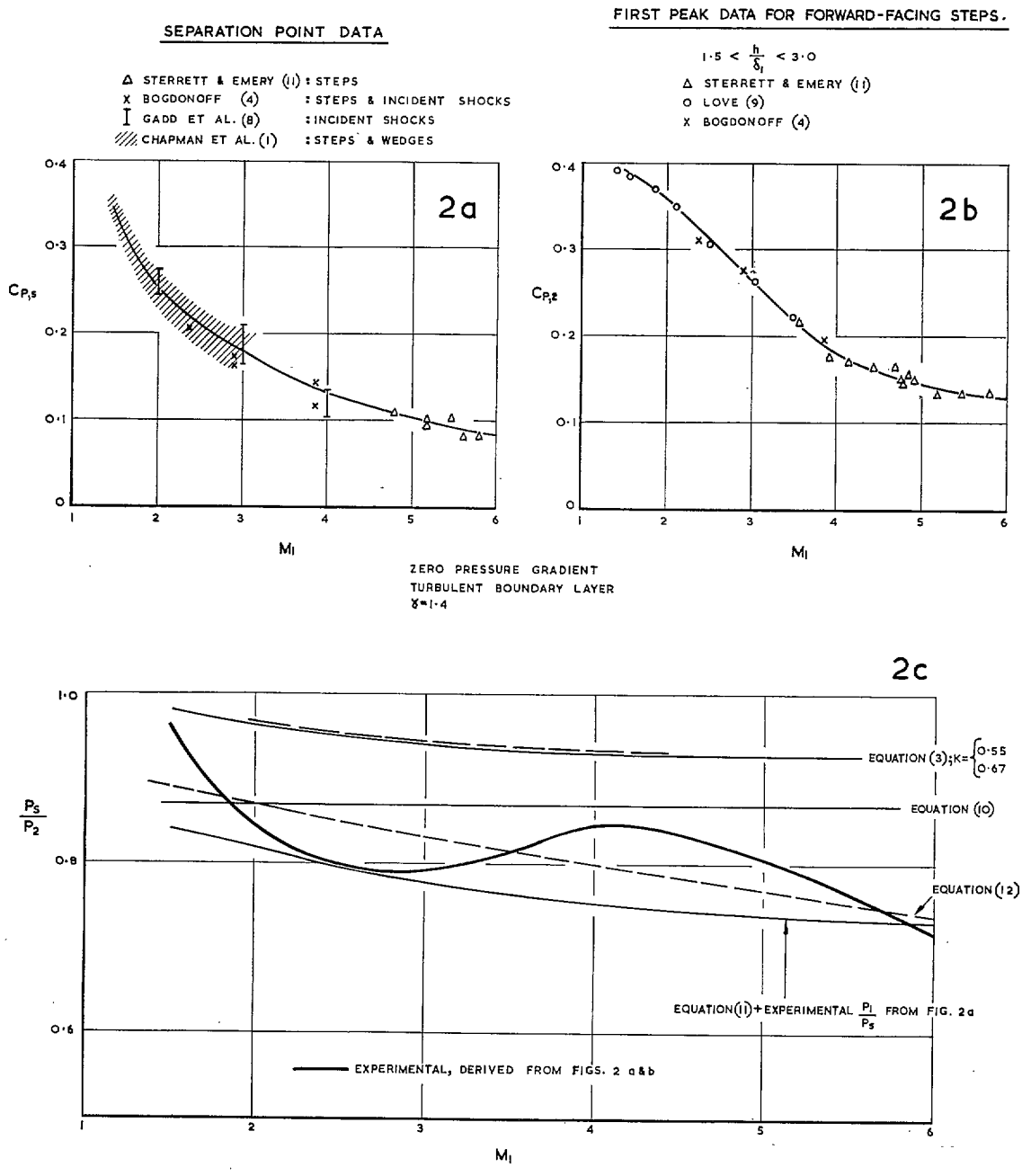

FIG. 2. Separation pressure ratio—II.

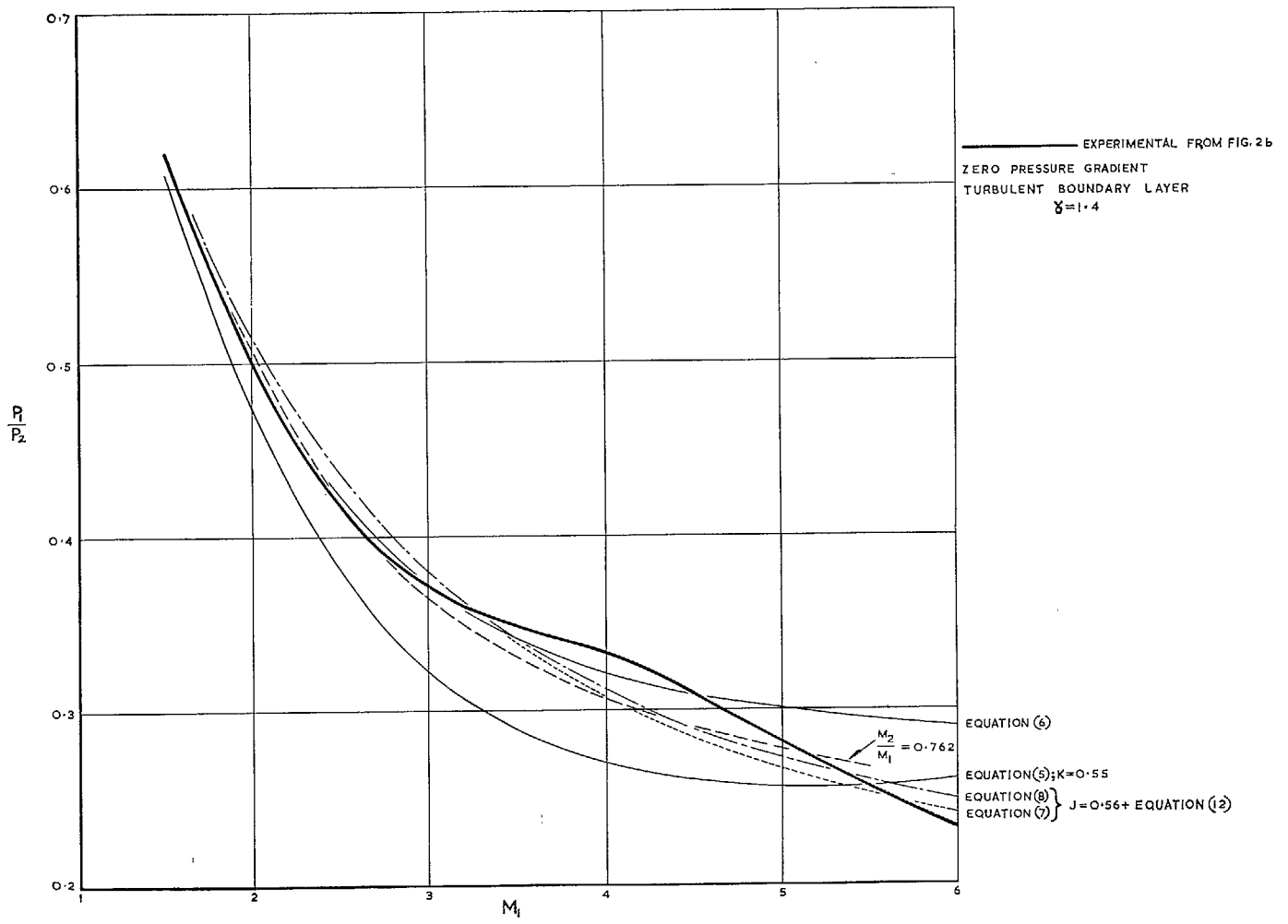

FIG 3. Separation pressure ratio—III.

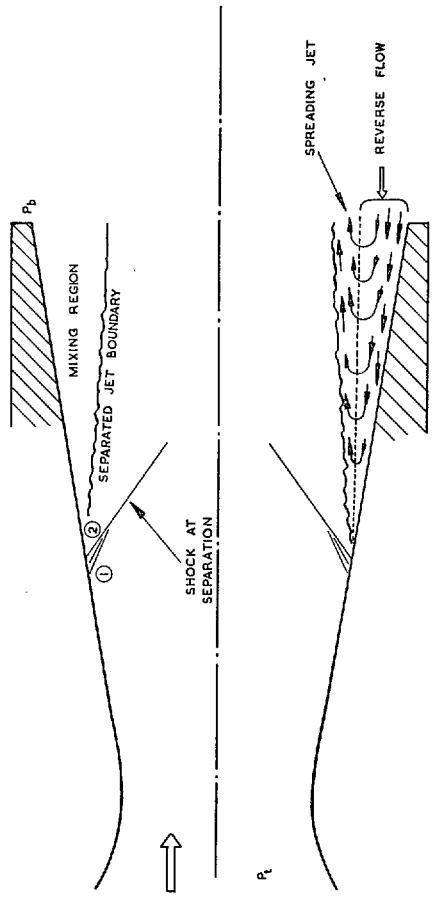

FIG. 4. Nozzle flow with separation.

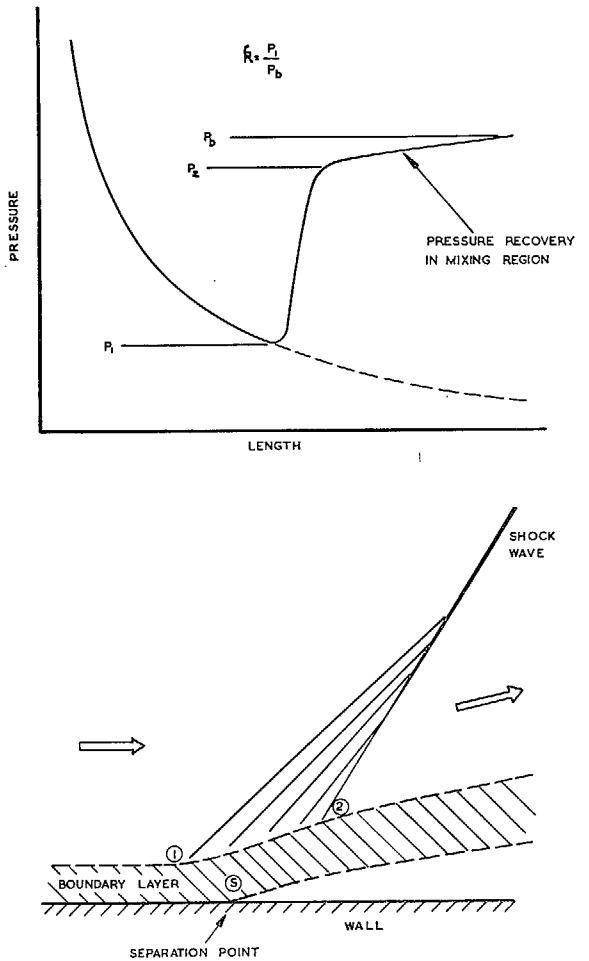

FIG. 5. Nozzle separation pressures.

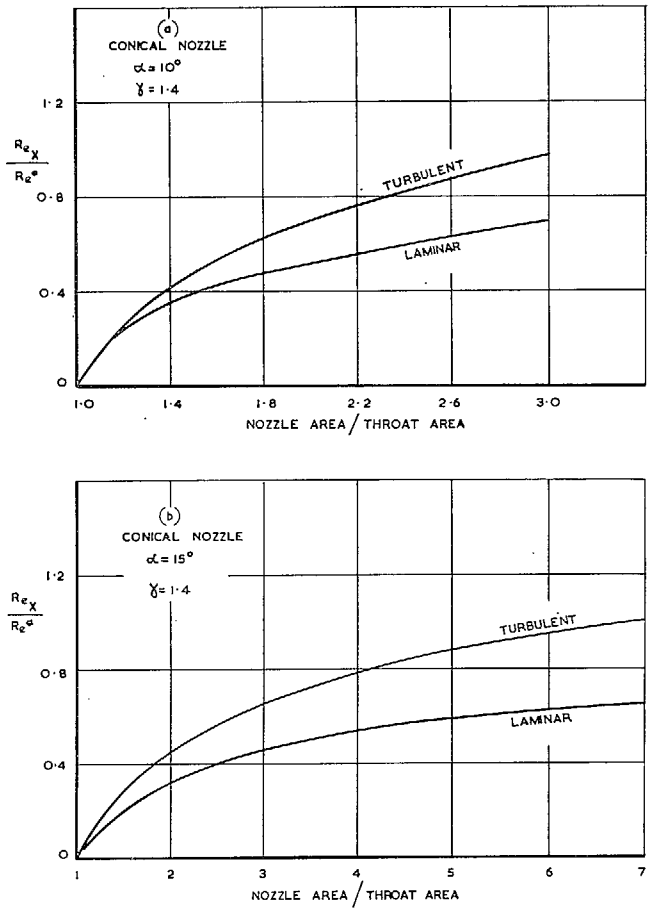

FIG. 6. Reynolds number variation along a nozzle.

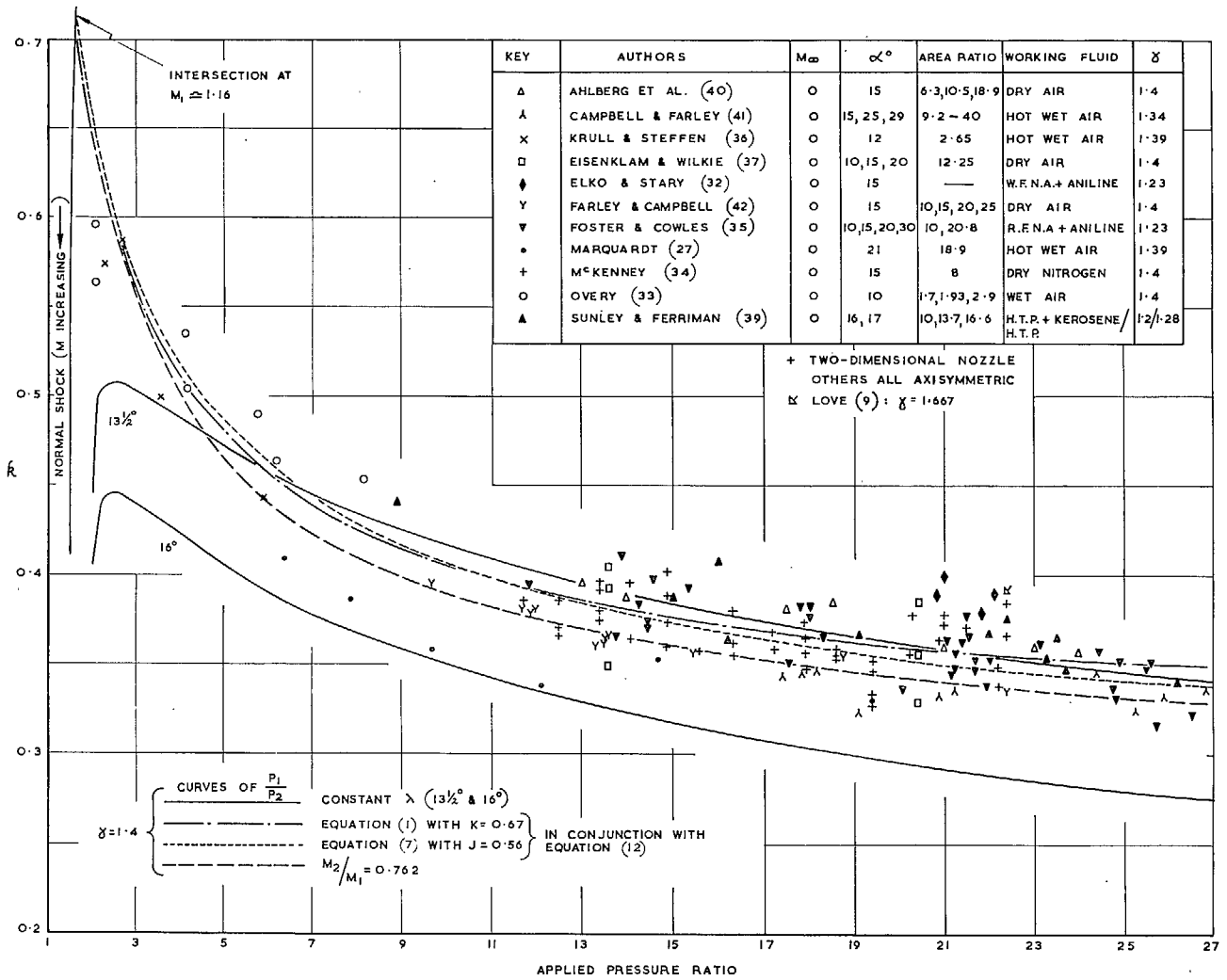

FIG. 7. Conventional nozzle separation data—I.

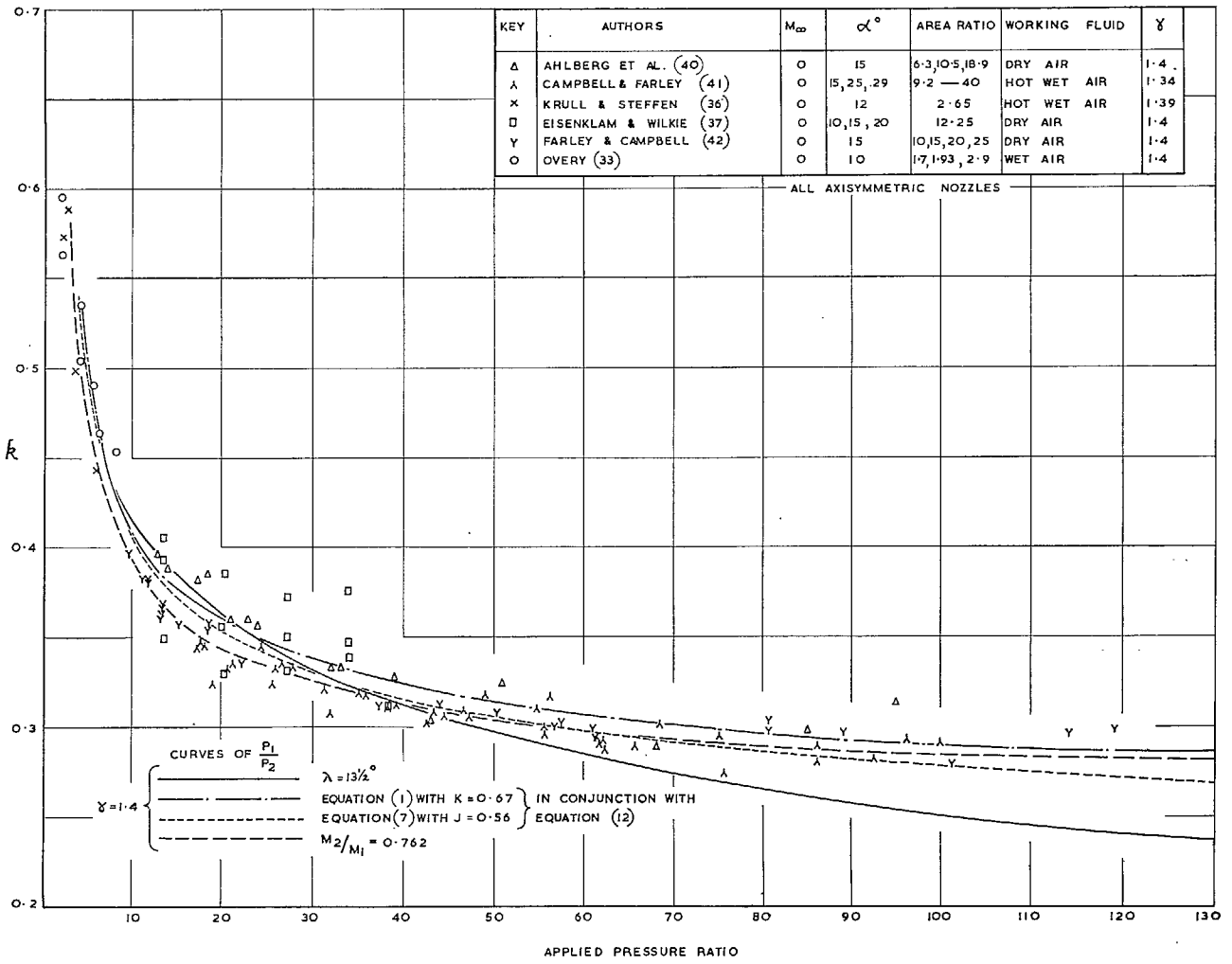

FIG. 8. Conventional nozzle separation data—II.

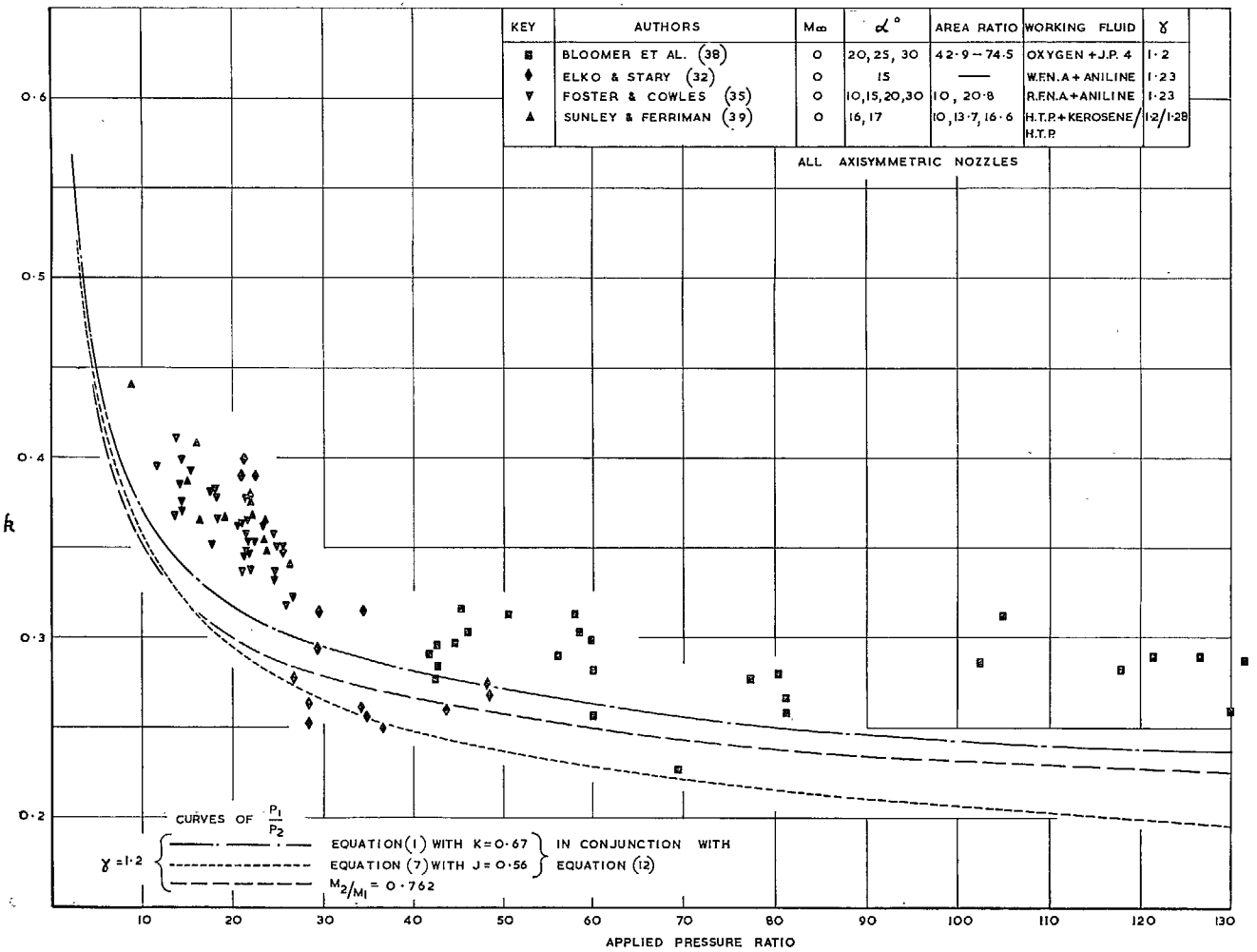

FIG. 9. Conventional nozzle separation data—III.

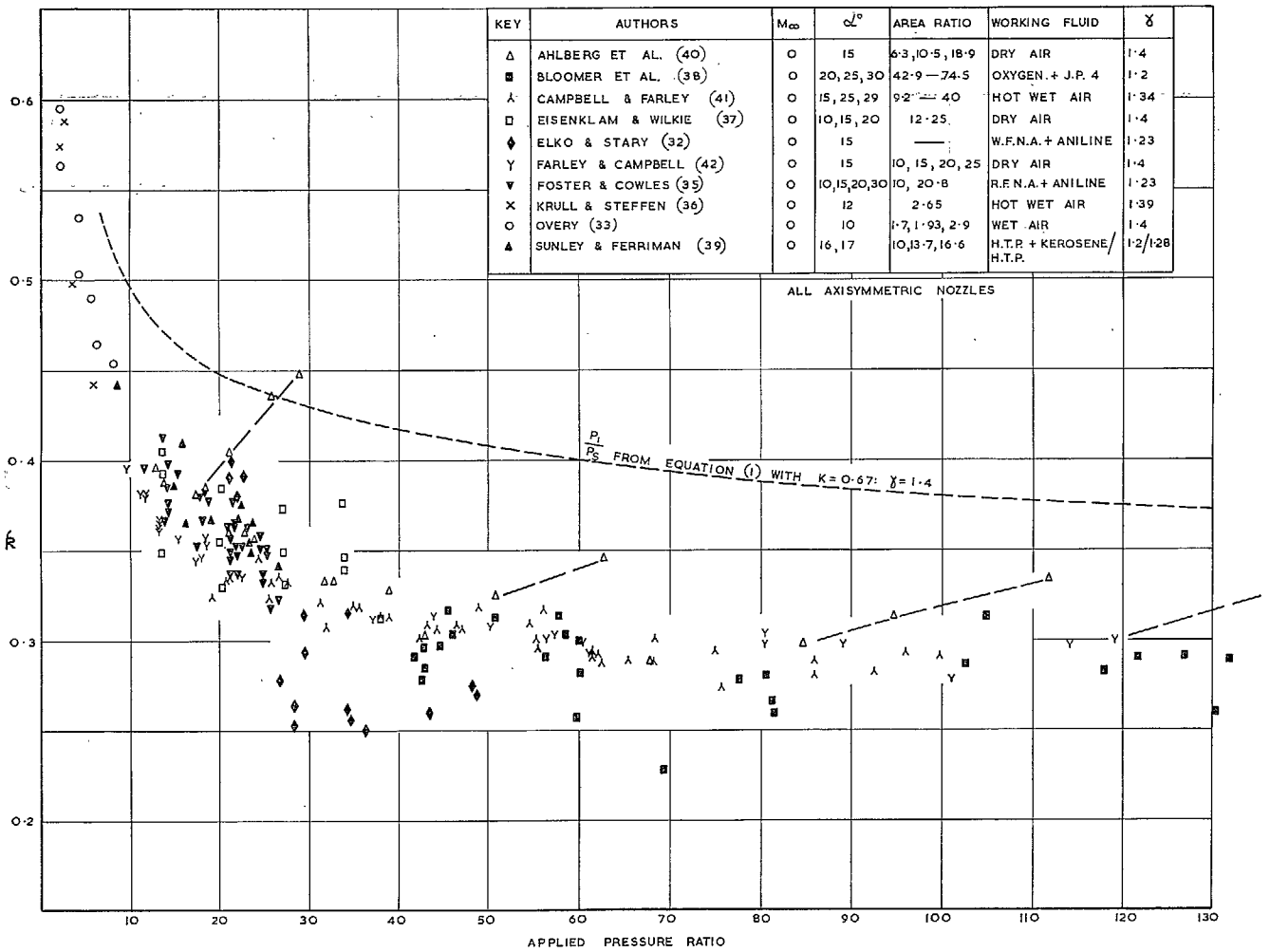

FIG. 10. Conventional nozzle separation data—IV.

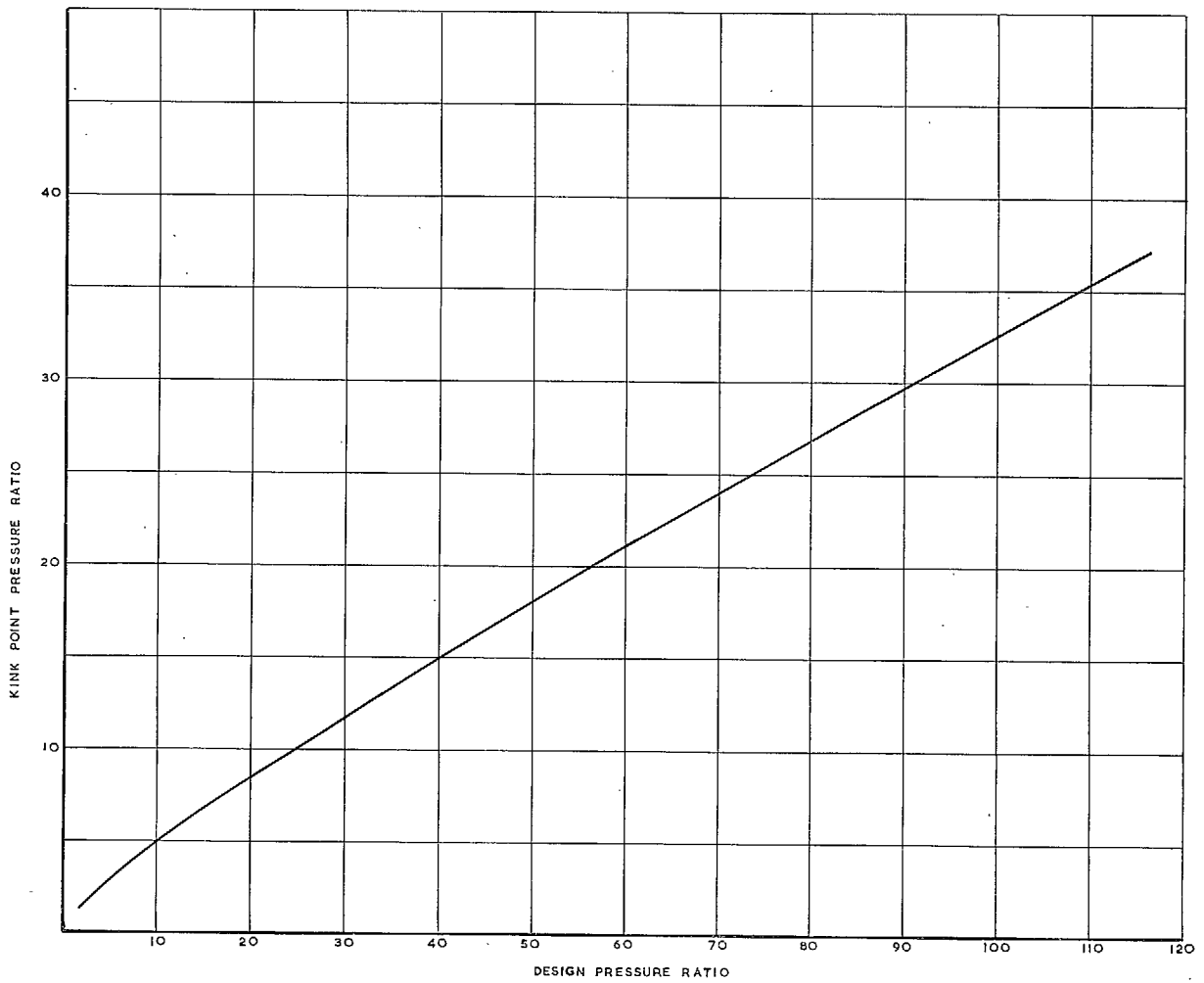

FIG. 11. Turbulent boundary-layer 'kink points'.

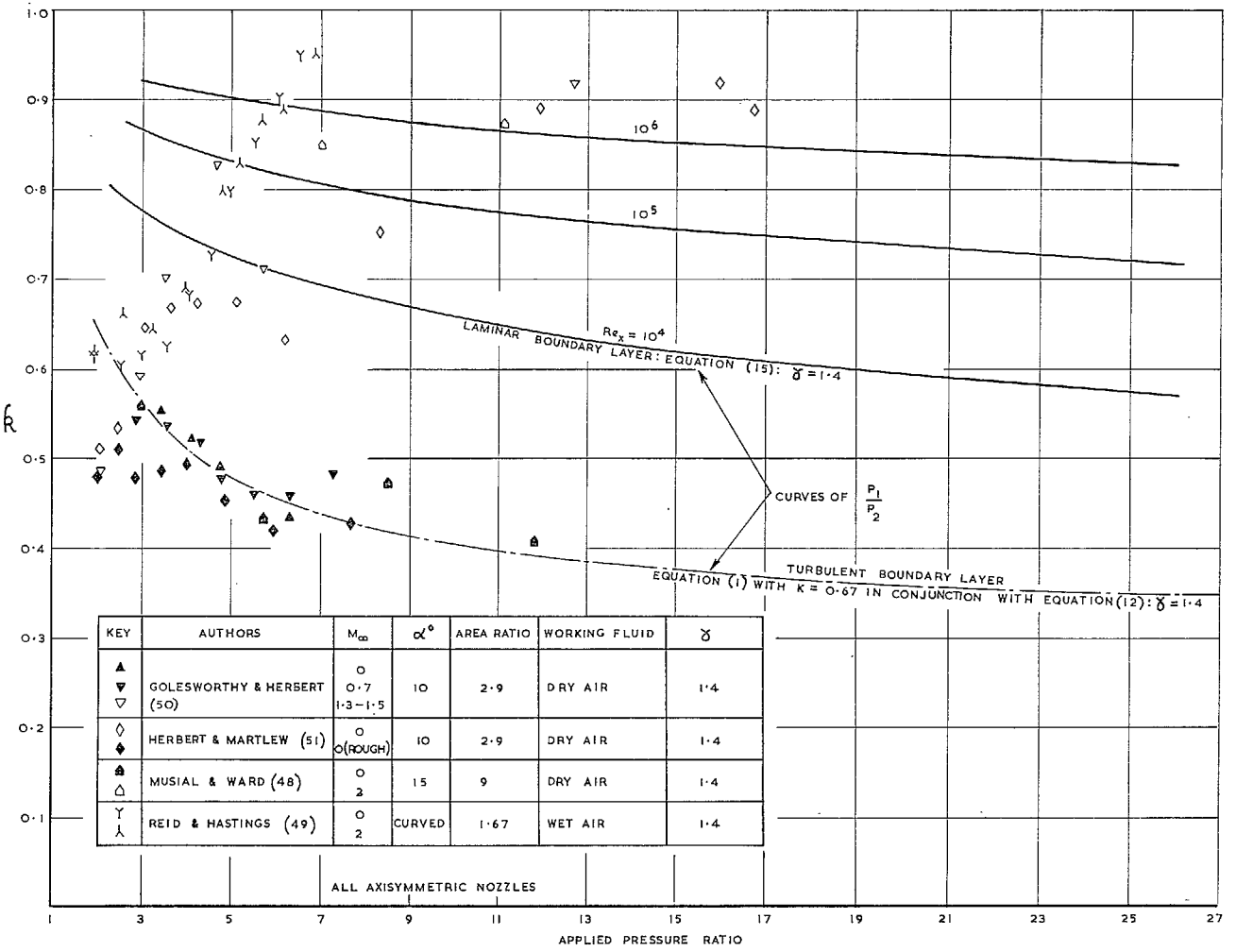

KEY	AUTHORS	M_∞	$\alpha°$	AREA RATIO	WORKING FLUID	γ
▲ ▼ ▽	GOLESWORTHY & HERBERT (50)	0 0·7 1·3–1·5	10	2·9	DRY AIR	1·4
◊ ◆	HERBERT & MARTLEW (51)	0 0(ROUGH)	10	2·9	DRY AIR	1·4
⏃ △	MUSIAL & WARD (48)	0 2	15	9	DRY AIR	1·4
Y ⅄	REID & HASTINGS (49)	0 2	CURVED	1·67	WET AIR	1·4

FIG. 12. Unconventional nozzle separation data.

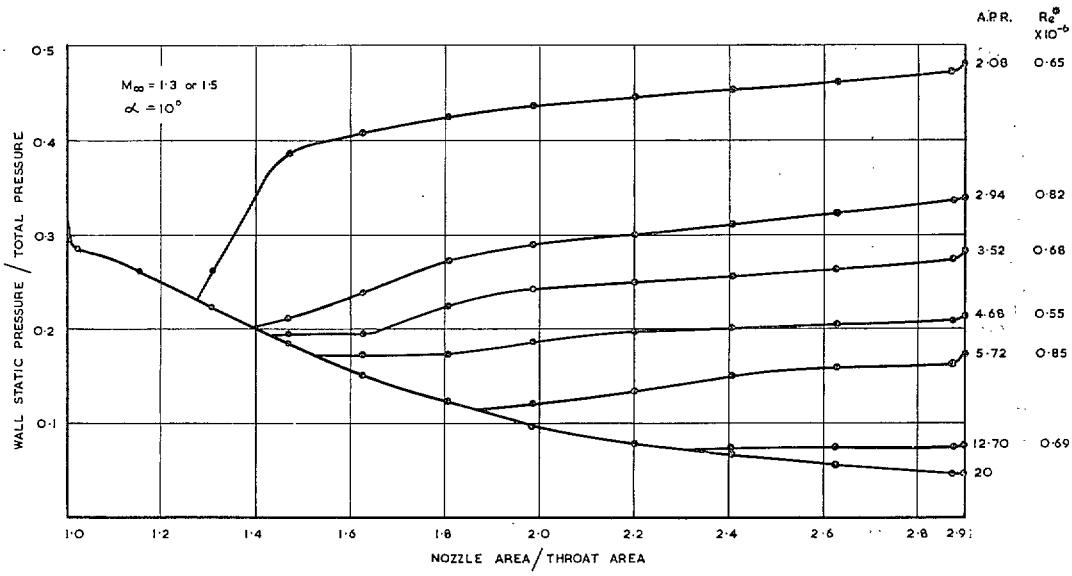

FIG. 13. Nozzle pressure distribution from Ref. 50—I.

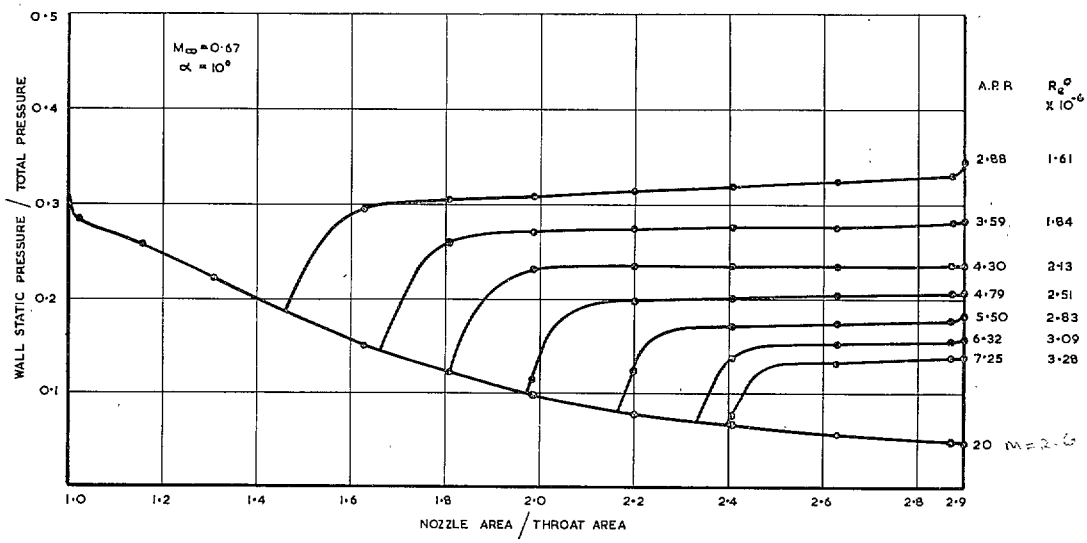

FIG. 14. Nozzle pressure distribution from Ref. 50—II.

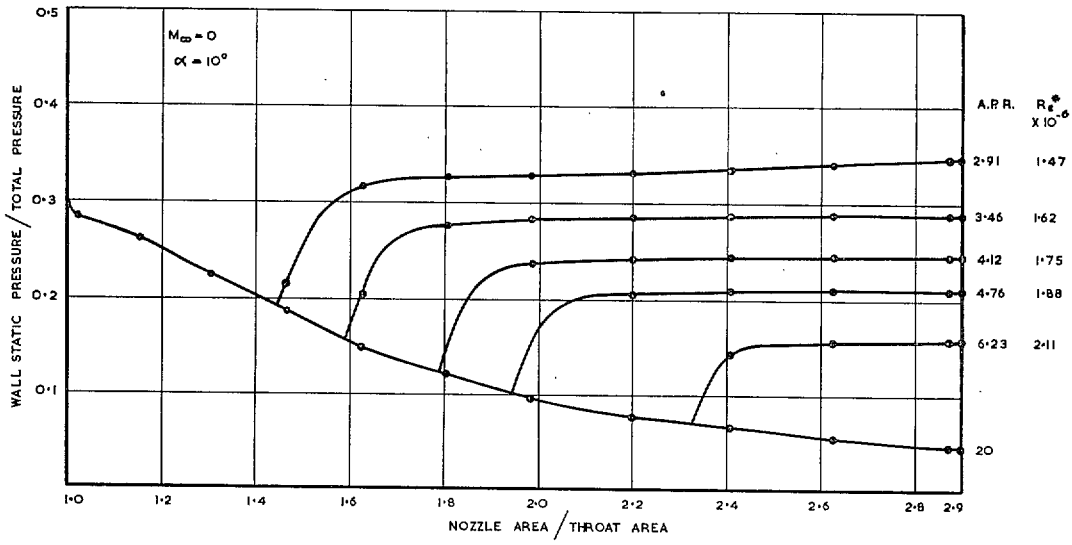

FIG. 15. Nozzle pressure distribution from Ref. 50—III.

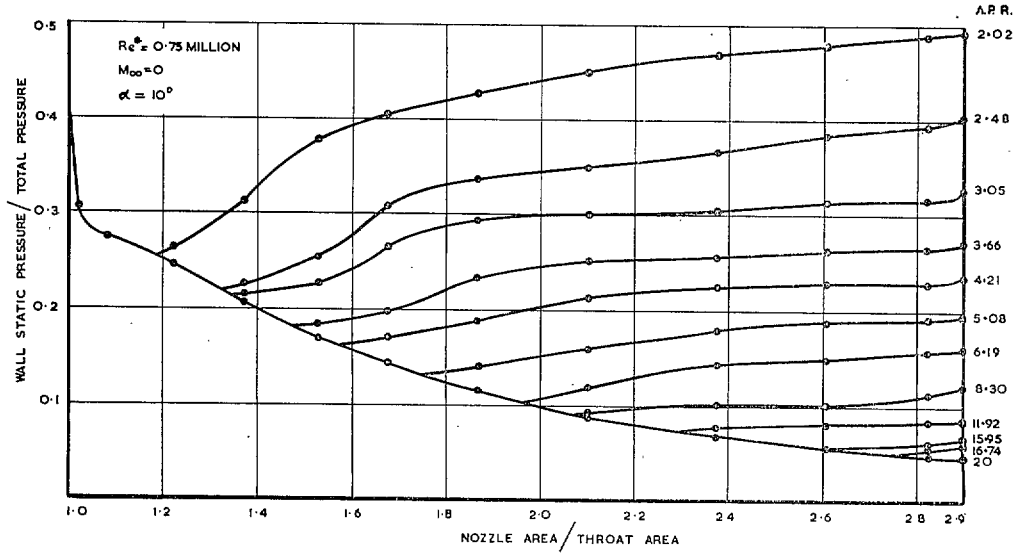

FIG. 16. Nozzle pressure distribution from Ref. 51—I.

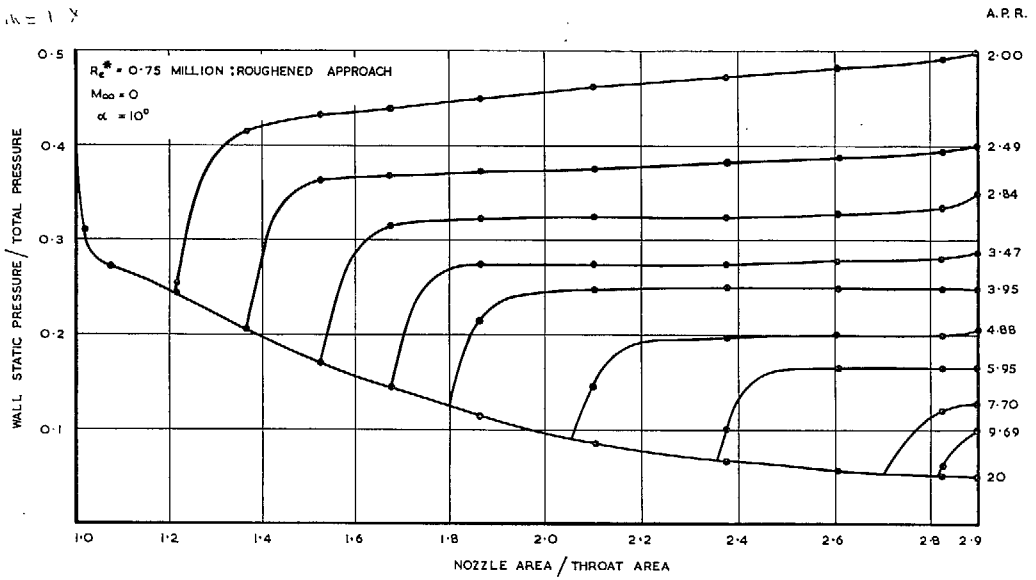

FIG. 17. Nozzle pressure distribution from Ref. 51—II.

KEY	AUTHORS	M_∞	$\alpha°$	AREA RATIO	WORKING FLUID	γ	RANGE OF M_1
▲ ▼ ▽	GOLESWORTHY & HERBERT (50)	0 0·7 1·3–1·5	10	2·9	DRY AIR	1·4	1·85 — 2·39 1·90 — 2·41 1·72 — 2·37
◇	HERBERT & MARTLEW (51)	0	10	2·9	DRY AIR	1·4	1·67 — 2·55
▲ △	MUSIAL & WARD (48)	0 2	15	9	DRY AIR	1·4	2·30 — 2·91 2·01 — 2·28
Y 人	REID & HASTINGS (49)	0 2	CURVED	1·67	WET AIR	1·4	1·69 — 1·91 1·71 — 1·95
○	OVERY (33)	0	10	1·7, 1·93, 2·9	WET AIR	1·4	1·99 — 2·53
●	UNPUBLISHED N.G.T.E. DATA	0–0·9	10	2·14, 2·44, 2·9	DRY AIR	1·4	1·80 — 2·55

ALL AXISYMMETRIC NOZZLES.
A.P.R. ≥ 3.
COMPUTATION AS FOR A TURBULENT BOUNDARY LAYER THROUGHOUT

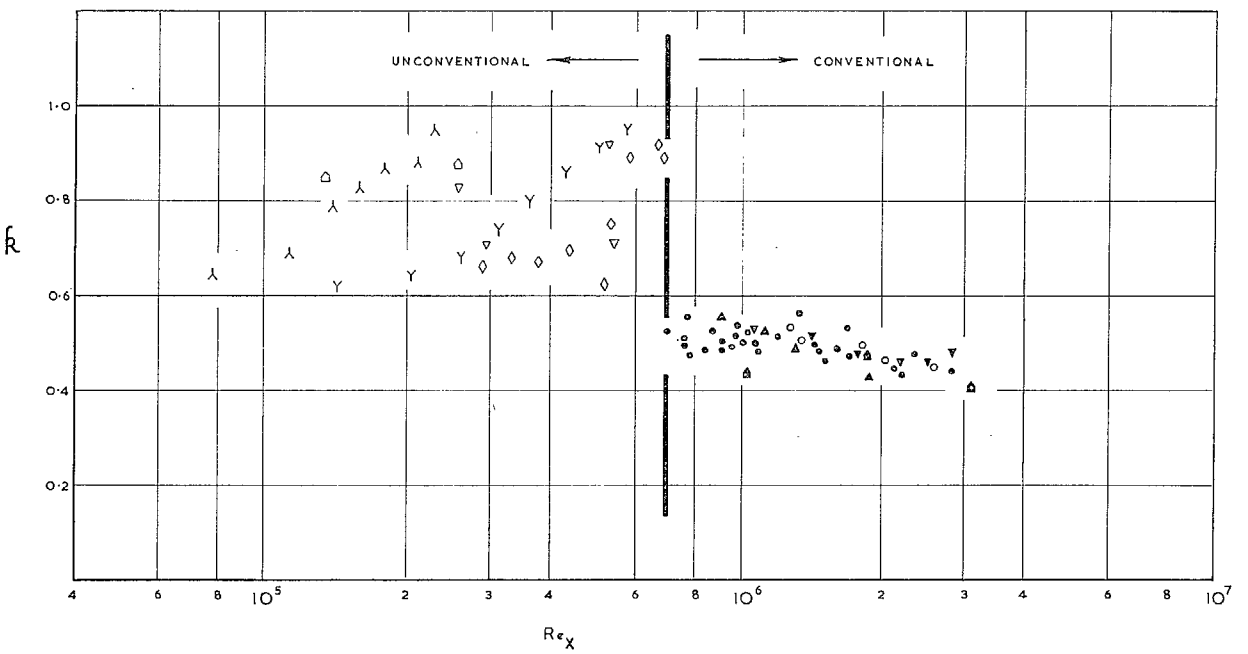

FIG. 18. Separation Reynolds number of some data.

KEY	AUTHORS	M_∞	α°	AREA RATIO	WORKING FLUID	γ	RANGE OF M_1
△	GOLESWORTHY & HERBERT (50)	0	10	2·9	DRY AIR	1·4	1·85 — 2·39
▼		0·7					1·90 — 2·41
▽		1·3–1·5					1·72 — 2·37
◇	HERBERT & MARTLEW (51)	0	10	2·9	DRY AIR	1·4	1·67 — 2·55
▲	MUSIAL & WARD (48)	0	15	9	DRY AIR	1·4	2·30 — 2·91
△		2					2·01 — 2·28
Y	REID & HASTINGS (49)	0	CURVED	1·67	WET AIR	1·4	1·69 — 1·91
⅄		2					1·71 — 1·95
○	OVERY (33)	0	10	1·7, 1·93, 2·9	WET AIR	1·4	1·99 — 2·53
●	UNPUBLISHED N.G.T.E. DATA	0–0·9	10	2·14, 2·44, 2·9	DRY AIR	1·4	1·80 — 2·55

ALL AXISYMMETRIC NOZZLES
A.P.R. ≥ 3

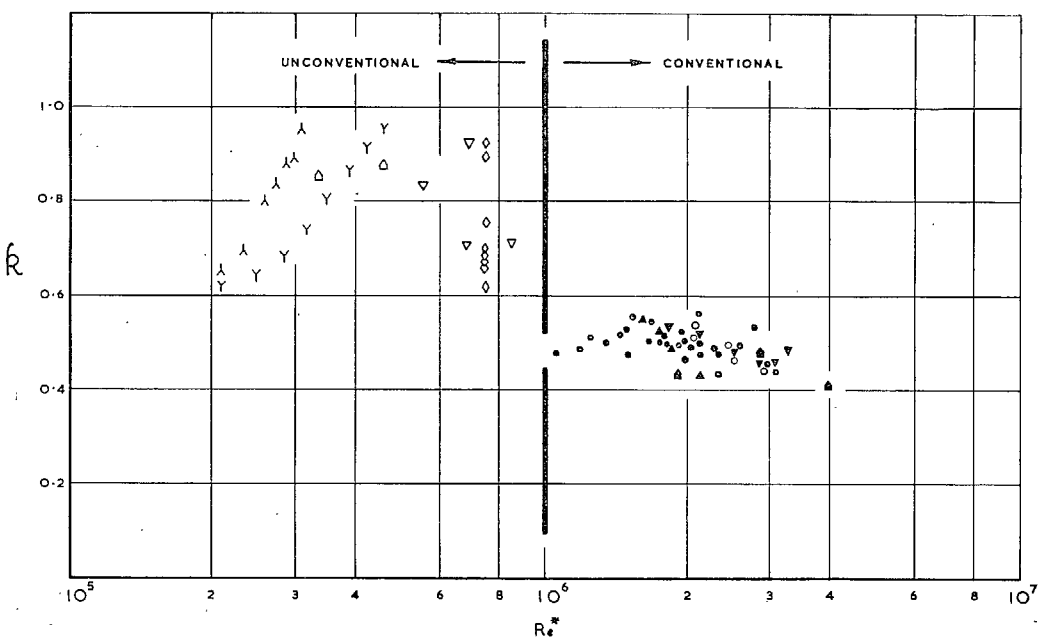

FIG. 19. Throat Reynolds number of some separation data.

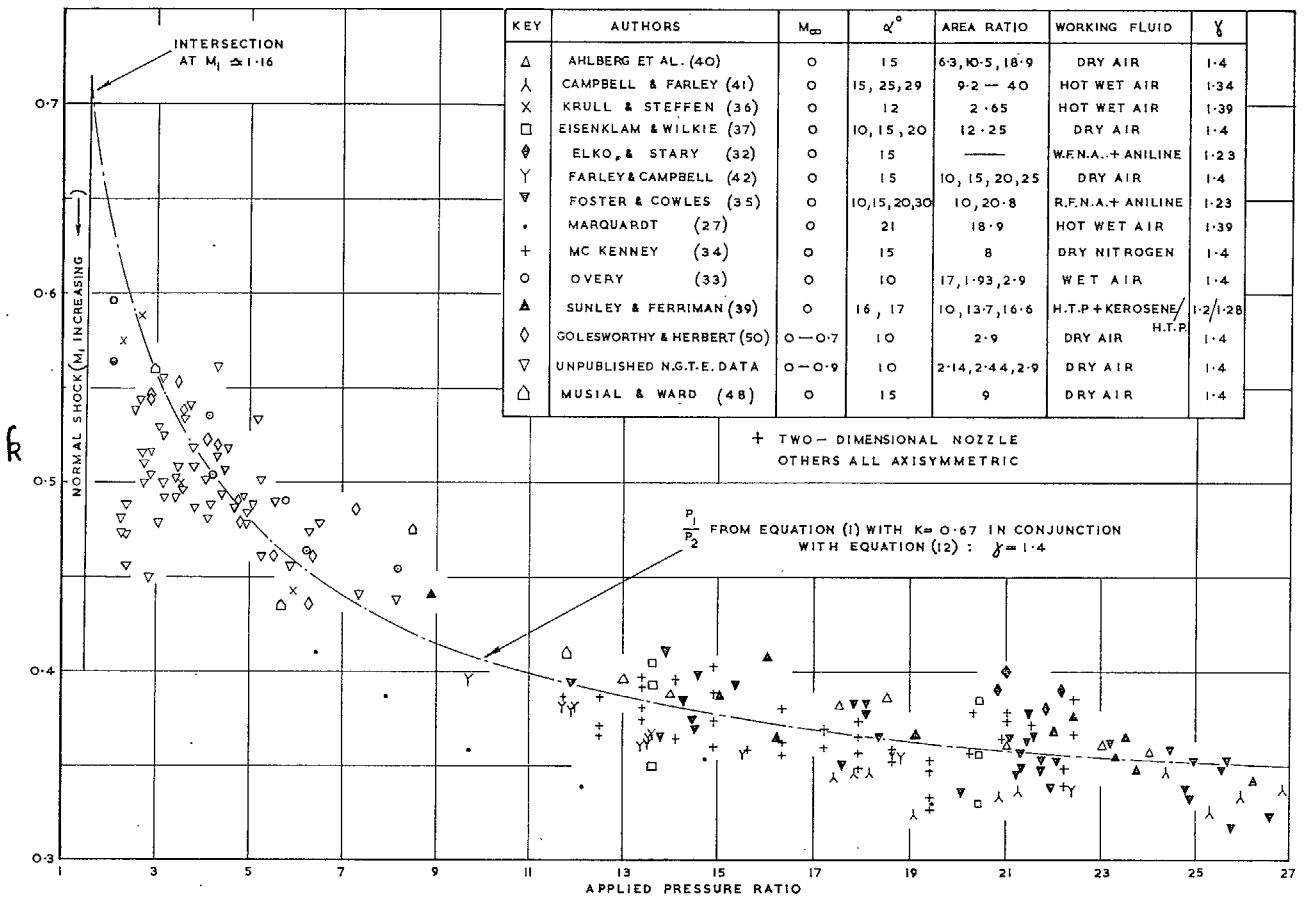

FIG. 20. Turbulent nozzle separation data at low applied pressure ratio.

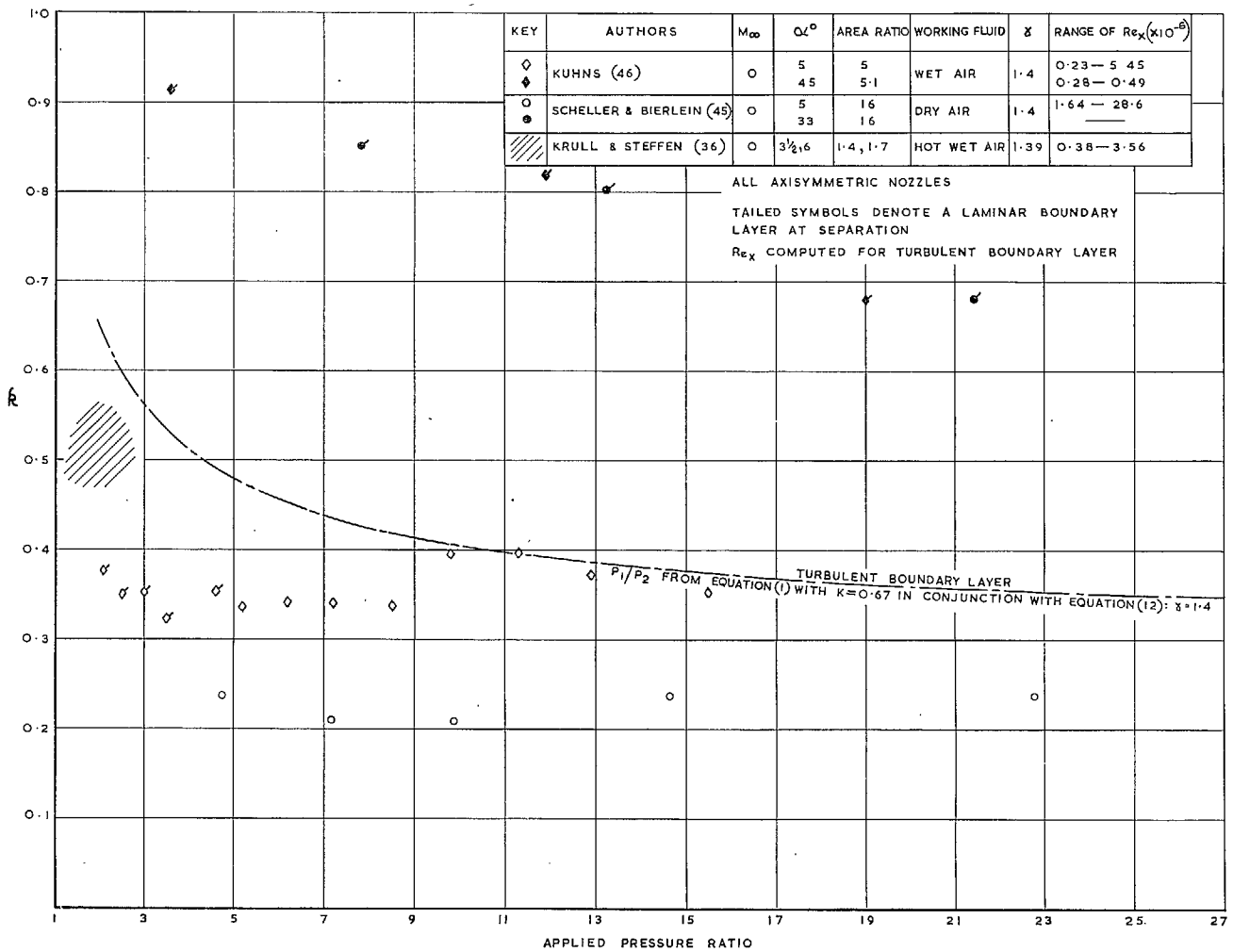

FIG. 21. The effect of divergence angle.

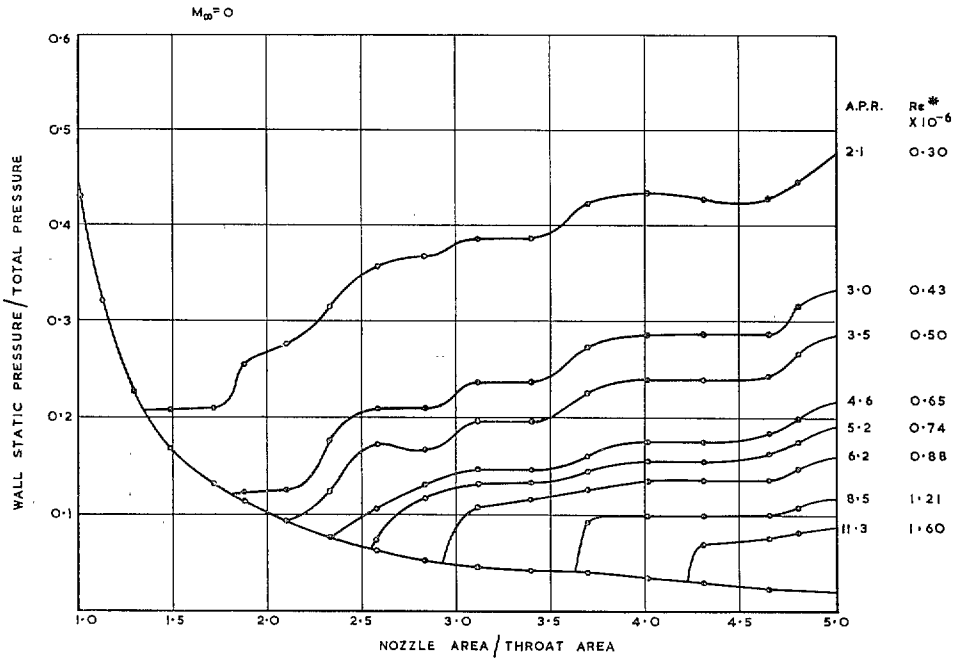

FIG. 22. Pressure distribution down Kuhns 5° nozzle.

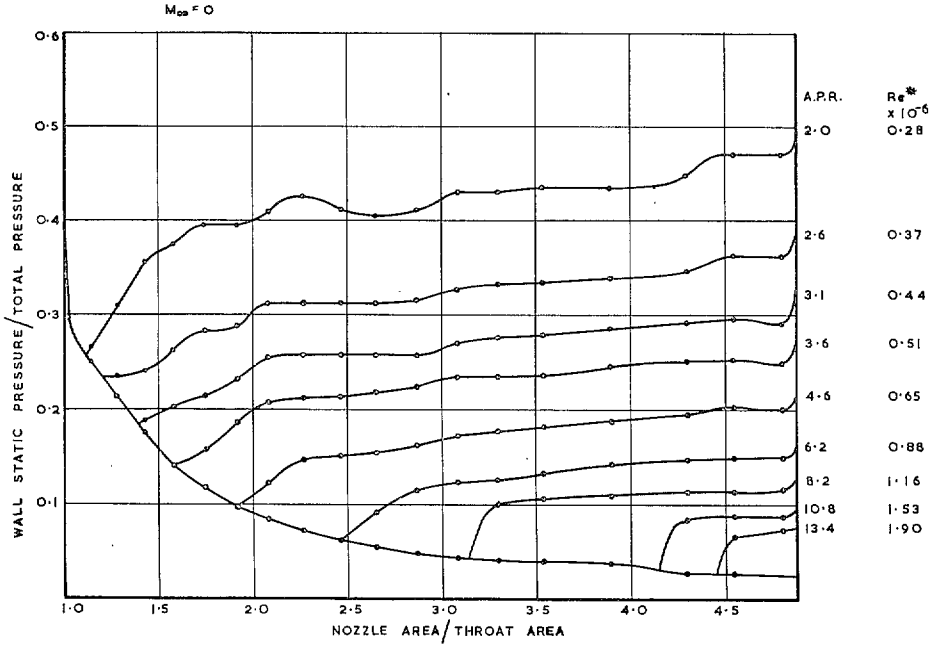

FIG. 23. Pressure distribution down Kuhns 10° nozzle.

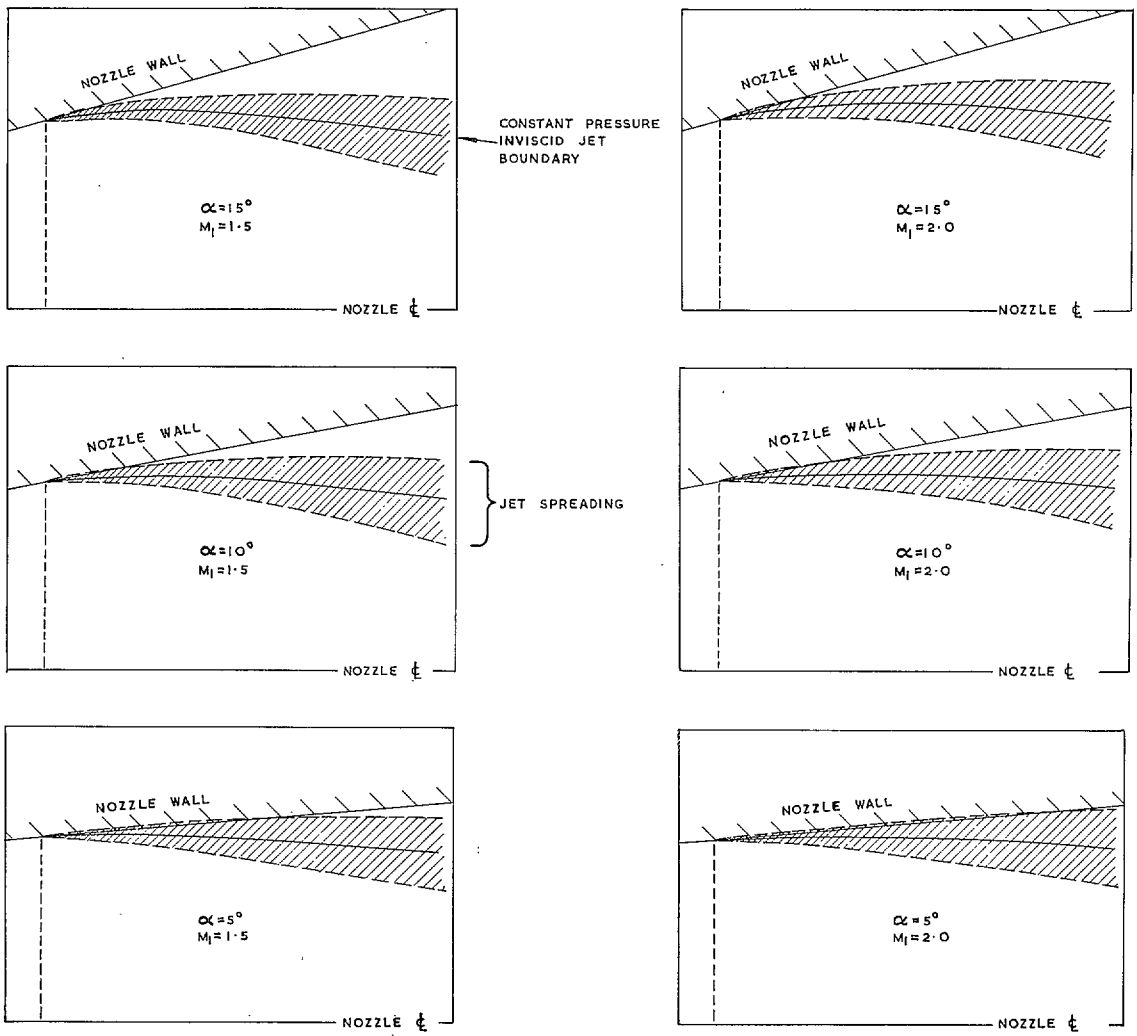

FIG. 24. Free jet boundaries after laminar separation.

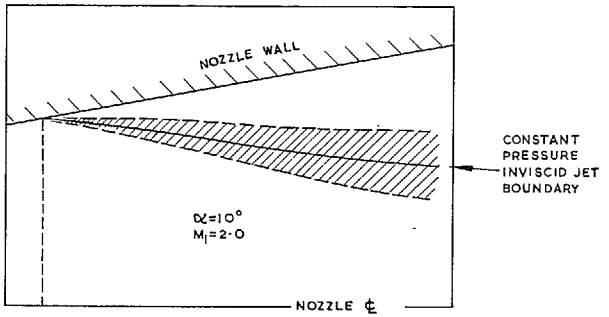

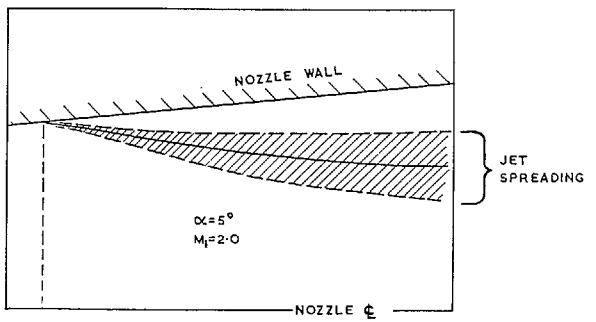

FIG. 25. Free jet boundaries after turbulent separation.

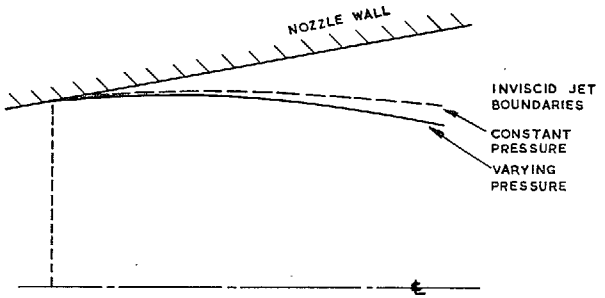

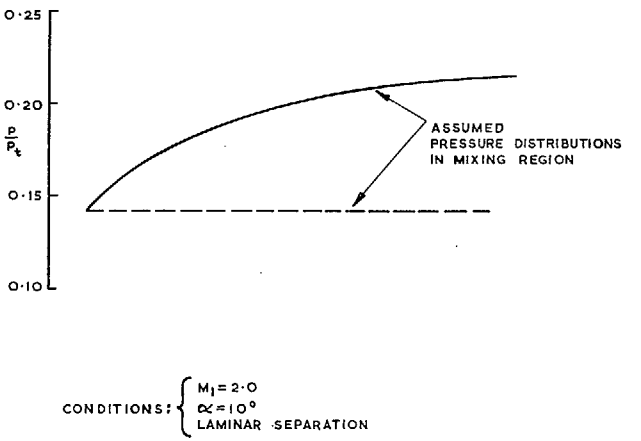

FIG. 26. Modification to jet boundary caused by pressure rise in mixing region.

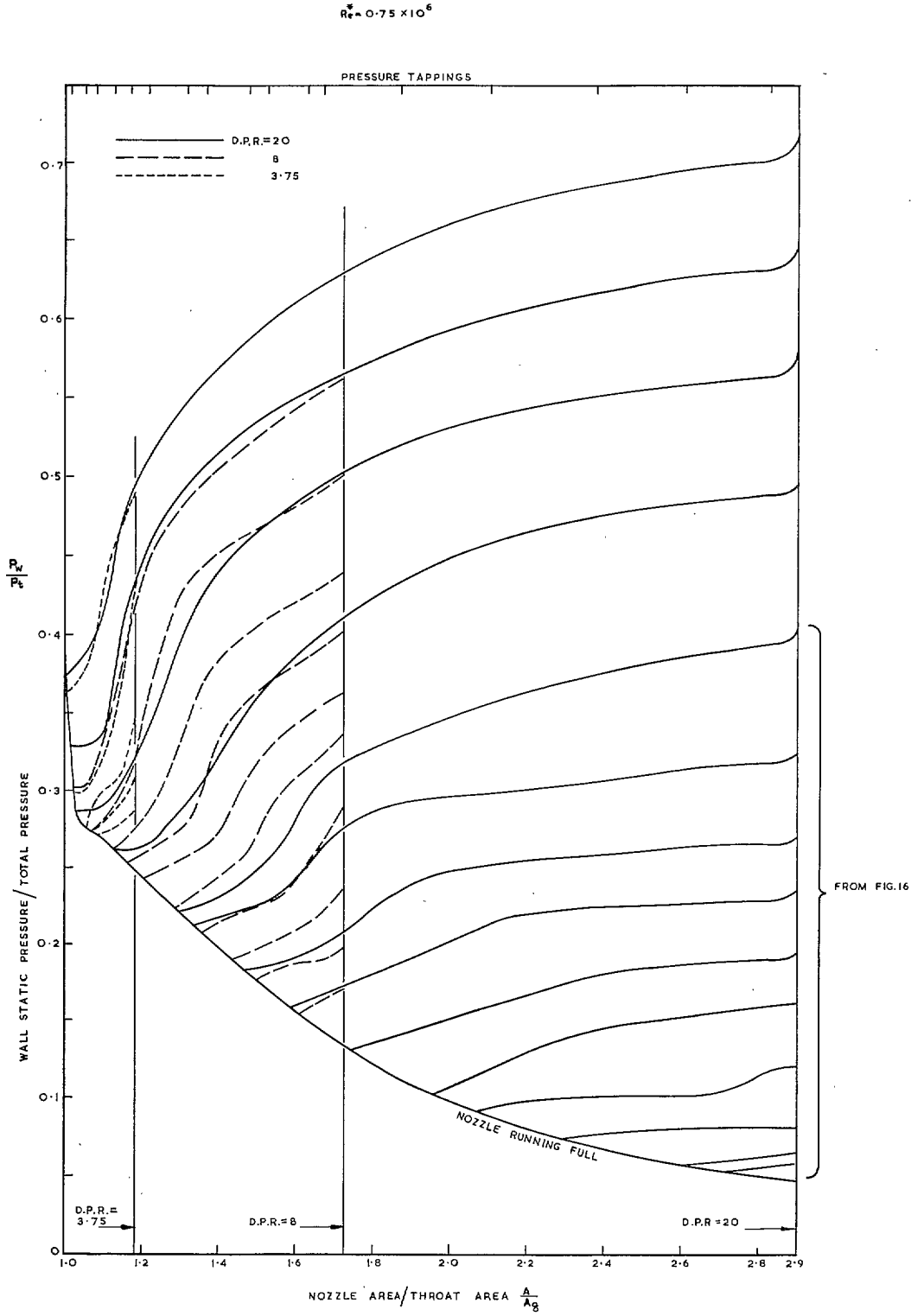

FIG. 27. Pressure distributions in several 10° conical nozzles.

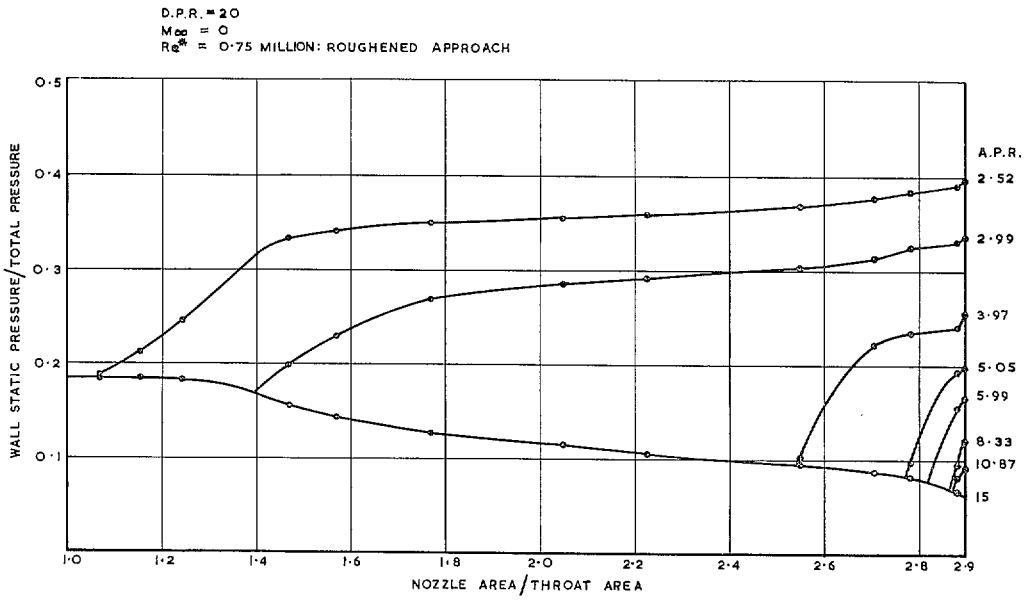

FIG. 28. 'Tulip' nozzle pressure distribution from Ref. 51—I.

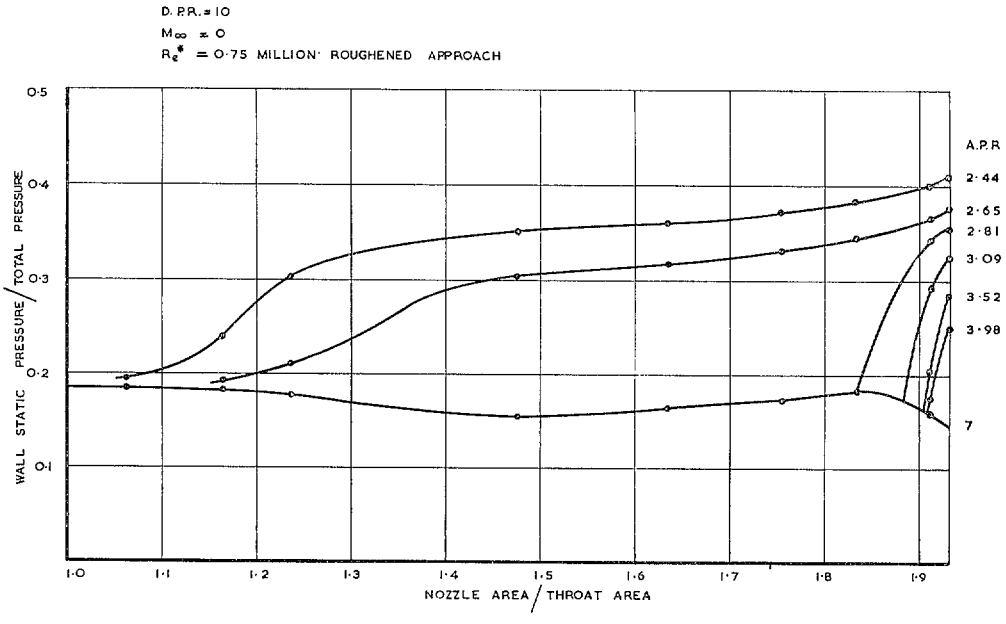

FIG. 29. 'Tulip' nozzle pressure distribution from Ref. 51—II.

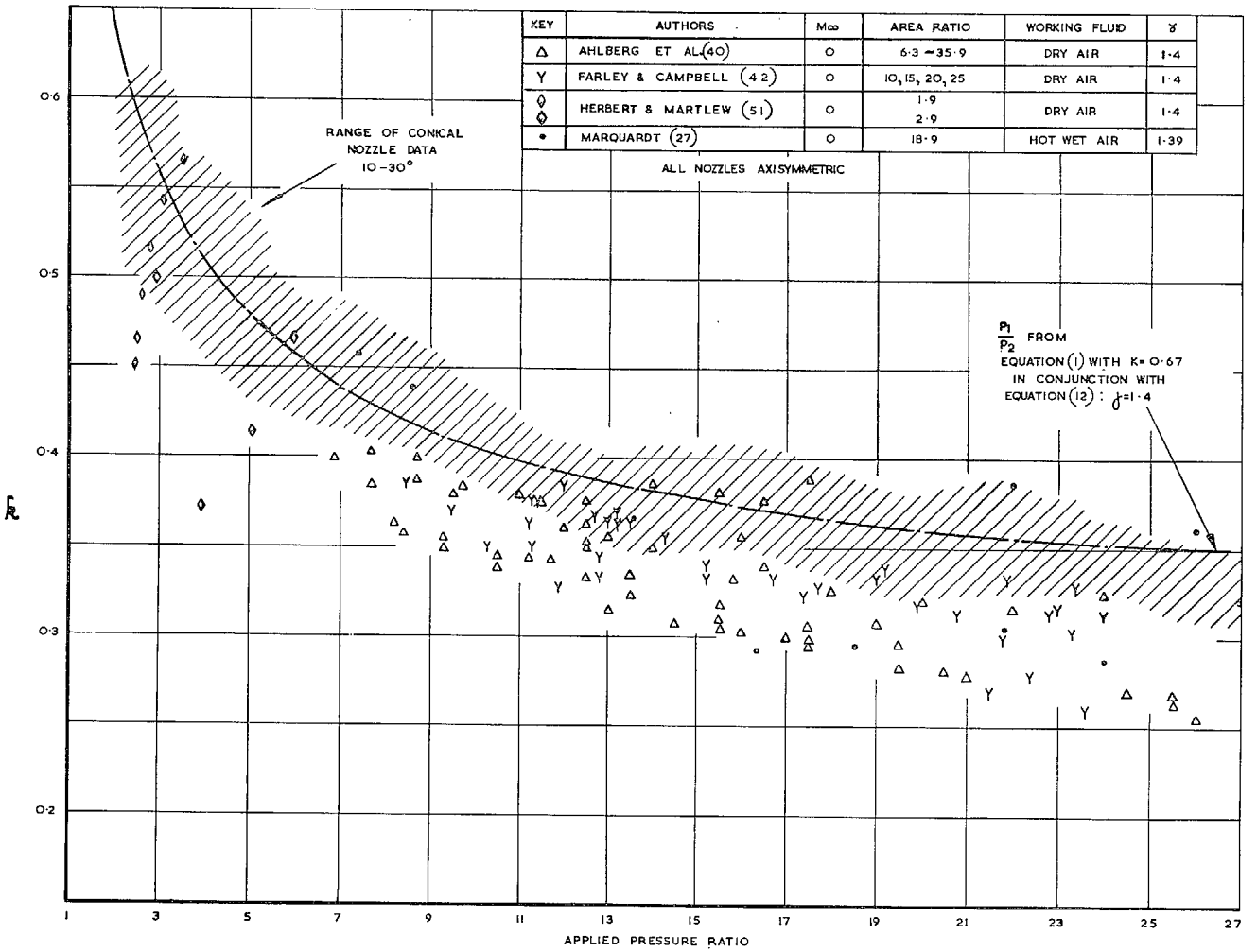

FIG. 30. Turbulent separation data for contoured nozzles—I.

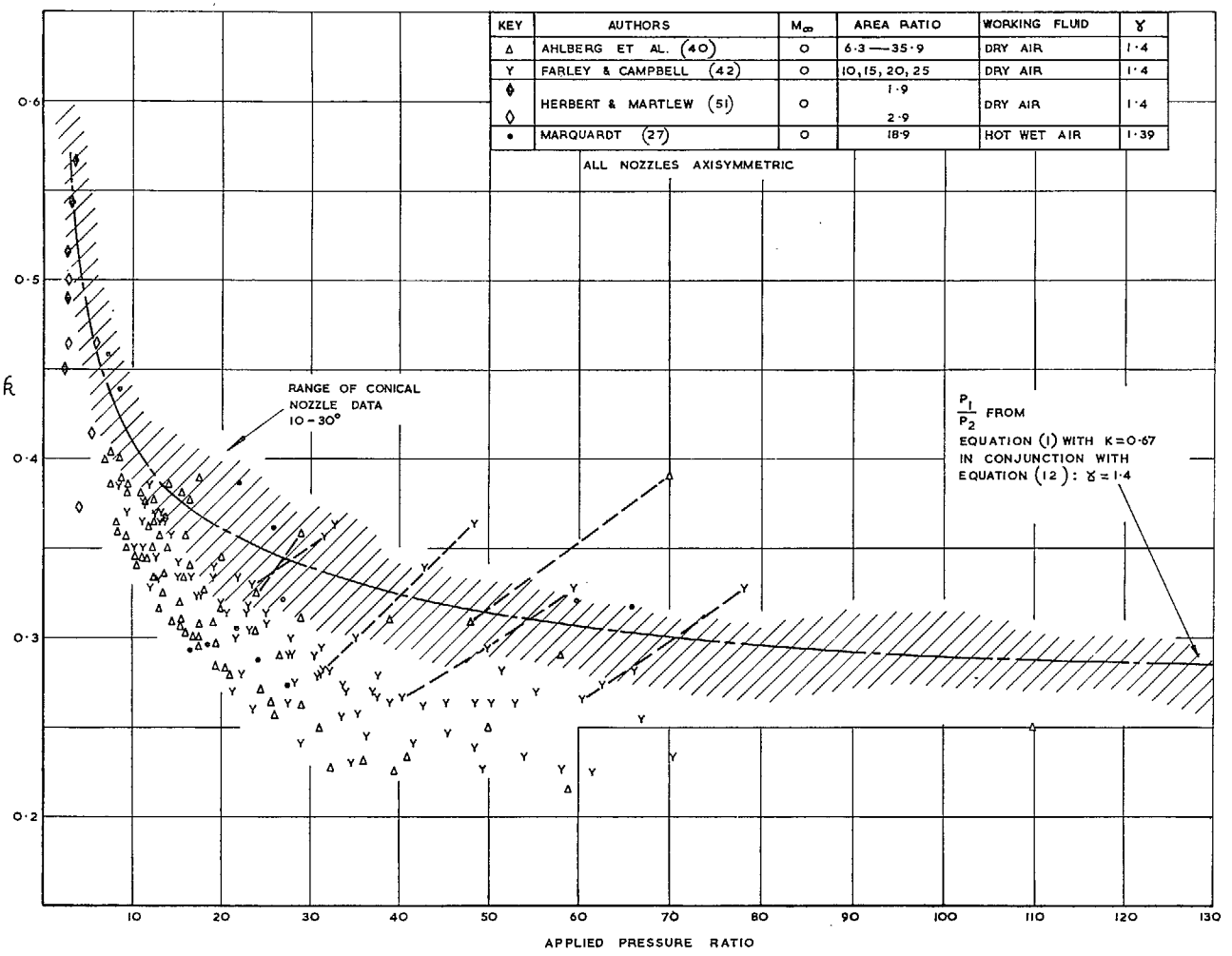

FIG. 31. Turbulent separation data for contoured nozzles—II.

(91646) Wt. 66/2301 K5 8/66 Hw.

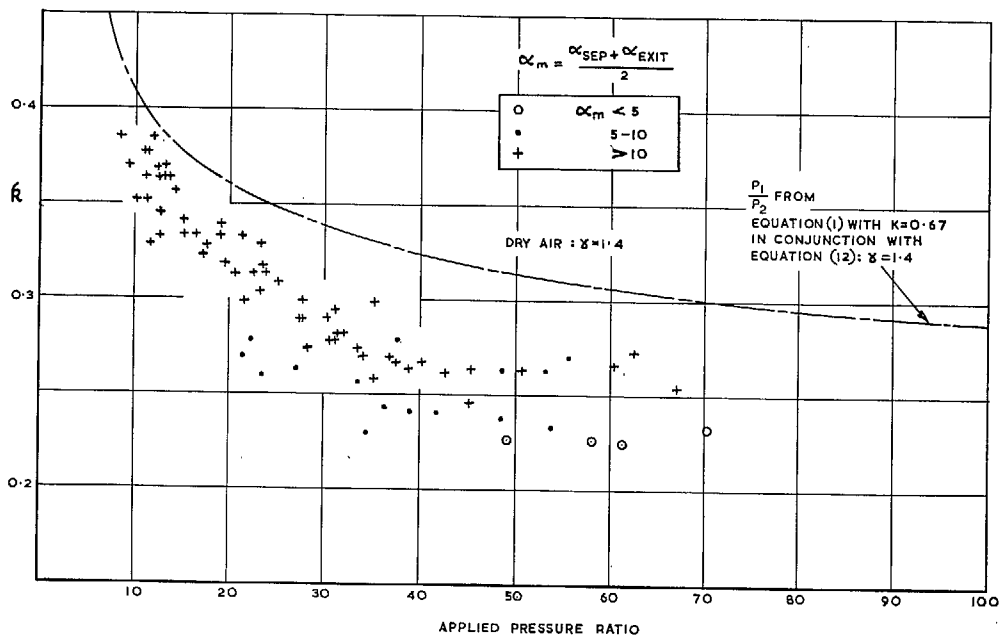

FIG. 32. Effect of mean wall angle on performance of contoured nozzles (from Ref. 42).

Publications of the Aeronautical Research Council

ANNUAL TECHNICAL REPORTS OF THE AERONAUTICAL RESEARCH COUNCIL (BOUND VOLUMES)

1945 Vol. I. Aero and Hydrodynamics, Aerofoils. £6 10*s*. (£6 13*s*. 6*d*.)
Vol. II. Aircraft, Airscrews, Controls. £6 10*s*. (£6 13*s*. 6*d*.)
Vol. III. Flutter and Vibration, Instruments, Miscellaneous, Parachutes, Plates and Panels, Propulsion. £6 10*s*. (£6 13*s*. 6*d*.)
Vol. IV. Stability, Structures, Wind Tunnels, Wind Tunnel Technique. £6 10*s*. (£6 13*s*. 3*d*.)

1946 Vol. I. Accidents, Aerodynamics, Aerofoils and Hydrofoils. £8 8*s*. (£8 11*s*. 9*d*.)
Vol. II. Airscrews, Cabin Cooling, Chemical Hazards, Controls, Flames, Flutter, Helicopters, Instruments and Instrumentation, Interference, Jets, Miscellaneous, Parachutes. £8 8*s*. (£8 11*s*. 3*d*.)
Vol. III. Performance, Propulsion, Seaplanes, Stability, Structures, Wind Tunnels. £8 8*s*. (£8 11*s*. 6*d*.)

1947 Vol. I. Aerodynamics, Aerofoils, Aircraft. £8 8*s*. (£8 11*s*. 9*d*.)
Vol. II. Airscrews and Rotors, Controls, Flutter, Materials, Miscellaneous, Parachutes, Propulsion, Seaplanes, Stability, Structures, Take-off and Landing. £8 8*s*. (£8 11*s*. 9*d*.)

1948 Vol. I. Aerodynamics, Aerofoils, Aircraft, Airscrews, Controls, Flutter and Vibration, Helicopters, Instruments, Propulsion, Seaplane, Stability, Structures, Wind Tunnels. £6 10*s*. (£6 13*s*. 3*d*.)
Vol. II. Aerodynamics, Aerofoils, Aircraft, Airscrews, Controls, Flutter and Vibration, Helicopters, Instruments, Propulsion, Seaplane, Stability, Structures, Wind Tunnels. £5 10*s*. (£5 13*s*. 3*d*.)

1949 Vol. I. Aerodynamics, Aerofoils. £5 10*s*. (£5 13*s*. 3*d*.)
Vol. II. Aircraft, Controls, Flutter and Vibration, Helicopters, Instruments, Materials, Seaplanes, Structures, Wind Tunnels. £5 10*s*. (£5 13*s*.)

1950 Vol. I. Aerodynamics, Aerofoils, Aircraft. £5 12*s*. 6*d*. (£5 16*s*.)
Vol. II. Apparatus, Flutter and Vibration, Meteorology, Panels, Performance, Rotorcraft, Seaplanes. £4 (£4 3*s*.)
Vol. III. Stability and Control, Structures, Thermodynamics, Visual Aids, Wind Tunnels. £4 (£4 2*s*. 9*d*.)

1951 Vol. I. Aerodynamics, Aerofoils. £6 10*s*. (£6 13*s*. 3*d*.)
Vol. II. Compressors and Turbines, Flutter, Instruments, Mathematics, Ropes, Rotorcraft, Stability and Control, Structures, Wind Tunnels. £5 10*s*. (£5 13*s*. 3*d*.)

1952 Vol. I. Aerodynamics, Aerofoils. £8 8*s*. (£8 11*s*. 3*d*.)
Vol. II. Aircraft, Bodies, Compressors, Controls, Equipment, Flutter and Oscillation, Rotorcraft, Seaplanes, Structures. £5 10*s*. (£5 13*s*.)

1953 Vol. I. Aerodynamics, Aerofoils and Wings, Aircraft, Compressors and Turbines, Controls. £6 (£6 3*s*. 3*d*.)
Vol. II. Flutter and Oscillation, Gusts, Helicopters, Performance, Seaplanes, Stability, Structures, Thermodynamics, Turbulence. £5 5*s*. (£5 8*s*. 3*d*.)

1954 Aero and Hydrodynamics, Aerofoils, Arrester gear, Compressors and Turbines, Flutter, Materials, Performance, Rotorcraft, Stability and Control, Structures. £7 7*s*. (£7 10*s*. 6*d*.)

Special Volumes

Vol. I. Aero and Hydrodynamics, Aerofoils, Controls, Flutter, Kites, Parachutes, Performance, Propulsion, Stability. £6 6*s*. (£6 9*s*.)
Vol. II. Aero and Hydrodynamics, Aerofoils, Airscrews, Controls, Flutter, Materials, Miscellaneous, Parachutes, Propulsion, Stability, Structures. £7 7*s*. (£7 10*s*.)
Vol. III. Aero and Hydrodynamics, Aerofoils, Airscrews, Controls, Flutter, Kites, Miscellaneous, Parachutes, Propulsion, Seaplanes, Stability, Structures, Test Equipment. £9 9*s*. (£9 12*s*. 9*d*.)

Reviews of the Aeronautical Research Council

1949–54 5*s*. (5*s*. 5*d*.)

Index to all Reports and Memoranda published in the Annual Technical Reports

1909–1947 R. & M. 2600 (out of print)

Indexes to the Reports and Memoranda of the Aeronautical Research Council

Between Nos. 2451–2549: R. & M. No. 2550 2*s*. 6*d*. (2*s*. 9*d*.); Between Nos. 2651–2749: R. & M. No. 2750 2*s*. 6*d*. (2*s*. 9*d*.); Between Nos. 2751–2849: R. & M. No. 2850 2*s*. 6*d*. (2*s*. 9*d*.); Between Nos. 2851–2949: R. & M. No. 2950 3*s*. (3*s*. 3*d*.); Between Nos. 2951–3049: R. & M. No. 3050 3*s*. 6*d*. (3*s*. 9*d*.); Between Nos. 3051–3149: R. & M. No. 3150 3*s*. 6*d*. (3*s*. 9*d*.); Between Nos. 3151–3249: R. & M. No. 3250 3*s*. 6*d*. (3*s*. 9*d*.); Between Nos. 3251–3349: R. & M. No. 3350 3*s*. 6*d*. (3*s*. 10*d*.)

Prices in brackets include postage

Government publications can be purchased over the counter or by post from the Government Bookshops in London, Edinburgh, Cardiff, Belfast, Manchester, Birmingham and Bristol, or through any bookseller

Printed and published by
HER MAJESTY'S STATIONERY OFFICE

To be purchased from
49 High Holborn, London WC1
423 Oxford Street, London W1
13A Castle Street, Edinburgh 2
109 St. Mary Street, Cardiff
Brazennose Street, Manchester 2
50 Fairfax Street, Bristol 1
35 Smallbrook, Ringway, Birmingham 5
80 Chichester Street, Belfast 1
or through any bookseller

Printed in England

S.O. Code No. 23-3421